2002

High-throughput single molecule screening and selective single molecule PCR for early stage disease diagnosis based on capillary electrophoresis

Hanlin Li
Iowa State University

High-throughput single molecule screening and selective single molecule PCR for early stage disease diagnosis based on capillary electrophoresis

by

Hanlin Li

A dissertation submitted to the graduate faculty

in partial fulfillment of the requirements for the degree of

DOCTOR OF PHILOSOPHY

Major: Analytical Chemistry

Program of Study Committee:
Edward S. Yeung, Major Professor
Donald C. Beitz
James H. Espenson
Robert S. Houk
Dennis C. Johnson

Iowa State University

Ames, Iowa

2002

UMI Number: 3051486

UMI Microform 3051486

ProQuest Information and Learning Company
300 North Zeeb Road
P.O. Box 1346
Ann Arbor, MI 48106-1346

Graduate College

Iowa State University

This is to certify that the doctoral dissertation of

Hanlin Li

has met the dissertation requirement of Iowa State University

Signature was redacted for privacy.

Major Professor

Signature was redacted for privacy.

For the Major Program

To my parents and my well-beloved husband

TABLE OF CONTENTS

ABSTRACT

The purpose of this research was to develop high throughput approaches for single molecule and single cell screening for early stage disease diagnosis. High sensitivity as well as high selectivity is essential for the success screening.

We first demonstrated a laser-induced fluorescence imaging method that allows screening many single molecules at a time based on their electrophoretic mobilities. YoYo-I labeled DNA molecules were tracked by a charge-coupled device (CCD) camera under a microscope while migrating in the electric field. The purpose is not to separate the DNA molecules but to identify each one on the basis of the measured electrophoretic mobility. Three different procedures were developed to measure the individual molecular mobilities, multi-frame method, streak method, and multi-spot method. Based on their difference in mobility, 2k and 49k bp DNA fragments were unambiguously differentiated. Each measurement only requires a few milliseconds to complete, which opens up the possibility of screening tens of thousands of molecules every second. The results correlate well with normal capillary electrophoresis (CE) experiments for the same samples (2-49 kb dsDNA) under identical separation conditions. The implication is that any electrophoresis protocols from slab gels to CE should be adaptable to single-molecule screening for disease diagnosis.

We also developed on-line capillary polymerase chain reaction (PCR) coupled with laser-induced fluorescence detection for individual DNA molecules. A single 30-μm-i.d. fused-silica capillary was used both as the reaction vessel and for isolating single molecules. SYBR green I dye was added into the reaction mixture for dynamic fluorescent labeling. Because of the small inside diameter of the capillary, PCR-amplified DNA fragments from single molecules were localized in the capillary, providing discrete product zones with

concentrations at readily detectable levels. By counting the number of peaks in the capillary via electromigration past a detection window, the number of starting DNA molecules could be determined. With selective primer design, only the molecule of interest was detected. Amplification of the 110-bp fragment from an individual human β-globin gene and the 142-bp fragment from an individual HIV-1 DNA was demonstrated.

Finally, we demonstrated the direct online capillary PCR amplification from crude biological samples. Individual lymphoblast cells were loaded into the PCR cocktail and on-line lysed by hypotonic buffer in the reaction capillary right before thermal cycling. Human β-actin gene within individual lymphoblast cells was successfully amplified and detected in the capillary with no extra sample preparation step. Partial dark field microscopy online cell counting provided the actual initial cell positions, which correlated very well with final amplified DNA peaks. This would provide highly selective and sensitive disease diagnosis at a very early stage when there are only a few infected cells. The problem reduces to identifying the suitable primer pairs for each disease marker. The feasibility for continuous-flow PCR monitoring, along with the well-developed capillary array electrophoresis techniques, will provide the high throughput and high sensitivity for large-scale clinical diagnosis.

CHAPTER 1. GENERAL INTRODUCTION

Dissertation Organization

This dissertation begins with a general introduction of the background information. Recent research and progress are also provided in the literature. The following chapters are presented as three complete scientific manuscripts with accompanying literature cited, tables and figures. General conclusions summarize the work and provide some prospective for future research. Appendix comprises supporting information.

Single Cell/Single Molecule Analysis

Background

Single cell analysis will potentially benefit clinical diagnosis and treatment. Briefly, there are two major reasons. First, sensitivity beyond what is presently available is needed to establish molecular profiles for species that are now inaccessible because they are present at low concentrations in tissues or at small quantities in a single cell. Single-molecule assays would be the ultimate solution. Finding and quantifying such species will allow us to pose "new testable hypotheses" and to recognize minor molecular alterations. This will open the door for studies in the very early stages of disease or cancer. In regular blood test, usually hundreds or thousands of cells are homogenized to provide sufficient amounts of analyte for quantification. However, at the early stages of disease, only a few cells may carry the specific chemical or biochemical markers indicative of infection. Such markers are likely to be completely masked by the averaged contents of the overabundant healthy cells. On the other hand, if the cell population is examined one cell at a time, each abnormal cell will be easily

recognized against normal ones. Such digital discrimination (abnormal/normal) is much more reliable and sensitive than analog discrimination based on small changes in an averaged value. Second, profiling individual cells and probing single DNA molecules can also reveal and quantify the diversity of a population, offer the opportunity to perform differential diagnosis and may provide mechanistic insights that homogenized cell samples cannot give. With sensitive detection, it is likely that biochemical changes can be recognized well before physical changes occur in the progress of a disease. In the treatment of diseases, it is also likely that the uptake of pharmaceuticals can be very different between healthy and disease-stricken cells. The understanding of such variability can lead to better drug design and control of side effects.

Detection (Sensitivity)

For detecting single molecules, one must have sufficient signal to record the event. In nearly all reported single-molecule experiments, compounds with a conjugated π-electron system (i.e., an organic dye) have been used. Usually, detection of these molecules has been performed by sensitive detection of their laser-induced fluorescence. Large molecules such as biopolymers (i.e., DNA) can possess many fluorescent centers per molecule, increasing the signal in the measurement. Not surprisingly, one of the earliest demonstrations of single-molecule detection is based on multiple fluorescent labeling of DNA molecules deposited at a low concentration on a glass slide. Another approach to increase the signal level would be by amplifying the sample itself from limited amount to detectable level by an enzyme-catalyzed reaction, such as polymerase chain reaction (PCR).

Background reduction is more of an issue than signal enhancement in single molecule detection. A serious source of background can be attributed to spurious fluorescence due to impurities. This source of background could be lowered by using ultra pure solvent and purified equipment.[1] Another source of background, nearly inevitable, is Rayleigh and/or Raman scattering of the bulk medium. Several approaches have been used to minimize the contributions of scattering to the background, including the use of extremely high rejection optical filters, time-gating detectors,[2, 3] and the use of near infrared (near-IR) excitation.[4] Background can also be suppressed by spatial discrimination, which has the effect of increasing the apparent concentration of the molecule of interest, i.e., reducing the sample volume.[5, 6]

Identification (Selectivity)

Sensitivity is not all for the detection of single biomolecules; the ability to recognize the target species in an overwhelming excess of very similar molecules is also a must. To this end, hybridization probes for DNA and antibodies to selected antigens are the most generally useful classes of highly specific probes for biorecognition. Fluorescence *in situ* hybridization (FISH) is certainly among the most promising tools for genetics research. The hybridization of a nucleic acid strand to its complement target is one of the most specific molecular recognition events known. The FISH technique is based on the hybridization of a specific nucleic acid sequence in cells, tissue or metaphase chromosomes with a fluorescently tagged sequence. However, FISH is limited by the high levels of cellular autofluorescence and involves tedious sample work up. Other in vitro hybridization approaches for nucleic acids such as molecular beacons[7, 8, 9] and Taqman assay[10, 11] employ a single-stranded DNA

molecule composed of a hairpin-shaped oligonucleotide that contains both a fluorophore and a quencher group.[12] The signal transduction mechanism is based on fluorescence energy transfer. However, at the present stage, all these hybridization approaches involve complicated probe design for each target molecule investigated, which is time consuming and not cost effective, therefore, not suitable for high-speed, high-throughput applications. Electrophoretic mobility, alternatively, is one of the most well defined universal molecular properties, provides selective detection too. At the single-molecule level, electrophoretic mobility has been reported in a micrometer-sized flow stream by correlating the photon-bursts created at two laser beams that are axially separated[13] or by autocorrelation of photon bursts within a single laser beam.[14] There, only one DNA molecule at a time can be probed and the measurement time is limited by the distance of separation between the two laser beams.

Imaging analysis

Imaging analysis with charge-coupled device (CCD) camera has shown great progress in recent years in accordance with the progress in high-sensitive fluorescent staining dyes for both DNAs and proteins.[15, 16, 17] Today, it draws even more attention because of the high level of interest in the analysis of proteins by two-dimensional gel electrophoresis in the field of proteomics research.[18] Other than fluorescence detection, CCD cameras also enable the detection of chemiluminescence, where specific DNA or proteins were blotted to a membrane. In the CCD camera system, emitted light from the sample is gathered through microscope lens and focused onto the CCD. CCD is a device possessing many light receiving elements (photopixels). Each element generates electrons in respond to the incident light and

forms one of the pixels of the digital image.[17] The size of each element contributes to both signal strength and dynamic range.

In this report, we applied CCD imaging technique in single molecule studies. The most attractive feature of CCD imaging is that it allows the observation of many distinct molecules simultaneously; thus, substantially improving throughput in single molecule analysis. Thousands of molecules could be screened within seconds.[19]

Chromosomes, DNA And Gene

Within the nucleus of each eukaryotic cell are a number of chromosomes (46 for human), each composed of a single molecule of DNA and a roughly equal mass of proteins. The DNA molecule, as is now common knowledge, is the carrier of genetic information; the proteins help effect the ordered condensation, or compaction, of the very long, very thin DNA molecule.[20] The determination of the structure of DNA by James Watson and Francis Crick in 1953 is often said to mark the birth of modern molecular biology. The usual configuration of DNA is shown in figure 1. Two strands of repeated chemical units are coiled together into a double helix. A sugar with an attached organic base and phosphate group constitutes the basic repeat unit of a DNA strand, a nucleotide. The nucleotides fall into four types: deoxyadenosine (A), deoxycytidine (C), deoxyguanosine (G), and deoxythymidine (T). The two strands of DNA are held together by hydrogen bonds between complementary bases, known as Chargaff's Rules: base A is always paired with T (A and T are complementary bases) and base C is always linked to G (C and G is called a base pair). Genetic information is encoded by the sequence of bases in the DNA strands. Human genome has about 3000 mega bases encoding about 50,000 to 100,000 genes.

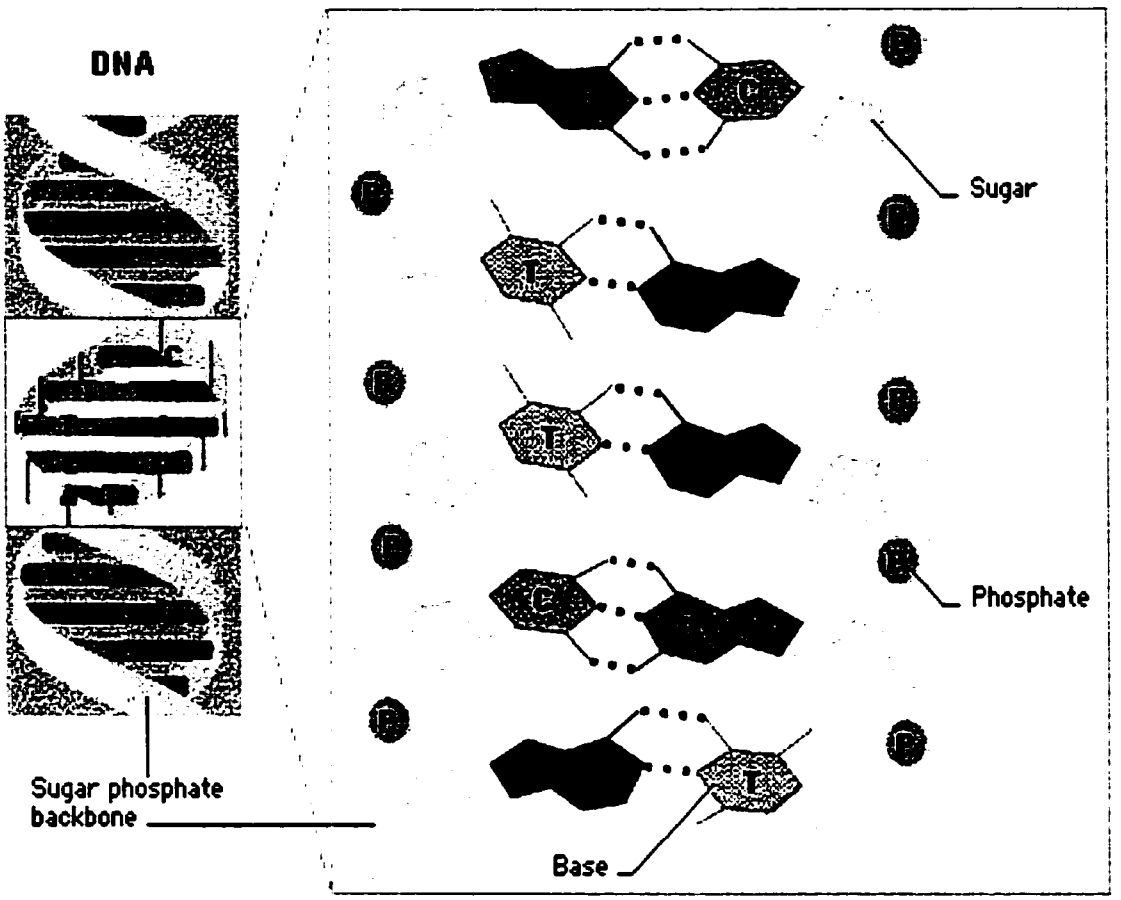

FIGURE 1 Structure of DNA

A = adenine, T = thymine, C = cytosine, G = guanine

Studying the Human Genome was one of the greatest enterprises of 20th Century science—and one that carries modern molecular biology well into the 21st Century.[21] Tremendous information from genomic maps and DNA sequence information to genome function was obtained from the exhilarating Human Genome Project. The Human Genome Project results in an unprecedented understanding of the basic biochemical processes of living organisms, and in particular, will enable the creation of a new "molecular medicine" based on early detection of individual diseases, effective preventive medicine, efficient drug development and personalized therapies.[22]

In recent years, hundreds of human diseases have been identified that have a genetic basis. Some are as mild as red-green color blindness, while others are as severe as complex diseases such as diabetes, cardiovascular disease or even cancer. Genetic research has already had a great impact in clinical diagnosis, as investigators have successfully isolated and identified disease genes including those responsible for breast cancer (BRCA1[23] and BRCA2[24]), early-onset Alzheimer's disease[25], Duchenne muscular dystrophy, cystic fibrosis, and the fragile X syndrome.[26, 27]

Polymerase Chain Reaction (PCR)

Background

There is no doubt that the advent of PCR had revolutionized the field of molecular biology since its introduction in 1985[28], because it mitigated problems with limited sample amounts by enabling amplification of genetic materials to detectable levels. Briefly, the PCR reaction is an enzyme-catalyzed DNA synthesis reaction that is analogous to the process by which cells replicate their DNA.[29] PCR allows the amplification of specific DNA sequences *in vitro*

using DNA polymerase and two short oligonucleotide primers flanking the DNA region of interest.

A typical amplification reaction includes the sample of target DNA, a thermostable DNA polymerase, two oligonucleotide primers, deoxynucleotide triphosphates (dNTPs), reaction buffer, magnesium and optional additives. The amplification process itself consists of a three-step cycle:

1. The initial step in a cycle denatures the target DNA by heating it to 94°C or higher for 15 seconds to 2 minutes. In the denaturation process, the two intertwined strands of DNA separate from one another, producing the necessary single-stranded DNA template for the thermostable polymerase.
2. The next step of a cycle reduces the temperature to approximately 40-60°C for 30-60 seconds. At this temperature, the oligonucleotide primers can form stable associations (anneal) with the separated target DNA strands and serve as primers for DNA synthesis by DNA polymerase.
3. Finally, the synthesis of new DNA begins when the reaction temperature is raised to the optimum for the DNA polymerase, typically 72°C. Extension of the primer by the thermostable polymerase lasts about 1-2 minutes. This step completes one cycle, and the next cycle begins with a return to 94°C for denaturation.

Each PCR cycle theoretically doubles the amount of targeted template sequence (amplicon) in the reaction. 20 cycles in theory multiply the amplicon by a factor of more than a million in a matter of hours. (Figure 2)

Application of PCR has now spread far and wide throughout biotechnology. In particular, the reaction has found many uses in molecular biology for cloning[30, 31], gene mapping,[32,33]

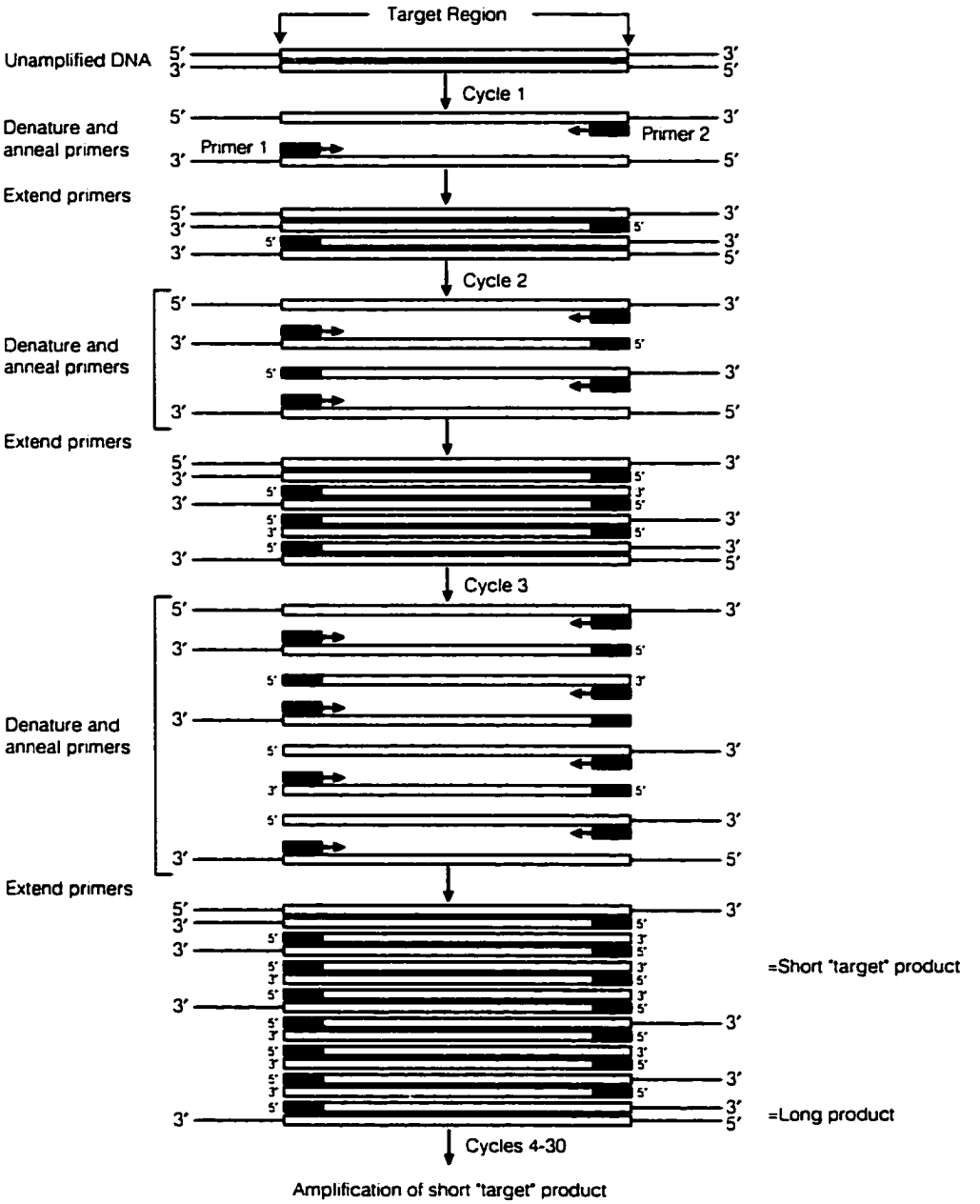

FIGURE 2 Principle of Polymearse Chain Reaction

forensic analysis, cDNA library construction[34] and so forth. In medicine, PCR has proven useful not only for the identification of infectious agents, such as human immunodeficiency virus (HIV),[35, 36] hepatitis B and C viruses,[37, 38, 39] etc., but also in the diagnosis of genetic disease and in the understanding of the pathogenesis of disease processes. [40, 41]

Single-Cell/Single Molecule PCR

In recent studies, the sensitivity of PCR has reached an extreme level where a single copy sequence within a single cell or a few cells can be detected[42]. The area of diagnostic science most affected by the advent of this ultra-sensitive single-cell PCR has undoubtedly been pre-implantation genetic analysis[43, 44, 45], which was used to investigate numerous genetic disorders before pregnancy has occurred. Other than the field of prenatal diagnosis, single-cell PCR also has a great impact on gene expression analysis[46, 47, 48], immunology and oncology research. [49,50]

The biggest challenge in single cell/molecule PCR is to achieve the single molecule sensitivity. Two approaches are commonly used to improve the sensitivity: nested PCR and primer extension pre-amplification (PEP). For nested PCR, two or more sequential rounds of amplification have to be performed, usually using nested primers. The first round is a standard amplification of 30 to 35 cycles. A small aliquot of the initial amplification is diluted 1:20 to 1:50 and added to the second round of amplification with 30 to 44 cycles.[51, 52, 53] Two different primer sets are used for the two rounds of amplification. The second amplification uses a nested set of primers that bind to the target just inside the first set of primers. Nested PCR can increase the sensitivity from limited amounts of target; however, it is time consuming and also accentuates problems with carry-over contamination.[54] Another

method often used for low copy number amplification is PEP, also termed whole genome amplification[55, 56], in which the entire genome was first amplified, thus providing enough DNA for subsequent PCRs. Unfortunately PEP also has two major disadvantages: it is also time consuming, for PEP usually takes 8-12 h; although the whole genome can be amplified, the amplification seems random, in practice, only ~80% of the genome is effectively amplified. The remaining 20% of the genome, which may contain the gene of interest, may not be amplified at all.[57]

Both nested PCR and PEP involve at least two rounds of amplification and liquid transfer between rounds. What we presented in our work is a new approach with only one-step, one primer pair PCR for single cell/single molecule amplification. We reasoned that the sensitivity of laser-induced fluorescence (LIF) detection could be improved to enable detection of single starting molecules if reaction volume were reduced. Therefore, miniaturization of PCR is introduced.

Miniaturization of PCR

The advent of biological microdevices[58]allows one to consider conducting bioanalytical assays such as PCR at very small volumes to increase the speed of these assays, reduce the amount of material and reagents needed, improve sensitivity and accomplish automation.[59] The first microfabricated PCR reactors were constructed from silicon and glasss and amplified DNA from template concentrations down to roughly 2000 copies/μL and in volumes down to 1 μL.[60] Since then, stand-alone PCR reactors have been constructed in silicon,[61, 62, 63] glass,[64, 65, 66] polymeric materials,[67, 68] and fused silica capillaries.[69] Unfortunately, most of these materials are less ideal for DNA amplification because of the

tendency of proteins (DNA polymerase) to be deactivated by adsorption to the surface. Surface passivation has to be made through several approaches, such as oxidation,[60] dynamic coatings using polymers such as polyvinyl pyrrolidone (PVP)[66], polyethylene glycol (PEG), hydroxyethylcellulose (HEC) ect.[70], and preliminary treatment with bovine serum albumin (BSA).[71] Rapid thermal cycling near 17s/cycle has been demonstrated in microchips by having a small thermal mass and decreasing PCR dwell times. Such a device was used to detect bacterial DNA by a real-time TaqMan PCR assay in 7 min.[72] Continuous flow PCR was performed in a glass chip with times ranging from 1.5 to 18.5 min.[64]

However, the most challenging and important issue in the submicroliter miniaturization of DNA analyses is the integration of the various amplification and analysis steps, because a good substrate for PCR amplification may not meet the electrical requirements of electrophoresis.[71] Several groups have developed integrated microfluidic devices combing rapid thermal cycling PCR amplification with capillary electrophoresis and demonstrated the feasibility of portable microchip-based instrumentation platforms.[73, 74, 75, 68, 71] Combination of amplification and CE components on a single fused silica capillary was also reported.[76]

Isolation and Purification of DNA

DNA isolation and purification are essential techniques for molecular biology studies. The quality and integrity of DNA isolated directly affect the results of scientific research. The extraction and purification of nucleic acid (DNA or RNA) from a biological sample requires lysis of the cell membrane, inactivation of the cellular nuclease, and separation of the desired nucleic acid from the cellular debris. Cell lysis is crucial to the success of amplification, especially in the case of single cell PCR. Although the reasons for amplification failure from

single cells are likely to be numerous, including problems with sample preparation; e.g., failure to transfer the cell, degradation or loss of the target sequence and /or problems associated with PCR, the major cause of the PCR failure, however, is probably due to inefficient cell lysis.[77] This is reflected by the fact that failure appears to vary with cell type used,[42] probably because different cell types, with their different structure and nature, respond differently to lysing process.[78] A number of methods have been developed and commonly used to lyse cells so that DNA may be PCR amplified, such as phase extraction, enzymatic treatment, detergents, and boiling. Traditionally, DNA extraction was accomplished by phase separation, e.g. phenol-chloroform, which preferentially partitions the nucleic acid into the aqueous phase and the other cellular components including connective proteins, into organic phase or phase interface. However, phase separation has the disadvantage of a relatively high loss of material, thus decreasing the efficiency and reproducibility of the procedure. The cost and use of organic solvent are also a concern. Enzymatic lysing with proteinase K[79] is a simpler and cleaner method than phase extraction. The advantage of using proteinase K is that it will not only break down the cell membranes and expose DNAs, but also digest some intracellular proteins that may prohibit PCR reactions. Detergents such as sodium dodecyl sulfate (SDS), Triton X-100 and NP-40 can be used alone or in combination with proteinase K in lysing cells.[51, 80] Charged surfactants, e.g. SDS, are more effective than neutral ones. Yet, none of the above methods or components is compatible with PCR reagents. Extra steps of centrifugation, incubation and liquid transferring have to be taken before PCR analysis. Boiling cells in distilled water[81, 82, 83] or PCR reaction mixture[74, 55] on the other hand, is a good alternative method, which could achieve cell lysis and PCR amplification in one module. The disadvantage of this method is it

does not contain any purification steps in DNA isolation; therefore, it may also have a decreased efficiency when PCR inhibitors remain in the reaction mix.

Post-PCR analysis—Capillary Electrophoresis (CE)

Capillary zone electrophoresis

Capillary zone electrophoresis (CZE) is defined as an electrophoresis in free homogeneous solution. The capillary and the buffer reservoirs are filled with background electrolyte, which conducts practically all the electric current and provides buffering capacity. There are no interactions between the substances and a gel in CZE. Separations are achieved based on different charge-to-mass ratio of the analytes. CZE has been used to separate a wide range of charged simple organic molecules,[84] inorganic ions,[85] carbohydrates,[86] peptides[87, 88] and proteins.[89, 90] Various additives such as cyclodextrins[91, 92] as well as other chiral discriminating agents[93] have been added to the separation buffers as chiral selectors to perform chiral separations by CZE. However, DNA molecules cannot be separated directly in CZE, because oligonucleotides larger than 10 bp would have very similar mass to charge ratio, regardless of their sizes. Therefore, a sieving matrix has to be introduced to separate DNAs based on size difference.

Capillary gel electrophoresis

Traditionally, slab gel electrophoresis was used for DNA analysis, such as sequencing, restricted fragment length polymorphism, and mutation tests. The gel has two functions: it is used as an anticonvective medium as well as a sieving matrix for separation. This method usually is very slow because of the poor heat dissipation; thus, only lower voltage can be

applied compared with capillary electrophoresis. Capillary electrophoresis, on the other hand, is superior to classical slab-gel electrophoresis since it offers high resolution, high sensitivity and the possibility for automation.

Due to the small dimensions of the capillaries (typical inner diameters are between 50 and 100μm), convection is rather low. Thus, CE offers the possibility of gel-free separation. But in case of biopolymers such as DNA, RNA or SDS-proteins, which have a constant charge:size ratio, no electrophoretic separation occurs in free solution. One solution to this problem is the use of a separation matrix as in traditional electrophoresis.[94] The first spectacular electropherograms, published in the late 1980s by Cohen and Karger[95, 96] using capillary gel electrophoresis, demonstrated an opportunity for significant advances in the practice of separation science. At first, electrophoretic separation was adapted from slab format to capillary format by using the same matrices, e.g., cross-linked polyacrylamide or agarose.[97,98] The gels are prepared in the same manner as slab gels, i.e., by adding the catalysts to the monomer solution shortly before it is pumped into the capillary, where polymerization takes place. Single-base separations of polyoligonucleotides have been achieved in minutes[99] and DNA sequencing runs resolving 350 bases have been completed in 1 hour[100] with gel-filled capillaries. Unfortunately, capillaries filled with polyacrylamide only have very limited lifetime and the gel filling process also lacks of reproducibility. Therefore, nowadays they only play a minor role in DNA separation applications.

A number of different polymer solutions soon replaced cross-linked polymers in DNA separations with CE. Most of the polymers used are modified polysaccharides: agarose and its derivatives and various cellulose derivatives such as hydroxyethylcellulose (HEC)[101] and hydroxypropylcellulose (HPC)[102]. In addition, synthetic polymers have been found superior

over polymers from natural sources. Frequently used synthetic polymers are PEG[103], polyethylene oxide (PEO)[104], PVP[105] and linear polyacrylamide.[106, 107, 108, 109]

Separation mechanisms in polymer solutions

The mechanism of DNA movement in a porous matrix under the influence of an electric field has been studied in detail. Three models were postulated.

Ogston model

The earliest model is Ogston model, developed in 1950s, where gel is assumed to be a static, infinite network of long, inert and randomly distributed linear fibers having a certain "average pore size". DNA is suggested to electrophorese through this network as an unperturbed spherical coil, which must diffuse laterally until it encounters a pore large enough to permit its passage.

Reptation model

Obviously, Ogston model is not valid for the situation when DNA molecules are larger than the pores of the gel; then, the reptation model was developed. According to this model, randomly coiled DNAs, too large to fit through a pore while maintaining a coiled conformation, will migrate headfirst, snakelike, through "tubes" defined by the fibers (for a rigid mesh) or the "blobs" (for a flexible network) surrounding it. No lateral motion is allowed within the tube, and DNAs are thought to alternately stretch and relax as they slither through the tube. Thus, the reptation model assumes that large DNAs, instead of migrating as undeformable particles, can be deformed and stretched according to local conditions.

Biased reptation model

According to this model, at high electric fields, and/or DNAs larger than 40 kbp, field-induced orientation extends the stretching periods of DNA, causing their random walk to

become strongly biased in the forward direction so that DNA is stretched to a rod-like conformation.[110]

Transient entanglement coupling

All of the above three models apply to DNA separations in entangled polymer solutions, where separation occurs by DNA "sieving" through polymer networks. However, at concentrations well below the polymer entanglement threshold (c*), even at about two orders of magnitude below c*, where no polymer network exists, separation of dsDNA was still found.[101] This suggests that the mechanism of DNA separation in such dilute polymer solutions must be quite different from the mechanisms postulated for DNA movement in gels and entangled polymer solutions, which assume the existence of "pores" or "tubes". Baron et al. proposed a simple hypothesis to explain the successful separation in unentangled polymer solutions.[111] It is based on the idea that DNA molecules, while migrating, collide with the matrix polymers. These polymers are then caught and dragged along by the DNA until eventually they slide away. This "transient entanglement coupling mechanism" creates a size-dependent drag force, i.e., large DNA molecules will have a higher probability of entangling with one or more polymer molecules than smaller ones; thus, large ones will be more retarded than smaller ones. The catching and dragging is primarily based on physical interactions rather than chemical interactions such as hydrogen bonding between DNA and polymer chains.[112] This model was applied in our report for large DNA separations. (Chapter 2)

Our Goal

The emphasis in health care will continue to evolve from management to prophylaxis. There is usually a better chance for therapy if the disease could be recognized at its early stage. Our goal is to develop a highly selective and sensitive approach for single molecule screening, which would benefit the disease diagnosis at its very early stage when only very few cells out of a large population are infected. Integration of the total analysis process with increased throughput is also addressed for the practical use of the technique for large-scale clinical diagnosis.

REFERENCES

1. Zander, C. *Fresenius J. Anal. Chem.* **2000**, 366, 745-751.
2. Shera, E. B.; Seitzinger, N. K.; Davis, L. M.; Keller, R. A.; Soper, S. A. *Chem. Phus. Lett.* **1990**, 174, 553-557.
3. Johnson, M. E.; Goodwin, P. M.; Ambrose, W. P.; Martin, J. C.; Marrone, B. L.; Jett, J. H.; Keller, R. A. *Proc. SPIE* **1993**, 1895, 69-78.
4. Soper, S. A.; Legendre, L. B.; Huang, J. *Chem. Phys. Lett.* **1995**, 237, 339-345.
5. Nie, S.; Chiu, D. T.; Zare, R. N. *Anal. Chem.* **1995**, 67, 2849-2857.
6. Keller, R. A.; Ambrose, W. P.; Goodwin, P. M.; Jett, J. H.; Martin, J. C.; Wu, M. *Appl. Spectrosc.* **1996**, 50, 12A-32A.
7. Kostrikis, L. G.; Tyagi, S.; Mhlanga, M. M.; Ho, D. D.; Kramer, F. R. *Science* **1998**, 279, 1228-1229.
8. Fang, X.; Tan, W. *Anal. Chem.* **1999**, 71, 3101-3105.

9. Fang, X.; Li, J.; Perlette, J.; Tan, W.; Wang, K. *Anal. Chem.* **2000**, 72, 747A-753A.

10. Holland, P. M.; Abramson, R. D.; Watson, R.; Gelfand, D. H. *Proc. Natl. Acad. Sci. USA* **1991**, 88, 7276-7280.

11. Livak, K. J.; Flood, S. J. A.; Marmaro, J.; Giusti, W.; Deetz, K. *PCR Methods Applicat.* **1995**, 4, 357-362.

12. Tyagi, S.; Kramer, F. R. *Nat. Biotech.* **1996**, 14, 303-308.

13. Castro, A.; Shera, E. B. *Anal. Chem.* **1995**, 67, 3181-3186.

14. Van Orden, A.; Keller, R. A. *Anal. Chem.* **1998**, 70, 4463-4471.

15. Steinberg, T. H.; Jones, L. J.; Haugland, R. P.; Singer, V. L. *Anal. Biochem.* **1996**, 239, 223-237.

16. Berggren, K.; Steinberg, T. H.; Lauber, W. M.; Carroll, J. A.; Lopez, M. F.; Chernokalskaya, E.; Zieske, L.; Diwu, Z.; Haugland, R. P. *Anal. Biochem.* **1999**, 276, 129-143.

17. Miura, K. *Electrophoresis* **2001**, 22, 801-813.

18. Spibey, C. A.; Jackson, P.; Herick, K. *Electrophoresis* **2001**, 22, 829-836.

19 Shortreed, M. R.; Li, H.; Huang, W. H.; Yeung, E. S. *Anal Chem.* **2000**, 72, 2879-2885.

20. Wagner, R. P. *The Human Genome Project: Deciphering the Blueprint of Heredity,* Cooper, N. G. (Ed), Mill Valley, CA, University Science Books, **1994**.

21. Dressler, D. *The Human Genome Project: Deciphering the Blueprint of Heredity,* Cooper, N. G. (Ed), Mill Valley, CA, University Science Books, **1994**.

22. Uddhav K.; Ketan, S. *Mol. Biol. Rep.* **1998**, 25, 27-43.

23. Miki, Y.; Swensen, J.; Shattuck-Eidens, D.; Futreal, P. A.; Harshman, K.; Tavtigian, S.; Liu, Q.; Cochran, C.; Bennett, L. M.; et al. *Science*, **1994**, 266(5182), 66-71.

24. Wooster, R.; Bignell, G.; Lancaster, J.; Swift, S.; Seal, S.; Mangion, J.; Collins, N.; Gregory, S.; Gumbs, C.; et al. *Nature* **1995**, 378(6559), 789-792.

25. Chartier-Harlin, M. C.; Crawford, F.; Houlden, H.; Warren, A.; Hughes, D.; Fidani, L.; Goate, A.; Rossor, M.; Roques, P.; et al. *Nature* **1991**, 353(6347), 844-846.

26. Boguski, M. S. *New Engl. J. Med.* **1995**, 333, 645-647.

27. Handyside, A. H.; Lesko, J. G.; Tarin, J. J.; Winston, R. M. L; Hughes, M. R. *New Engl. J. Med.* **1992**, 327, 905-909.

28. Saiki, R. K.; Scharf, S.; Faloona, F.; Mullis, K. B.; Horn, G. T.; Erlich, H. A.; Arnheim, N. *Science* **1985**, 230, 1350-1354.

29. Erlich, H. A. *PCR Technology: principles and applications for DNA amplification* New York, Stockton Press, **1989**.

30. Deng, Y. M.; Lee, J. H.; Moran, C.; Jin, J. H.; Tuch, B. E.; Rawlinson, W. D. *Nucleic Acids Res.* **2000**, 28(23), e103/1-e103/4.

31. Schaefer, B. C. *Anal. Biochem.* **1995**, 227(2), 255-273.

32. Campbell, I. G.; Bryan, E. J. *Methods Mol. Med.* **2000**, 39(Ovarian Cancer), 365-374.

33. Arnheim, N.; Li, H.; Cui, X. *Genomics* **1990**, 8(3), 415-419.

34. Brady, G.; Iscove, N. N. *Methods enzymol.* **1993**, 225, 611-623.

35. Ou, C. Y.; Kwok, S.; Mitchell, S. W.; Mack, D. H.; Sninsky, J. J.; Krebs, J. W.; Feorino, P.; Warfield, D.; Schochetman, G. *Science* **1998**, 239, 295-297.

36. Fiscus, S. A. *Methods Mol. Med.* **1999**, 20, 129-139.

37. Larzul, D.; Guigue, F.; Sninsky, J. J.; Mack, D. H.; Brechot, C.; Guesdon, J. L. *J. Virol. Methods* **1988**, 20, 227-237.

38. Kaneko, S.; Miller, R. H.; Feinstone, S. M.; Unoura, M.; Kobayashi, K.; Hattori, N.; Purcell, R. H. *Proc. Natl. Acad. Sci. USA* **1989**, 86, 312-316.

39. Allen, M. I.; Gauthier, J.; DesLauriers, M.; Bourne, E. J.; Carrick, K. M.; Baldanti, F.; Ross, L. L.; Lutz, M. W.; Condreay, L. D. *J. Clin. Microbiol.* **1999**, 37(10), 3338-3347.

40. McMahon, G.; Davis, E.; Wogan, G. N. *Proc. Natl. Acad. Sci. USA*. **1987**, 34, 4974

41. Bos, J. L.; Fearon, E. R.; Hamilton, S. R. *Nature* **1987**, 327, 293

42. Li, H. H.; Gyllensten, U. B.; Cui, X. F.; Saiki, R. K.; Erlich, H. A.; Arnheim, N. *Nature* **1988**, 335, 414-417.

43. Hahn, S.; Zhong, X. Y.; Troeger, C.; Burgemeister, R.; Gloning, K.; Holzgreve, W. *Cell. Mol. Life Sci.* **2000**, 57, 96-105.

44. Garvin, A. M.; Holzgreve, W.; Hahn, S. *Nucleic. Acids Res.* **1998**, 26(15), 3468-3472.

45. Rechitsky, S.; Verlinsky, O.; Amet, T.; Rechitsky, M.; Kouliev, T.; Strom, C.; Verlinsky, Y. *Mol. Cell. Endocrinol.* **2001**, 183(Suppl. 1), S65-S68.

46. Ebervine, J.; Yeh, H.; Miyashiro, K.; Cao, Y.; Nair, S.; Finnell, R.; Zettel, M.; Coleman, P. *Proc. Natl Acad. Sci. USA* **1992**, 89, 3010-3014.

47. Cheng, T.; Shen, H.; Giokas, D.; Gere, J.; Tenen, D. G.; Scadden, D. T. *Proc. Natl Acad. Sci. USA* **1996**, 93, 13158-13163.

48. Hu, M.; Krause, D.; Greaves, M.; Sharkis, S.; Dexter, M.; Heyworth, C.; Enver, T. *Genes Dev.* **1997**, 11, 774-785.

49. Gellrich, S.; Lukowsky, A.; Schilling, T.; Rutz, S.; Muche, J. M.; Jahn, S.; Audring, H.; Sterry, W. *J. Invest. Dermatol.* **2000**, 115(4), 620-624.

50. Attuil, V.; Bucher, P.; Rossi, M.; Mutin, M.; Maryanski, J. L. *Proc. Natl. Acad. Sci. USA* **2000**, 97(15), 8473-8478.

51. Garvin, A. M.; Holzgreve, W.; Hahn, S. *Nucleic Acids Res.* **1998**, 25(15), 3468-3472.

52. Gravel, S.; Delsol, G.; Al Saati, T. *Blood*, **1998**, 91(8), 2866-2874.

53. Roers, A.; Montesinos-Rongen, M.; Hansmann, M. L.; Rsjewsky, K.; Küppers, R. *Eur. J. Immunol.* **1998**, 28, 2424-2431.

54. Kalinina, O.; Lebedeva, I.; Brown, J.; Silver, J. *Nucleic Acids Res.* **1997**, 25(10), 1999-2004.

55. Zhang. L.; Cui, X. F.; Schmitt, K.; Hubert, R.; Navidi, W.; Arnheim, N. *Proc Natl Acad Sci USA* **1992**, 89, 5847-5851.

56. Kristjansson, K.; Chong, S. S.; Vandenveyver, I. B.; Subramanian, S.; Snabes, M. C.; Hughes, M. R. *Nat Genet* **1994**, 6, 19-23.

57. Findlay, I. *British Med. Bulletin* **2000**, 56(3), 672-690.

58. Van den Berg, A.; Olthuis, W.; Bergveld, T. *Micro Total Analysis Systems 2000*, Kluwer Academic Publishers: Dordrecht, The Netherlands, **2000**.

59. Cheng, J.; Fortina, P.; Surrey, S.; Kricka, L. J.; Wilding, P. *Mol. Diagn.* **1996**, 1, 183.

60. Cheng, J.; Shoffner, M. A.; Hvichia, G. E.; Kricka, L. J.; Wilding, P. *Nucleic Acids Res.* **1996**, 24, 380-385.

61. Wilding, P.; Kricka, L. J.; Cheng, J.; Hvichia G.; Shoffner, M. A.; Fortina, P. *Anal. Biochem.* **1998**, 257, 95-100.

62. Northrup, M. A.; Benett, B.; Hadley, D.; Landre, P.; Lehew, S.; Richards, J.; Stratton, P. *Anal Chem.* **1998**, 70, 918-922.

63. Chaudhari, A. M.; Woudernberg, T. M.; Albin, M.; Goodson, K. E. *J. Microelectromech. Syst.* **1998**, 7, 345-355.

64. Oda, R. P.; Strausbauch, M. A.; Huhmer, A. F. R.; Borson, N.; Jurrens, S. R.; Craighead, J.; Wettstein, P. J.; Echloff, B.; Kline, B.; Landers, J. P. *Anal. Chem.* **1998**, 70, 4361-4368.

65. Taylor, T. B.; Harvey, S. E.; Albin, M.; Lebak, L.; Ning, Y.; Mowat, I.; Schuerlein, T.; Principe, E. *Biomed. Microdevices* **1998**, 1, 65-70.

66. Kopp, M. U.; de Mello, A. J.; Manz, A. *Science* **1998**, 280, 1046-1048.

67. Soper, S. A.; Ford, S. M.; Xu, Y.; Qi, S.; McWhorter, S.; Lassiter, S.; Patterson, D.; Bruch, R. C. *J. Chromatogr. A* **1999**, 853, 107-120.

68. Hong, J. W.; Fujii, T.; Seki, M.; Yamamoto, T.; Endo, I. *Electrophoresis* **2001**, 22, 328-333.

69. Zhang, N. Y.; Tan, H. D.; Yeung, E. S. *Anal. Chem.* **1999**, 71, 1138-1145.

70. Giordano, B. C.; Copeland, E. R.; Landers, J. P. *Electrophoresis* **2001**, 22, 334-340.

71. Khandurina, J.; McKnight, T. E.; Jacobson, S. C.; Waters, L. C.; Foote, R. S.; Ramsey, M. J. *Anal. Chem.* **2000**, 72, 2995-3000.

72. Belgrader, P.; Benett, W.; Hadley, D.; Richards, J.; Stratton, P.; Mariella, R.; Milanovich, F. *Science* **1999**, 284, 449-450.

73. Woolley, A. T.; Hadley, D.; Landre, P.; de Mello, A. J.; Mathies, R. A.; Northrup, A. M. *Anal. Chem.* **1996**, 68(23), 4081-4086.

74. Waters, L. C.; Jacobson, S. C.; Kroutchinina, N.; Khandurina, J.; Foote, R. S.; Ramsey, M. J. *Anal. Chem.* **1998**, 70(1), 158-162.

75. Lagally, E. T.; Medintz, I.; Mathies, R. A. *Anal. Chem.* **2001**, 73(3), 565-570.

76. Li, H.; Xue, G.; Yeung, E. S. *Anal. Chem.* **2001**, 73(7), 1537-1543.

77. Findlay, I.; Matthews, P.; Quirke, P. *Prenat. Diagn.* **1998**, 18, 1413-1421.

78. El-Hashemite, N.; Delhanty, J. D. *Mol. Hum. Reprod.* **1997**, 3(11), 975-978.

79. Taylor, R. W.; Taylor, G. A.; Durham, S. E.; Turnbull, D. M. *Nucleic Acids Res.* **2001**, 29(15), e74.

80. Cheng, T.; Shen, H.; Giokas, D.; Gere, J.; Tenen, D. G.; Scadden, D. T. *Proc. Natl. Acad. Sci. USA* **1996**, 93, 13158-13163.

81. Saiki, R. K.; Bugawan, T. L.; Horn, G. T.; Mullis, K. B.; Erlich, H. A. *Nature* **1986**, 324, 163-166.

82. Li, H.; Gyllensten, U. B.; Cui, X.; Saiki, R. K.; Erlich, H. A.; Arnheim, N. *Nature* **1998**, 335, 414-417.

83. Erickson, C. E.; Castora, F. J. *Biochim. Biophys. Acta* **1993**, 1181, 77-82.

84. Terabe, S.; Yashima, T.; Tanaka, N.; Araki, M. *Anal. Chem.* **1988**, 60, 1673-1677.

85. Morin, P.; Amran, M. B.; Favier, S.; Heimburger, R.; Leroy, M. Fresenius. J. *Anal. Chem.* **1992**, 42(4-5), 357-62.

86. Colon, L. A.; Dadoo, R.; Zare, R. N. *Anal. Chem.* **1993**, 65(4), 476-81.

87. Grossman, P. D.; Wilson, K. J.; Petrie, G.; Lauer, H. H. *Anal. Biochem.* **1988**, 173, 265-270.

88. Moseley, M. A.; Deterding, L. J.; Tomer, K. B.; Jorgenson, J. W. *Anal. Chem.* **1991**, 63(2), 109-14.

89. McCormick, R. M. *Anal. Chem.* **1988**, 60, 2322-2328.

90. Loo, J. A.; Jones, H. K.; Udseth, H. R.; Smith, R. D. *J. Microcolumn Sep.* **1989**, 1(5), 223-229.

91. Otsuka, K.; Terabe, S. *J. Chromatogr.* **1990**, 515, 221

92. Nielen, M. W. F. *Anal. Chem.* **1993**, 65, 885-893.

93. Kuhn, R.; Erni, F.; Bereuter, T.; Haeusler, J. *Anal. Chem.* **1992**, 64, 2815-2820

94. Heller, C. *Electrophoresis* **2001**, 22, 629-643.

95. Cohen, A. S.; Karger, B. L. *J. Chromatogr.* **1987**, 397, 409-417.

96. Cohen, A. S.; Paulus, A.; Karger, B. L. *Chromatographia* **1987**, 24, 15-24.

97. Cohen, A. S.; Najarian, D. R.; Paulus, A.; Guttman, A.; Smith, J. A.; Karger, B. L. *Proc. Natl. Acad. Sci. USA* **1988**, 85, 9660-9663.

98. Motsch, S. R.; Kleemiß, M. H.; Schomburg, G. *J. High Resol. Chromatogr.* **1991**, 14, 629-632.

99. Karger, B. L.; Cohen, A. S.; Guttman, A. *J. Chromatogr.* **1989**, 492, 585-614.

100. Drossman, H.; Luckey, J. A.; Kostichka, A.; D'Cunha, J.; Smith, L. M. *Anal. Chem.* **1990**, 62(9), 900-903.

101. Barron, A. E.; Soane, D. S.; Blanch, H. W. *J. Chromatogr.* **1993**, 652, 3-16.

102. Baba, Y.; Ishimaru, N.; Samata, K.; Tsuhako, M. *J. Chromatogr.* **1993**, 653, 329-335.

103. Menchen, S.; Johnson, B.; Winnik, M. A.; Xu, B. *Electrophoresis* **1996**, 17, 1451-1459.

104. Fung, E. N.; Yeung, E. S. *Anal. Chem.* **1995**, 67, 1913-1919.

105. Gao, Q.; Yueng, E. S. *Anal. Chem.* **1998**, 70, 1382-1388.

106. Heiger, D. N.; Cohen, A. S.; Karger, B. L. *J. Chormatogr.* **1990**, 516, 33-48.

107. Chiari, M.; Nesi, M.; Fazio, M.; Righetti, R. G. *Electrophoresis* **1992**, 13, 690-697.

108. Paulus, A.; Hüsken, D. *Electrophoresis* **1993**, 14, 27-35.

109. Pariat, Y. F.; Berka, J.; Heiger, D. N.; Schmitt, T.; Vilenchik, M.; Cohen, A. S.; Foret, F.; Karger, B. L. *J. Chromatogr.* **1993**, 652, 57-66.

110. Righetti, P. G.; Gelfi, C. in: Righetti, P. G. (Ed.), *Capillary Electrophoresis in Analytical Biotechnology*, CRC Press, **1996**, pp431-476.

111. Barron, A. E.; Blanch, H. W.; Soane, D. S. *Electrophoresis* **1994**, 15, 597-615.

112. Barron, A. E.; Sunada, W. M.; Blanch, H. W. *Electrophoresis* **1996**, 17(4), 744-757.

CHAPTER 2. HIGH THROUGHPUT SINGLE-MOLECULE DNA SCREENING BASED ON ELECTROPHORESIS

A paper published in Analytical Chemistry*

Michael R. Shortreed, Hanlin Li, Wei-Hua Huang and Edward S. Yeung

ABSTRACT

In electrophoresis, the migration velocity is used for sizing DNA and proteins or for distinguishing molecules based on charge and hydrodynamic radius. Many protein and DNA assays relevant to disease diagnosis are based on such separations. However, standard protocols are not only slow (minutes to hours) but also insensitive (many molecules in a detectable band). We successfully demonstrated a high-throughput imaging approach that allows determination of the individual electrophoretic mobilities of many molecules at a time. Each measurement only requires a few ms to complete. This opens up the possibility of screening single copies of DNA or proteins within single biological cells for disease markers without performing polymerase chain reaction or other biological amplification. The purpose is not to separate the DNA molecules, but to identify each one based on the measured electrophoretic mobility. We developed three different procedures to measure the individual

---

* Reprinted with permission from Analytical Chemistry 2000, 72, 2879-2885.

molecular mobilities. The results correlate well with capillary electrophoresis (CE) experiments for the same samples (2 kb to 49 kb dsDNA) under identical separation conditions. The implication is that any electrophoresis protocols from slab gels to CE should be adaptable to single-molecule screening for disease diagnosis.

INTRODUCTION

Genetic analysis is arguably at the vanguard of several modern scientific arenas including the etiology and diagnosis of disease. The advent of the polymerase chain reaction (PCR) technique mitigated problems with limited sample amounts by enabling amplification of genetic materials to detectable levels and significantly decreasing the time from disease onset to diagnosis. Complications arising directly from PCR, however, are well known.[1] In principle, any DNA sample can be amplified provided that suitable conditions can be established. While so-called PCR kits establish good starting points, the user is still required to provide high-quality DNA template material and unambiguous primer pairs. Any contamination (introduction of extraneous DNAs) may cause a misidentification or misdiagnosis. Developing PCR protocols is a formidable task even for well-known and understood DNA samples. Heterogeneous DNA samples (e.g. DNA with partial mutations or deletions) complicate the issue further. For instance, DNA with a significant deletion or mutation may not be amplified because the complementary primer sequence is either missing or compromised. For known deletions or mutations, alternative primer pairs can be created. But, everything fails for unknown samples. Screening of samples at the single-molecule level may expose heretofore unidentified DNAs. Single-molecule DNA screening as a complement to PCR may unleash significant analytical and medical progress.

How will single-molecule assays contribute to medical progress? Briefly, there are three major reasons. First, sensitivity beyond what is presently available is needed to establish molecular profiles for species that are now inaccessible because they are present at low concentrations in tissues or at small quantities in a single cell.[2, 3] Single-molecule assays will be the ultimate solution. Finding and quantifying such species will allow us to pose "new testable hypotheses" and to recognize minor molecular alterations. This will open the door for studies in the very early stages of disease or cancer. In the specific example of HIV detection, the most sensitive PCR tests (e.g. for HIV RNA) require 20-50 copies per mL.[4, 5] The need for detecting 1 copy per mL versus the current level of 20 copies per mL is now documented by recent case studies.[6] Second, profiling individual cells and probing single DNA molecules can reveal and quantify the diversity of a population which may tell what fraction of cells need to be infected (mutated) before disease (cancer) becomes unchecked.[7] Similarly, the effects of low numbers of mutations can be assessed. With sensitive detection, it is likely that biochemical changes can be recognized well before physical changes occur in the progress of a disease. This improves diagnosis and prognosis, selection of more effective therapies for individual patients and more accurate monitoring of response to therapies. Third, single-molecule assay is better for quantitative information compared to present enzyme-linked assays or PCR assays. Amplification associated with either of these standard methods is subject to many interferences and complications such as temperature fluctuations, matrix variations, enzyme integrity and the significant variability of clinical samples. Amplification also takes time.

With the increased viability of single-molecule chemical analysis and disease

diagnosis, other issues arise. A credible single-molecule method must yield different, more useful or more bountiful information than its ensemble counterpart. Throughput is presently sacrificed for the sake of more detailed information. One reason is that single-molecule methods based on fluorescence are background limited. A sufficient signal-to-noise ratio (S/N) is achieved by reducing the solvent volume and concomitantly the Raman scatter from solvent molecules. With such a configuration, single-channel detectors (photomultiplier tubes or avalanche photodiodes) are often employed. Optical pinholes placed in strategic locations eliminate out-of-focus emission and further improve S/N. Extremely low concentrations are needed to prevent two molecules from being present in the detection volume simultaneously. While such tactics enable the undeniable detection of individual fluorescent molecules, in concert they squelch throughput.[8-12]

Naturally, single-molecule detection requires more than just getting a sufficient signal. High specificity is also needed to pinpoint a target. Independent means such as hybridization, immunological binding, and electrophoretic mobility provide such selectivity. At the single-molecule level, electrophoretic mobility has been reported in a micrometer-sized flow stream by correlating the photon bursts created at two laser beams that are axially separated [13] or by autocorrelation of photon bursts within a single laser beam.[14] There, only one DNA molecule at a time can be probed and the measurement time is limited by the distance of separation between the two laser beams. The relative intensities of dsDNA stained with intercalating dyes have been used to size DNA.[15-17] The precision depends on the fragment size, with a relative standard deviation of 50% for 7 kb and 11% for 50 kb DNA.[18]

Our method, which addresses the issue of high-throughput in single-molecule analysis, employs commonly available high-speed ICCD cameras, standard laser sources and scientific-grade microscopes.[19, 20] Many distinct molecules can be simultaneously illuminated and imaged with the camera and their time-dependent motion in free solution recorded for subsequent analysis. In this way, we can distinguish DNA fragments at the single-molecule level with high throughput based their electrophoretic mobilities.

EXPERIMENTAL SECTION

Capillary Column Pre-Treatment and Running Buffers.

An aqueous solution of 50 mM Gly-Gly buffer (Sigma Chemical Co., St. Louis, MO) was prepared and adjusted to pH 8.2 with several drops of 1.0 N NaOH (Sigma). This buffer was used to prepare all samples and solutions. The running buffer solution was 0.3% (wt./vol.) 600,000 M_r poly(ethylene oxide) (PEO). Before addition and dissolution of the PEO polymer, the buffer was filtered through a 0.2-μm filter. The dissolution was brought about using a magnetic stir-bar and plate. An extremely slow stirring rate was used to prevent destruction of the polymer. The running buffer was further treated by application of ultraviolet light from a hand-held mercury lamp for approximately 12 h, which reduced fluorescence from any impurities in the sample via photobleaching. Glass capillaries (140 μm o.d., 30.5 μm i.d., and 12 μm coating) were obtained from Polymicro Technologies, Inc. (Phoenix, AZ). For both imaging and bulk electrophoresis, the capillary columns were pre-treated for 10-30 min with 0.2-0.3% (wt./vol.) poly(vinylpyrrolidone) (PVP) 1,000,000 M_r in the Gly-Gly buffer previously described.

DNA Samples.

All DNA samples were prepared in the photobleached Gly-Gly buffer described above. DNA samples were labeled with YOYO-1 intercalator dye (Molecular Probes, Eugene, OR) at a ratio of 1 dye molecule per 5 bp. In general, DNA samples were in the concentration range of 50-200 pM. For the single-molecule electrophoresis experiments, these DNA samples were further diluted to 0.1-0.7 pM just prior to the start of the experiment. The appropriate volume of YOYO-1 dye was dissolved in the Gly-Gly buffer before addition of the DNA to prevent precipitation and to promote uniform labeling. Dye/DNA samples were allowed to incubate for about 2 h before further dilution and use. Lambda DNA (48,502 bp) was obtained from Molecular Probes (Eugene, OR). The other DNA sample (2,000 bp) was made in our laboratory using a standard PCR protocol. The PCR cocktail contained the following components: 10 µl (+)universal primer 20M13 (Amersham); 1 µl (–)primer 5' GCT CAC CCA GAA ACG CTG G 3' (Ames Laboratory DNA facility); 1 µl pGEM template –3zf(+) (Life Technologies); 4 µl dNTP (Amersham); 28 µl water; 5 µl 10× buffer (Amersham); and 1 µl Taq Polymerase 5U/µl (cloned) (Amersham). The cycle sequencing protocol was as follows: 1 cycle of 95 °C, 30 s (denature); 35 cycles of 95 °C, 30 s (denature), 60 °C, 20 s (anneal), and 72 °C, 180 s (extension); 1 cycle of 72 °C, 30 s (completion); and, 1 cycle of 4 °C, indefinite time (storage). The 2000 bp product was verified by slab-gel electrophoresis in comparison with lambda DNA/Hind III digest on 1.2% (wt./wt.) agarose visualized using ethidium bromide. The product was then isolated using a 1% agarose slab gel. The band was removed from the gel using a spin-column at 5000 g for 8 min followed with two aqueous washes. DNA

concentration was measured using standard UV absorbance methods.

Bulk Capillary Electrophoresis.

Capillary electrophoresis with laser-induced fluorescence (LIF) detection was used to determine the electrophoretic mobility of the DNA samples described above. Briefly, a high-voltage power supply (Glassman High Voltage Inc., Whitehouse Station, NJ, EH series 0-30 kV) was used to drive electrophoresis. The capillary had a 50 cm total length with 30 cm from the injection end to the detector. The excitation source was an argon-ion laser (488 nm, Uniphase, San Jose, CA, model 2213-75SLYW). The fluorescent signal from the photomultiplier tube (PMT) was directly converted to voltage by a 10-kΩ resistor then passed to an A/D converter. The voltage was sampled at 4 Hz and stored on a computer. A 500-550 nm band-pass filter (Oriel Instruments, Stamford, CT) was used to eliminate scattered laser light from entering the detector. After pre-treating the capillary with PVP (see above) the column was rinsed with the running buffer. A potential of 10 kV was applied to the capillary for a period of 10 min so that the capillary could reach equilibrium. The sample was injected with electrokinetic injection for 3 s at 200 V/cm. The running voltage for the separation was set at 80 V/cm. Between runs, the capillary was rinsed with the PVP solution and the running buffer respectively.

Single-Molecule Electrophoresis Capillary Holder and Sample Stage.

A 16-cm long capillary was used for all experiments with a 1-cm window cleared at 5.5-6.5 cm. The window was created by thermally vaporizing the polymer cladding in an electronically heated metal coil. The window was then washed repeatedly with methanol-

soaked lens cleaning paper before use. Larger o.d. capillaries (1 cm long) were glued to the sections of sample capillary adjacent to the window. These larger sections of capillary were inserted into an aluminum block and held in place with plastic setscrews. This configuration, as shown in Figure 1, provided a sturdy platform, which allowed sample changes without the need for re-alignment. One end of the capillary was glued into a 25 G syringe needle to facilitate filling the narrow o.d. capillary. The capillary was filled with the appropriate solution and the ends were inserted into plastic centrifuge tubes as reservoirs. Chromel wire was used as electrode material. The electrodes were connected to an in-house built −1250 V dc power supply.

Microscope and ICCD Camera.

A Pentamax 512-EFT/1EIA intensified CCD (ICCD, Princeton Instruments) camera was mounted on top of a Zeiss Axioskop upright microscope. The digitization rate of the camera was 5 MHz (12 bits) with software controller gain set at 3 and hardware intensifier gain set at 10. The camera was operated in the external synchronous mode with the intensifier-disabled open. The camera was also used in the frame-transfer mode. The excitation source was a Coherent Innova-90 argon ion laser operated at 488 nm. Extraneous light from the laser was eliminated with the aid of an equilateral prism and an optical pinhole. The laser beam was focussed at normal incidence to the capillary with a 1.5-inch focal-length lens. The microscope objective used was a Zeiss 10× Fluar (0.5 n.a.). Two 488-nm holographic notch filters (Kaiser Optical, HNFP) with optical density of > 6 and one wide-band interference filter were used between the objective and the ICCD. The notch filters were used to eliminate laser scattered from the capillary walls and the interference

filter was used to eliminate Raman scatter from water.

Single-Molecule Electrophoresis Timing.

The experimental timing was controlled with a Stanford Research Systems Model DG535 Four-Channel Digital Delay/Pulse Generator. The ICCD camera was triggered at time = 0 ms with a 5 ms duration TTL pulse. An Isomet Model 1205 acousto-optic modulator was used as a shutter. The first order dispersion was used as the source for the experiments and the digital delay generator used to control laser pulse duration and frequency with respect to the ICCD camera integration time. The optical arrangement is shown in Figure 2. The camera integration time (software controlled) was estimated to be delayed ~3 ms from the initial edge of the trigger pulse. The laser pulse onset, in all cases, began at time = +5 ms relative to the start of the trigger to the ICCD. Therefore, ~2 ms of dead time is present in each data frame.

Multi-frame method.

A running voltage of –78.1 V/cm was applied to the capillary. The ICCD camera exposure frequency was 20 Hz with an exposure time of 10 ms for each frame. The laser pulse time was 3 ms with an average power of 4 mW. Each frame consists of 106 (horizontal) × 91 (vertical) square pixels. Each pixel represents 1.25 × 1.25 μm of real space. The electrophoretic mobility of each molecule is determined by first calculating the distance it moves (cm) per unit time (s) and then dividing that by the applied voltage.

Streak method.

A running voltage of −78.1 V/cm was applied to the capillary. The ICCD camera exposure frequency for this sequence was 4 Hz with a 210 ms exposure time. Each frame consists of 106 (horizontal) × 91 (vertical) square pixels. Each pixel represents 1.25 × 1.25 μm. The electrophoretic mobility of each molecule is determined by first calculating the distance it moves (cm) per unit time (s) and then dividing by the applied voltage. The mobilities for these molecules are determined from the number of pixels in the streak.

Multi-spot method.

A running voltage of −78.1 V/cm was applied to the capillary. The ICCD camera exposure frequency for this sequence was ~2 Hz with an exposure time of 420 ms for each frame. The laser pulse frequency was 20 Hz with 3 ms long pulse duration. Each frame consists of 106 (horizontal) × 91 (vertical) square pixels. Each pixel represents 1.25 × 1.25 μm of real space. The electrophoretic mobility of each molecule is determined by first calculating the distance it moves (cm) per unit time (s) and then dividing by the applied voltage.

RESULTS AND DISCUSSION

Background Emission from Buffers.

It is well known that background emission reduction is fundamentally important for single-molecule imaging applications. In our experience with single-molecule imaging it was found that photobleaching buffers and solvents before use aided the background reduction.[21]

Several buffers with pKa in the range of 7.5-8.5 were investigated for use in this experiment. Solutions were prepared (50 mM) and injected into the capillary in the same manner and geometry used for the single-molecule electrophoresis experiments. The signals from photobleached and unbleached solutions were measured using typical experimental conditions and compared with the background from pure water. Among the solutions tested, four (Gly-Gly, bicine, tricine, and amp) had relatively low background. Gly-Gly buffer was found to have the lowest background emission in its unbleached form. The background from unbleached Gly-Gly was 7% higher than water. Upon photobleaching, the Gly-Gly buffer background was further reduced by one-half (3% above water). We attribute the residual emission to Raman scattering from the Gly-Gly molecules.

Selection of Intercalation Dyes.

An investigation of the commonly available fluorescent DNA intercalator dyes led to some important results. Four dyes (Picogreen, POPO-III, TOTO-1, and YOYO-1) were chosen which are excitable at 488 nm. Equimolar (200 pM) solutions of dye-labeled Lambda DNA (1 dye: 5 bp) were prepared and allowed to equilibrate for 2 h. At this high concentration, Picogreen-labeled DNA had the highest integrated intensity. This was followed by YOYO-1, TOTO-1, and POPO-III with 0.564, 0.089, and 0.002 relative emissions. When the average single-molecule emission intensities for dye-labeled Lambda DNA (50-500 fM) were compared it was found that the order was altered. YOYO-1 labeled DNA had the highest average single-molecule peak intensity. Therefore, dye affinity is critical when working with femtomolar solutions of DNA. The relative molar fluorescence intensity at high DNA:dye concentrations cannot be extended to lower concentrations

because of a shift in the chemical equilibrium, which favors dissociation. The dye we chose for this study is YOYO-1. This dye is extremely bright when bound to DNA, has practically no background in its unbound form, and has exceptional binding affinity. The high binding affinity is appropriate for working with the low concentrations (500 fM) of DNA typically encountered.

Bulk Capillary Electrophoresis.

The first step in achieving our goal was to develop bulk electrophoresis separation conditions, which were amenable to real-time single-molecule imaging. We investigated the relationship between sieving matrix concentration and separation efficiency. The three polymers tested (HEC, PEO, and PVP) are readily soluble in water and have exceptionally low viscosity in dilute concentration (0.3% wt./vol.). Low viscosity solutions are convenient for CE, because they are easy to prepare, filter and fill into the capillary. In addition, these polymer solutions are all below their entanglement threshold. HEC and PEO in specific molecular weight and concentration ranges were found to perform well in separating large DNAs with similar resolutions (Table 1). PVP is not as good. However, the PEO coating is not stable at pH 8.2 while HEC cannot be used as coating material. It was previously reported[22] that PVP is a good coating material for capillary walls and can substantially suppress EOF. With the pretreatment of PVP, the fused-silica capillary performed like a coated capillary with electrophoretic mobility dominating the movement of the analytes. Different concentrations of HEC polymers in TBE buffer were tested. As the polymer concentration approached the entanglement threshold, there was only a slight improvement in resolution but much higher fluorescent background. PEO polymers with different molecular

weights in buffer were tested as separation solutions. Large molecular weight PEO polymers (M_r = 1,000,000 and M_r = 8,000,000) and small PEO (M_r = 100,000) yielded poor resolution, while medium-sized PEO polymer (M_r = 600,000) yielded the highest resolution. A 50 mM solution of Gly-Gly (pH 8.2) with 0.3% PEO (M_r = 600,000) was found to provide the highest efficiency separation with the lowest fluorescence background. Finally, this matrix yields a typical separation resolution of 20-30% (absolute mobility) for the size range of 2000-48,502 bp with ~1-3% RSD.

The experimental configuration we developed for the single-molecule electrophoresis imaging is simply a miniaturized albeit more sophisticated version of a typical capillary electrophoresis set-up. Dye-labeled DNA is driven through the capillary under the influence of an applied dc electric field (–80 V/cm). For controlling the laser pulse duration, we chose to use an acousto-optic modulator. The rising and falling edges of the laser pulse intensity were sharp. Well-defined pulse shapes and periods could be produced in the range of 3-400 ms with little effort.

We developed three procedures to measure the individual molecular mobility. A detailed example of each method follows. The *multi-frame method* assembles information from a series of consecutive images (Figure 3). Each frame is a snapshot (3 ms) of all molecules within the field of view (30 micrometers wide and 100 micrometers long). A high frame rate (15-20 Hz) is used to track the molecular motion. We use this "movie" to follow the motion of each molecule through several consecutive frames. The total migration time and excursion distance of each molecule combined with the field strength yields the single-molecule mobility. With this method, we can track and characterize many molecules simultaneously. The sequence of nine consecutive images (Figure 3) is of five separate

Lambda DNA molecules (48,502 b.p. each) labeled with YOYO-1. A similar experiment was performed on the 2 kb DNA. The mobility was recorded for 50 molecules from each dataset. The calculated mobility for the lambda DNA molecules is 1.46E-04 $cm^2/V/s$. The calculated mobility for the 2 kb DNA molecules is 2.09E-04 $cm^2/V/s$. The relative standard deviations for these experiments are 1.0 and 3.1% respectively, which is better than intensity-based measurements.[18] The results agree well with those determined from standard capillary electrophoresis (Table I and Figure 4). It is therefore possible to distinguish 2 kb DNA from 50 kb DNA based on electrophoresis at the single molecule level with almost no ambiguity.

One requirement for using the multiframe method is that one must be able to correlate spots in consecutive frames as belonging to specific molecules. Since the measurements involve more than one image, the ability to store a large amount of raw data is also critical. Also, the laser pulse should be kept short compared to molecular diffusion times[19] to create a well-defined spot in the image.

Although the experimental conditions were chosen to display only a few molecules per image for the sake of clarity, a substantially higher density of spots can be accommodated to increase the data throughput. In Figure 3, as many as 5 × 10 molecules can fit into the subframe. If the full 512 × 512 CCD frame is used to image a larger area, 1250 molecules can be screened in 50 ms. Another factor of 10-50 increase in throughput is expected if higher electric fields, faster frame rates and higher laser powers are employed. The construction of a wider but thinner flow channel and synchronization of the applied voltage with the frame rate will guarantee that 100% of the molecules are characterized.

The second procedure (*streak method*) uses both long exposure time (low frame rate)

and long laser burst time (Figure 5). Since the molecules are moving relative to the camera during exposure, the trajectories show up as streaks in the image. From the physical length of the streak, the exposure time and the field strength, we can determine the mobility from just one of the frames. Faster molecules leave a longer streak and slower molecules leave a shorter streak so that data analysis is straightforward. The streak length is then used as a determinate in assigning the molecular identity. Correlation in between frames is not needed here. However, a requirement is that the entire streak must be within the field of view and the molecule does not go out of focus or otherwise become photobleached during each exposure. The S/N ratio is also lower than in the multi-frame method and photobleaching is more likely because longer total exposure times are used. Actual determination of mobilities using this method yield large variances, implying that in our case photobleaching is important.

The third procedure (*multi-spot method*) differs in that a relatively long exposure time is used in conjunction with short bursts of laser light (Figure 6). Typically, 275 ms ICCD camera exposure time is used with 3 ms laser shots at 15-20 Hz. The resulting image consists of linear groupings of spots within one image from each molecule. Assigning groups of spots to individual molecules is also trivial, as seen in several closely packed series of spots in Fig. 6. The mobility is measured by determining the distance between the first and the last visible spot and combining this with the number of spots, the burst rate of the laser, and the applied field strength. This method is advantageous because mobilities can be measured from each frame even if only a few spots per molecule are recorded due to photobleaching, focusing, or the physical location of the molecule. In addition, molecules can be viewed side by side and a qualitative determination of mobility used to identify the component molecule. In a mixed sample of two DNA molecules (one fast and one slow), the identity can be determined

immediately. One disadvantage of this method is that the S/N is worse than the multi-frame method due to the longer total irradiation time. However, S/N is better than the streak method because the sample is not continuously irradiated during a given exposure. An important feature in Figure 6 is that the intensities among the groups of spots show large variations. Even for a given molecule, the intensity varies considerably along its length. This confirms the need for uniform excitation and constant transit times for intensity-based DNA sizing[15-18] and the lack of such interference in electrophoresis-based measurements.

CONCLUSIONS

We demonstrated an imaging method that allows screening many single molecules at a time based on their electrophoretic mobilities. Unlike intensity-based methods, photobleaching and variations in excitation intensity do not interfere with the measurements. Since the measurement only depends on being able to follow a molecule for a few ms in solution, in principle very short DNA, e.g. 30 bp,[19] can be monitored even when it is labeled with only one fluorophor. We expect that by enlarging the imaged area, expanding the laser beam and increasing the laser intensity, tens of thousands of molecules can be screened every second. This high degree of throughput will naturally require the development of automatic image analysis software prior to implementation.

ACKNOWLEDGMENT

The Ames Laboratory is operated for the U.S. Department of Energy by Iowa State University under Contract No. W-7405-Eng-82. This work was supported by the Director of Science, Office of Basic Energy Sciences, Division of Chemical Sciences and by the

National Institutes of Health.

REFERENCES

1. Kimpton, C. P.; Oldroyd, N. J.; Watson, S. K.; Frazier, R. R. E.; Johnson, P. E.; Millican, E. S.; Urquhart, A.; Squrkes, B. L.; Grill, P. *Electrophoresis* **1996**, *17*, 1283-1293.
2. Yeung, E. S. *Acc. Chem. Res.* **1994**, *27*, 409-414.
3. Yeung, E. S. *J. Chromatogr. A* **1999**, *830*, 243-262.
4. Richman, D. D. *Science* **1996**, *272*, 1886-1888.
5. Cohen, J. *Science* **1997**, *276*, 1488-1491.
6. Cohen, J. *Science* **1997**, *277*, 32-33.
7. Mellors, J. W.; Rinaldo, J., Charles R.; Gupta, P.; White, R. M.; Todd, J. A.; Kingsley, L. A. *Science* **1996**, *272*, 1167-1170.
8. Briggs, J.; Elings, V. B.; Nicoli, D. F. *Science* **1981**, *212*, 1266-1267.
9. Kinjo, M.; Rigler, R. *Nucl. Acids Res.* **1995**, *23*, 1795-1799.
10. Schwille, P.; Oehlenschlager, F.; Walter, N. G. *Biochem.* **1996**, *35*, 10182-10193.
11. Oehlenschlager, F.; Schwille, P.; Eigen, M. *Proc. Natl. Acad. Sci. (USA)* **1996**, *93*, 12811-12816.
12. Walter, N. G.; Schwille, P.; Eigen, M. *Proc. Natl. Acad. Sci. (USA)* **1996**, *93*, 12805-12810.
13. Castro, A.; Shera, E. B. *Anal. Chem.* **1995**, *67*, 3181-3186.
14. Van Orden, A.; Keller, R. A. *Anal. Chem.* **1998**, *70*, 4463-4471.
15. Castro, A.; Fairfield, F. R.; Shera, E. B. *Anal. Chem.* **1993**, *65*, 849-852.

16. Petty, J. T.; Johnson, M. E.; Goodwin, P. M.; Martin, J. C.; Jett, J. H.; Keller, R. A. *Anal. Chem.* **1995**, *67*, 1755-1761.

17. Chou, H.-P.; Spence, C.; Scherer, A.; Quake, S. *Proc. Natl. Acad. Sci. (USA)* **1999**, *96*, 11-13.

18. Van Orden, A.; Keller, R. A.; Ambrose, W. P. *Anal. Chem.* **2000**, *72*, 37-41.

19. Xu, X.; Yeung, E. S. *Science* **1997**, *276*, 1106-1109.

20. Xu, X.-H.; Yeung, E. S. *Science* **1998**, *281*, 1650-1653.

21. Affleck, R. L.; Ambrose, W. P.; Demas, J. N.; Goodwin, P. N.; Schecker, J. A.; Wu, M.; Keller, R. A. *Anal. Chem.* **1996**, *68*, 2270-2276.

22. Gao, Q.; Yeung, E. S. *Anal. Chem.* **1998**, *70*, 1382-1388.

Table I. Observed Mobilities ($Cm^2/V \cdot S$) of DNA Fragments in Capillary Electrophoresis at an Electric Field Strength of 200 V/Cm.

Separation buffer	2 kb DNA (μ_1)	λ DNA mobility (μ_2)	Mobility difference $(\mu_1-\mu_2)/\mu_2$
0.1×TBE, 0.3% PVP (M_r = 1,000,000)	3.43×10^{-4}	3.21×10^{-4}	6.8%
0.5×TBE, 0.3% HEC (M_r = 250,000)	1.63×10^{-4}	1.36×10^{-4}	20%
50mM Gly-gly, 0.3% PEO (M_r = 600,000)	2.00×10^{-4}	1.61×10^{-4}	24%

FIGURE CAPTIONS

Figure 1. Experimental arrangement for single-molecule electrophoresis.

Figure 2. Optical arrangement for single-molecule electrophoresis. Laser: Coherent Innova 90 argon ion; AO: Isomet Model 1205c acousto-optic modulator; PH1: pinhole selection of first order diffracted beam; PR: equilateral prism to remove plasma lines; M1-3: steering mirrors; PH2-3: laser alignment pinholes; L: f=1" plano-convex lens; C: capillary and holders; and MI: microscope.

Figure 3. (*Multi-frame method*) This sequence of nine consecutive images (left to right, top to bottom) is of three separate Lambda DNA molecules (48,502 b.p. each) labeled with YOYO-1. Voltage (–78.1 V/cm) was applied in the horizontal direction, which caused the DNA molecules to migrate in that direction. The ICCD camera exposure frequency for this sequence was 20 Hz hence this series represents 0.45 s of real time. The calculated mobility for these three molecules is 1.45E-04 $cm^2/V/s$. The relative standard deviation for such an experiment is typically in the range of 1-3%.

Figure 4. Comparison of bulk electropherogram (bottom) with histogram (top) of migration times predicted from single-molecule mobilities. Depicted are results for DNA assay (2 kb vs. 48.5 kb)

Figure 5. (*Streak method*) This collection of images each contains several separate Lambda DNA molecules (48,502 b.p. each) labeled with YOYO-1. Voltage (–78.1 V/cm) was applied in the horizontal direction, which caused the DNA molecules to migrate in that direction. The ICCD camera exposure frequency for this sequence was 4 Hz

Figure 6. (*Multi-spot method*) This collection of images is of Lambda DNA molecules (48,502 b.p. each) labeled with YOYO-1. Voltage (–78.1 V/cm) was applied in the horizontal direction, which caused the DNA molecules to migrate in that direction. The ICCD camera exposure frequency for this sequence was ~2 Hz. More importantly, the laser shot frequency was exactly 20 Hz with 3 ms long pulse duration. The linear sequence of spots results from consecutive laser shots impinging on the each of the many molecules at different points in space and time. The calculated mobility for this data set is 1.49E-04 $cm^2/V/s$. The relative standard deviation for such an experiment is typically in the range of 1-3%.

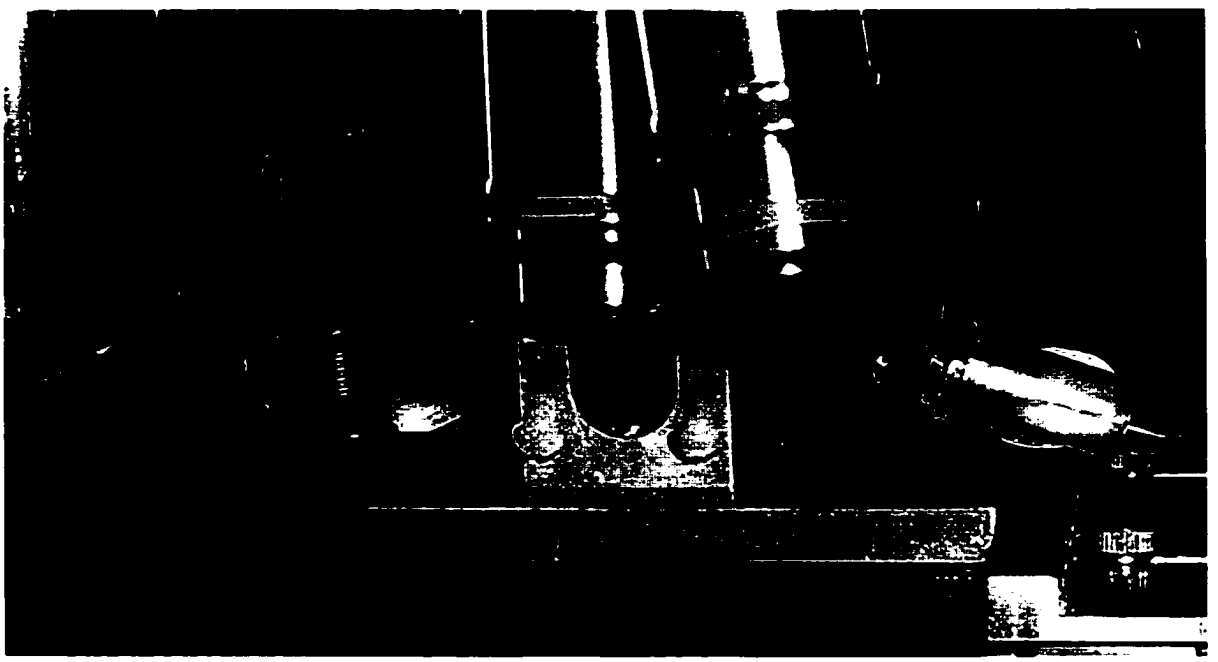

FIGURE 1

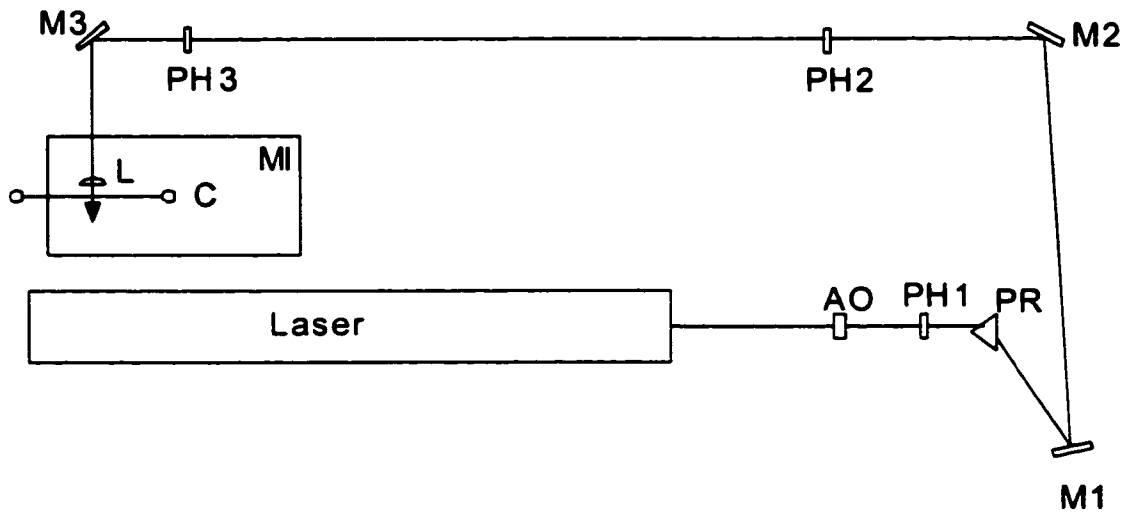

FIGURE 2

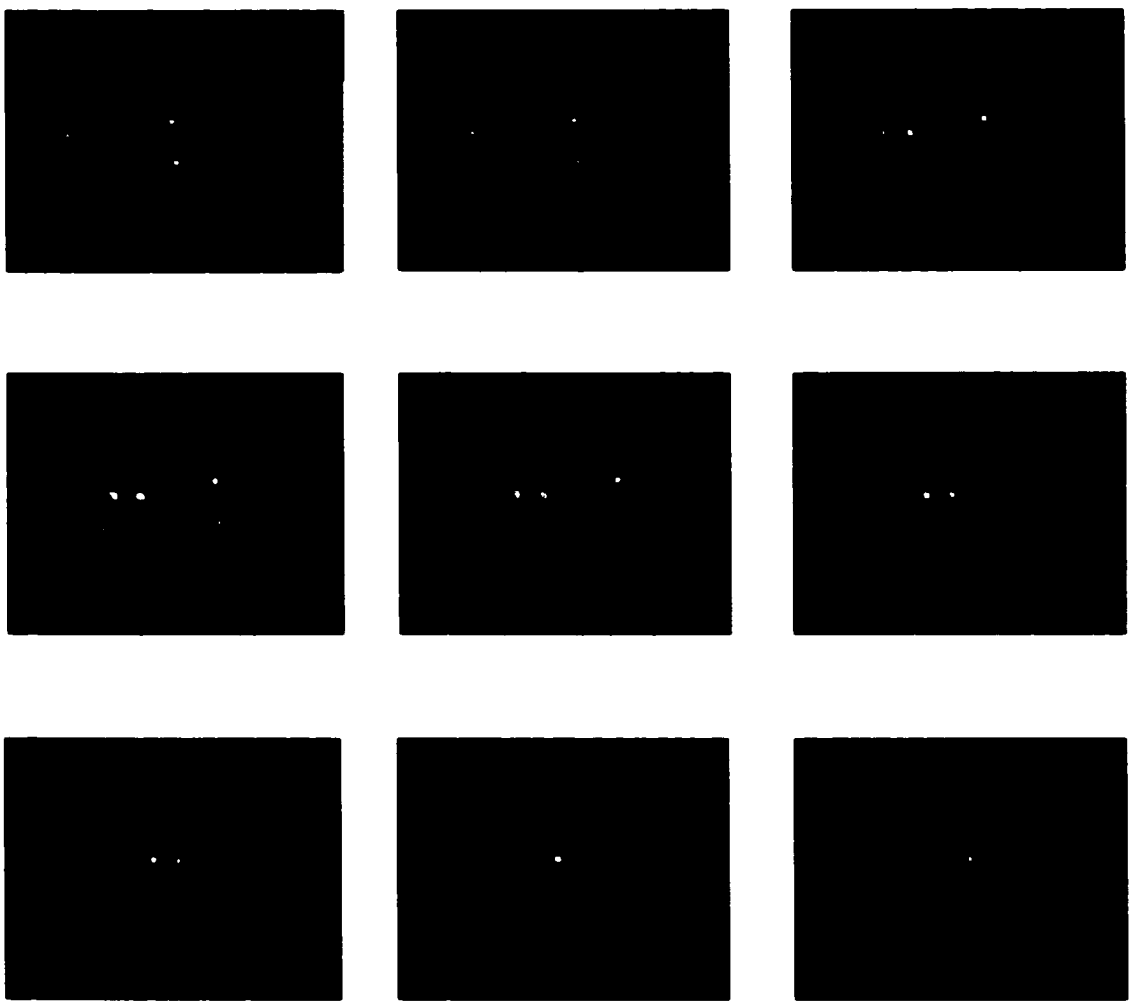

FIGURE 3

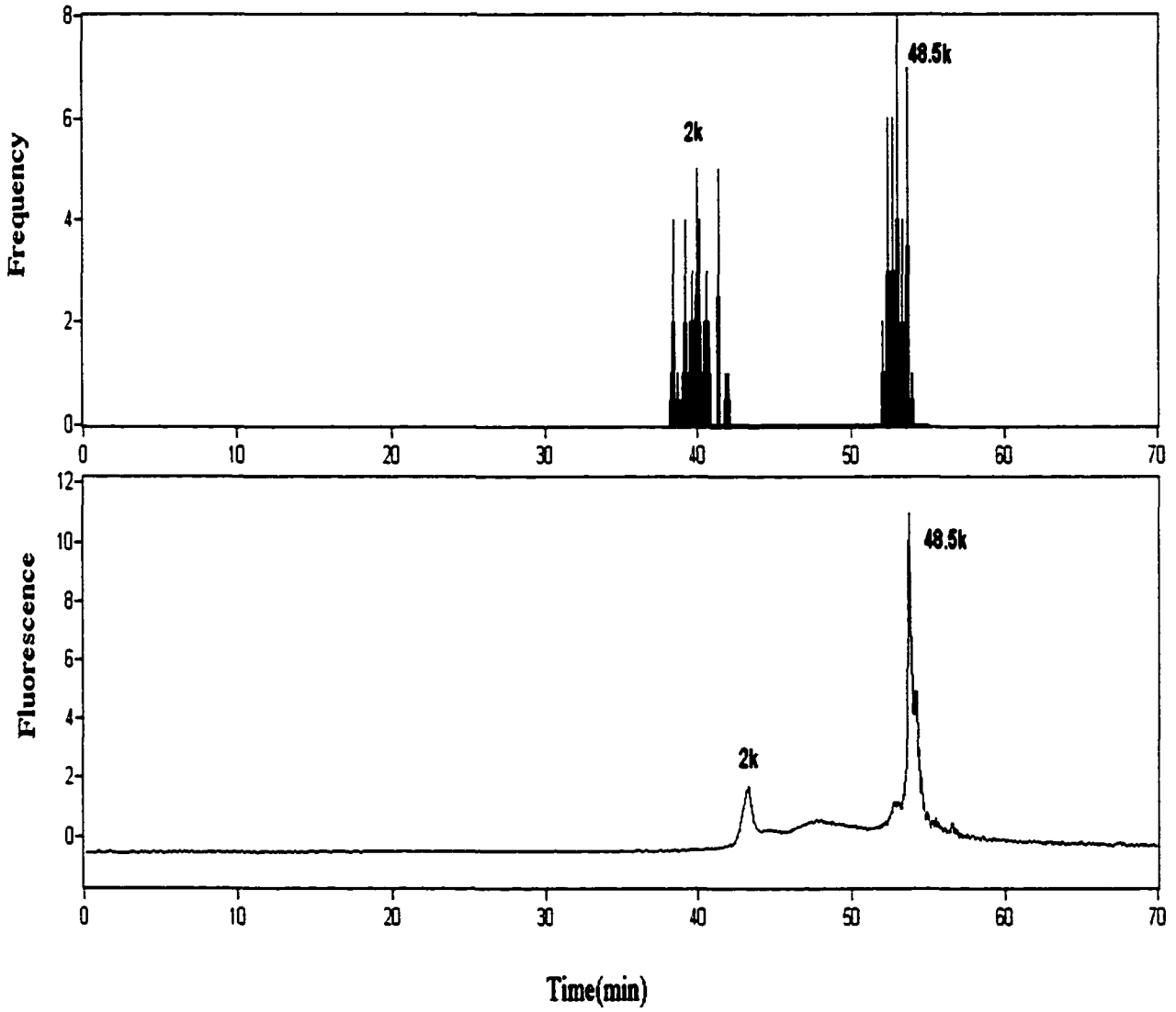
Frequency
8
6
4
2
0
2k
48.5k
0
10
20
30
40
50
60
70
Fluorescence
12
10
8
6
4
2
0
2k
48.5k
0
10
20
30
40
50
60
70
Time(min)

FIGURE 4

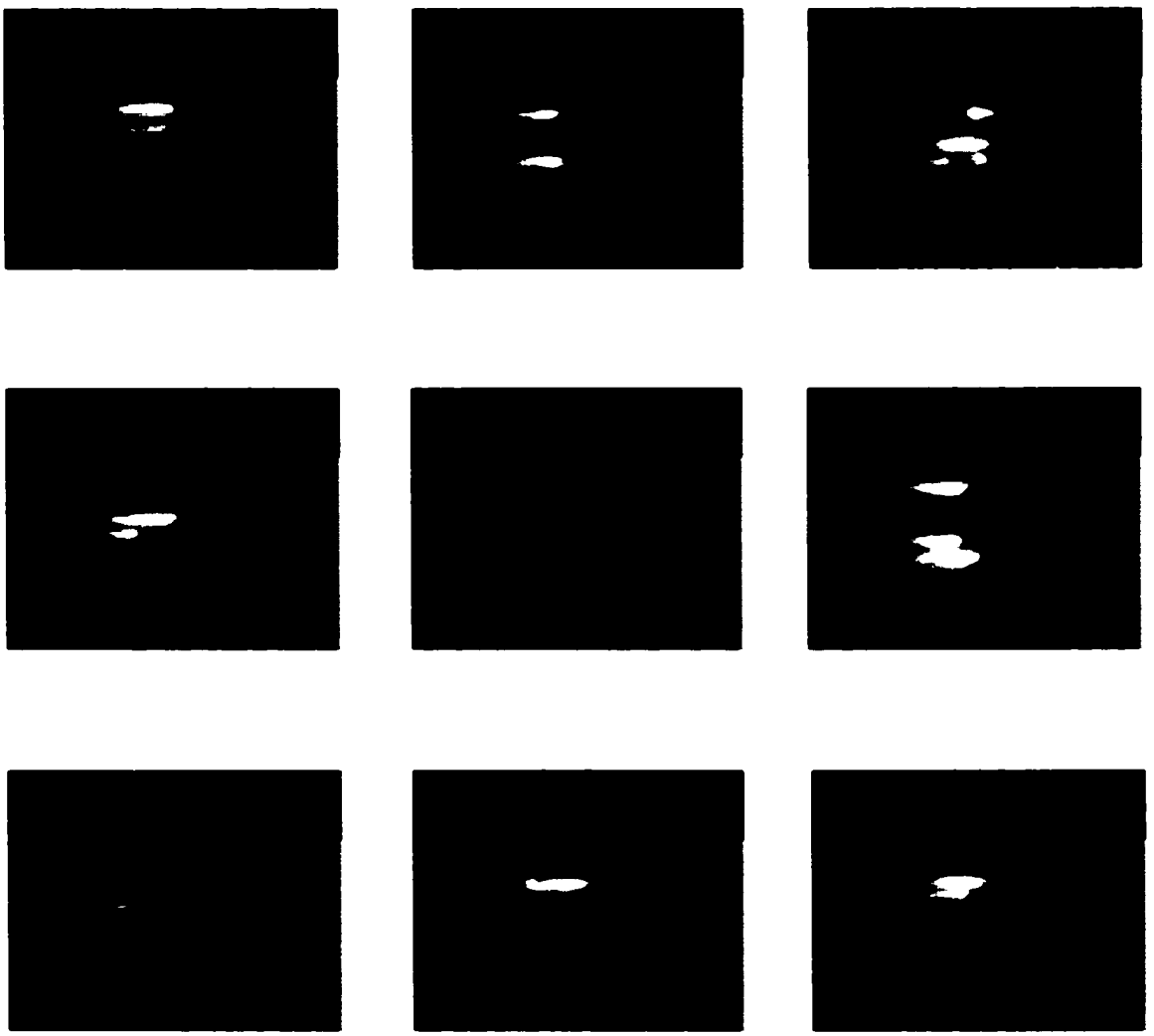

FIGURE 5

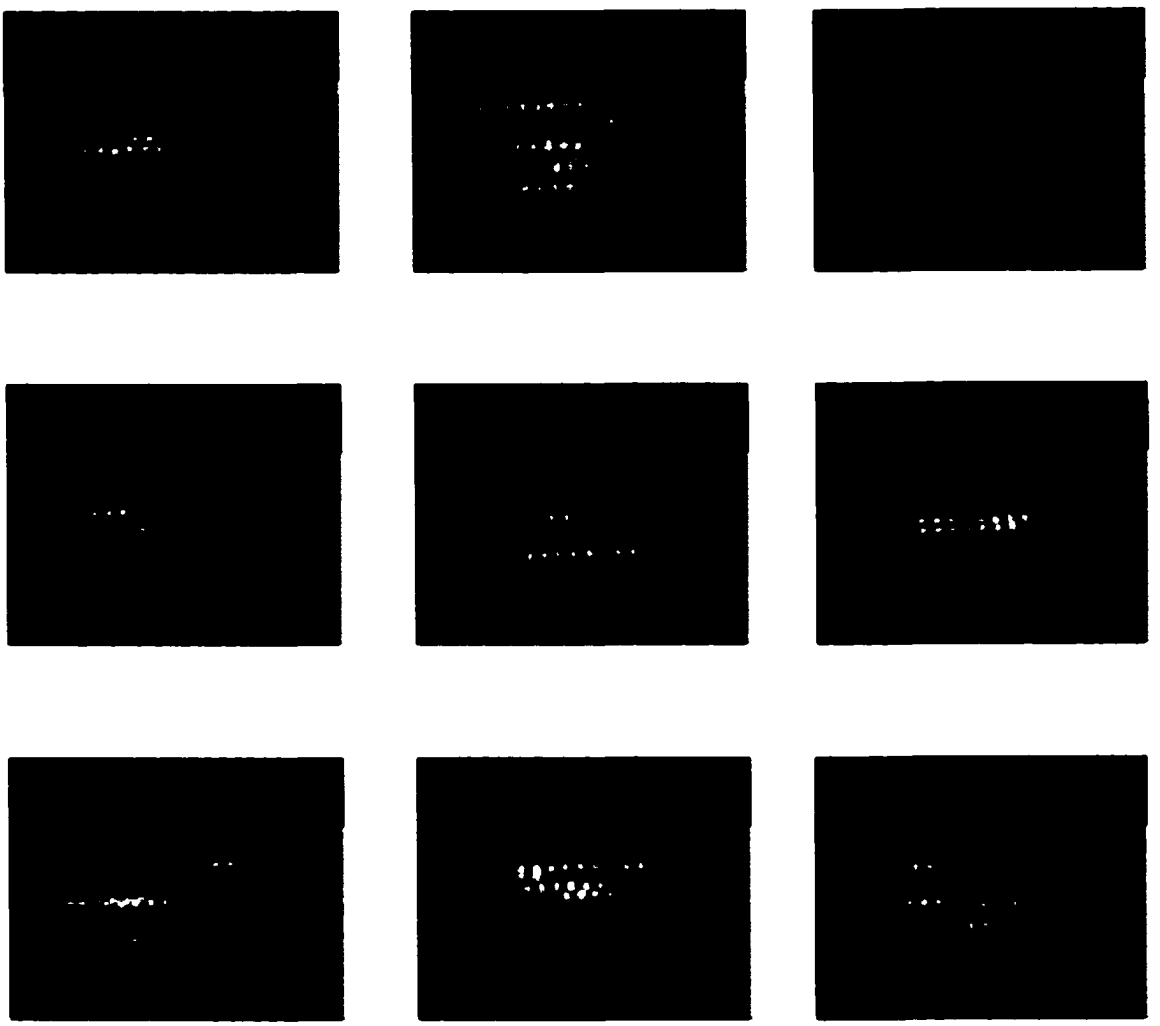

FIGURE 6

CHAPTER 3. SELECTIVE DETECTION OF INDIVIDUAL DNA MOLECULES BY CAPILLARY POLYMERASE CHAIN REACTION

A paper published in Analytical Chemistry*

Hanlin Li, Gang Xue and Edward S. Yeung

ABSTRACT

On-line capillary polymerase chain reaction (PCR) coupled with laser-induced fluorescence detection was successfully demonstrated for individual DNA molecules. A single 30-μm i.d. fused-silica capillary was used both as the reaction vessel and for isolating single molecules. SYBR Green I dye was added into the reaction mixture for dynamic fluorescent labeling. Because of the small i.d. of the capillary, PCR-amplified DNA fragments from single molecules were localized in the capillary, providing discrete product zones with concentrations at readily detectable levels. By counting the number of peaks in the capillary via electromigration past a detection window, the number of starting DNA molecules could be determined. With selective primer design, only the molecule of interest

---

* Reprinted with permission from Analytical Chemistry 2001, 73, 1537-1543.

was detected. Amplification of the 110-bp fragment from individual human β-globin gene and the 142-bp fragment from individual HIV-1 DNA was demonstrated. This opens the possibility of highly selective and sensitive disease diagnosis at a very early stage.

INTRODUCTION

The emphasis in health care will continue to evolve from management to prophylaxis. There is usually a better chance for therapy if the disease could be recognized at an early stage. For example, in the case of human immunodeficiency virus (HIV) infection, the standard blood test based on immunoassay requires a 6-month to 1-year incubation period after infection before a positive response can be obtained. By then, the virus may already have taken hold in the lymph nodes and would have time to mutate. At the early stages of other diseases, particularly cancer, only a few cells out of a large population are affected. These will not be detectable in a homogenized cell sample. A 5% change in the average contents in a given cell type is barely recognizable given the normal fluctuations in a healthy individual. But if the cell population is examined one at a time, then 5 "abnormal" out of 100 screened cells will show a change that is readily recognizable. In this way, we are looking for either a yes or a no answer for each cell examined. Such digital discrimination (yes/no) is much more reliable and sensitive than analog discrimination (100% vs. 95%) based on small changes in an averaged value. The more sensitive the technique, the fewer the number of infected cells will be needed for diagnosis. Also, there is a need for monitoring the progress of the therapy. It is therefore important to develop ultra-sensitive detection techniques, down to the level of a single cell and a single copy of DNA.

Recent advances in single-molecule detection and characterization[1-9] may lead to

new approaches for early disease diagnosis. Recognition of single DNA molecules based on their different electrophoretic mobilities[10] or spectral characteristics[11] was achieved using single-molecule imaging. The advantages of single-molecule screening are high speed and high throughput, since thousands of molecules could be screened within seconds. In the absence of sensitive imaging detectors, polymerase chain reaction (PCR) may provide an alternative solution for single-molecule detection.

PCR is a simple and powerful technique in molecular biology and is widely used for many applications.[12] The advent of PCR mitigated problems with limited sample amounts by enabling amplification of genetic materials to detectable levels. PCR already has a great impact on clinical diagnosis, such as HIV pathogen detection,[13-15] hepatitis B, hepatitis C infection,[16-18] and other genetic and viral diseases.[19-22] Many new patents were filed regarding various disease diagnoses and determinations based on PCR. In PCR, high specificity could be easily achieved by specific primer design. Only the fragment of interest will be amplified. It is relatively straightforward for only the mutant or exogenous DNA to be amplified and detected in a large excess of normal DNAs.

For post-PCR analysis, capillary electrophoresis (CE) with laser-induced fluorescence (LIF) is superior to traditional slab gel electrophoresis because of its high speed, high throughput and low cost. Many groups have demonstrated on-line coupling of PCR reaction and CE, which makes automation possible and greatly reduces the turnover time of the whole process. Our group successfully demonstrated fully automated genotyping from blood and DNA sequencing by on-line PCR and cycle sequencing.[23-26] Microfabricated devices have also been used to integrate PCR with electrophoresis.[27-29] More recently, on-column real-

time monitoring of PCR reaction was achieved using LightCycler.[30-33]

Generally, for PCR amplification of DNA from a single or low-copy template, it requires two sequential amplification reactions with nested primer pairs to achieve the necessary sensitivity.[34] However, we reasoned that the sensitivity of LIF detection could be improved to enable detection of single starting molecules if reaction volumes were reduced. Therefore, single-copy amplification could be realized with one-step PCR and one primer pair. Recently, Vogelstein and Kinzler made use of molecular beacon (MB) probes to detect PCR products derived from a two-step amplification of single DNA molecules.[35] Based on the intensity ratios of the fluorescence from two different probes, mutant DNA could be recognized. However, for different mutations, different MB probes would have to be designed and the PCR conditions would have to be re-optimized individually. That the MB probes had to be added after the PCR amplification was complete also made the approach less convenient.

In this article, we present a new scheme of on-line coupling of PCR reaction in capillary tubes. Individual DNA molecules of human β-globin gene and HIV-1 virus DNA are amplified and fluorescently labeled inside a 30-μm i.d. capillary by online PCR. Because of the negligible diffusion of the DNA molecules in such small i.d. capillaries, the PCR-amplified DNA fragments are highly localized near each template molecule. Individual starting template DNAs are thus identified as discrete DNA clusters along the capillary. Reliable and high sensitivity detection of single molecules can therefore be performed. Since PCR and fluorescence labeling are integrated in one step, this scheme is compatible with continuous flow PCR[28] and can readily be automated. A general intercalating dye served as

a universal fluorescent probe so that unmodified oligonucleotides can be used as primers. This concept is similar to that employed for detecting single enzyme molecules.[36-38] The difference is that PCR rather than enzymatic catalysis is responsible for generating the signal.

EXPERIMENTAL SECTION

Polymerase Chain Reaction

Human β-globin gene amplification. A 110-bp fragment of the β-globin gene was amplified with specific primers from human genomic DNA. Unless specified, all reagents were purchased from Roche Boehringer Mannheim Corp. (Indianapolis, IN). The 25-μL reaction mixture had the following final composition: standard 1× PCR buffer (50 mM KCl and 10 mM Tris/HCl), pH 8.3; 4.0 mM $MgCl_2$; 200 μM dNTP; 0.5 μM of each primer; 500 ng/μL bovine serum albumin (BSA, Idaho Technology, Salt Lake City, UT); 1:10000 dilution of intercalating dyes, 1.25 units of Taq polymerase, appropriate copies of human genomic DNA template (3×10^9 bp) and sterile water. Three dyes were tested: SYBR Green I at a stock concentration of 10 000×; PicoGreen at 10000×; and YOYO I at 1 mM. All dyes were purchased from Molecular Probes (Eugene, OR). The expected copies of templates were calculated based on one genomic equivalent of DNA per 3 pg.

For off-line experiments, 25 μL of reaction mixture was mixed in a 200 μL thin wall polypropylene PCR tube with 5 ng of human genomic DNA as template. The reaction was performed in a thermal cycler (Perkin-Elmer Model 9600) at the following temperatures: denaturation at 94 C for 90 s; 45 cycles of 94 C for 30 s, 55 C for 30 s, 72 C for 60 s; and 72 C for 10 min. On-line PCR was performed in a 360 μm o.d., 30 μm i.d. fused-silica

capillary (Polymicro Technologies, Phoenix, AZ) using Rapid Cycler (Idaho Technology). For each reaction, 10 μl of reaction mix was injected through a 75-100 cm long capillary by a glass syringe. 50 cm of the capillary was coiled inside the thermal-cycler chamber, which corresponds to an effective reaction volume of 0.35 μL. The temperature cycles were as follows: denaturation at 94°C for 90 s; 5 cycles of 94°C for 30 s, 55°C for 30 s, 72°C for 60 s; followed by 40 cycles of 94°C for 15 s, 55°C for 30 s, 70°C for 60 s; and 72°C for 10 min.

HIV-1 gag amplification. A 142 bp fragment from the *gag* region of HIV-1 DNA was amplified with primer pair SK145/SK431 (forward primer—SK145: 5'-AGTGGGGGGACATCAAGCAGCCATGCAAAT-3', reverse primer—SK431: 5'-TGCTATGTCAGTTCCCCTTGGTTCTCT-3', synthesized by DNA facility, Iowa State University, Ames, IA). In a 25-μL reaction mixture, it had the following final composition: 1× GeneAmp PCR buffer, pH 8.0, 25 ng HIV-1 negative control DNA (human placental DNA), appropriate copies of HIV-1 positive control DNA (stock solution at 10^3 copies/μL, Perkin Elmer, Foster City, CA), 2.5 mM $MgCl_2$, 200 μM dNTP, 0.5 μM of each primer, 500 ng/μL bovine serum albumin (BSA, Idaho Technology, Salt Lake City, UT), 1:10000 dilution of SYBR Green I, 1.25 units of Taq polymerase and sterile water. On-line capillary PCR of HIV-1 *gag* amplification was performed in the same setup as human β-globin gene amplification. The temperature cycles used were: denaturation at 94°C for 90 s; 5 cycles of 94°C for 30 s, 60°C for 60 s; followed by 40 cycles of 94°C for 15 s, 60°C for 60 s; and 72°C for 10 min.

Slab Gel Electrophoresis

The sizes of the PCR product for both human β-globin gene and HIV *gag* region were confirmed by gel electrophoresis using 4% high-resolution agarose E-Gels (Invitro Gen, Carlsbad, CA). 25-bp and 50-bp ladders (Life Technologies, Grand Island, NY) were loaded on the gel and co-migrated with the DNA sample. The total volume for each sample well was 20 μL. The image was taken under a UV lamp.

Capillary Electromigration

Setup. The setup for capillary PCR is the integration of an air thermal cycler and a single-capillary CE device. A 75-100 cm long capillary was coiled partially inside the thermal cycler where the amplification was performed. One end of the capillary was immersed in the buffer vial directly while the other end of the capillary with a ~1 cm detection window was fixed with a capillary holder and also immersed in the buffer vial. The 488-nm Ar^+ laser beam (Uniphase, San Jose, CA, model 2213-75SLYW) was focused by a convex lens with 12-mm focal length (Melles Griot, Irvine, CA) onto the capillary. Fluorescent signal was collected by a 10× microscope objective into the photomultiplier tube (PMT, R928, Hamamatsu Corp., Bridgewater, NJ). The PMT was terminated with a 10-kΩ resistor before connecting to an A/D converter. The signal was sampled at 2 Hz and stored in a computer. A 520-nm interference filter (Corion Optical Filters, Franklin, MA) was placed before the PMT to prevent scattered laser light from entering the detector. A high-voltage power supply (Glassman High Voltage Inc, Whitehorse Station, NJ, EH series 0-30kV) was used to drive electromigration.

The same capillary was used for both PCR reaction and electromigration in this

experiment. The capillary was pre-treated with 1% PVP (M_n = 1,000,000) in H_2O before use. Our experiments proved that PVP does not affect the PCR reactions but helps to reduce the electroosmotic flow during electromigration. +20 kV was applied to the detection end of the capillary after the reaction. DNAs moved towards the anode and passed through the detection window. When combined with ds-DNA, the fluorescence of SYBR Green I was greatly enhanced, which made it possible for the detection of the PCR product through LIF.

Buffer and reagents. The running buffer for electromigration had the following composition: 50 mM KCl, 10 mM Tris/HCl, 3.0 mM $MgCl_2$, pH 8.3; 500 ng/μL BSA; 1:10000 dilution of SYBR Green I dye; and 0.2% MW 1,000,000 PVP (Sigma, St. Louis, MO).

RESULTS AND DISCUSSION

Polymerase chain reaction has the advantage of exponential replication, which is capable of amplifying the limited amount of genetic materials by a factor of a million. However, this process is usually done in 200-μL thin wall polypropylene tubes in a metal-block thermal cycler. With the traditional 20-μL reaction mixture, the PCR product of a single copy of DNA would be diluted to 8.3×10^{-14} M. For a 100-bp DNA, the corresponding base pair concentration would be 8.3×10^{-12} M, which is below the current fluorescent labeling and detection level. But if PCR is carried out in a 30-μm i.d. capillary, the local concentration of DNA would be much higher than in traditional vials. Also starting with a single copy of DNA, even with lower amplification efficiency, e.g., 1×10^5 fold, the final concentration would be 5×10^{-12} M, or 100 times that of conventional PCR. The

volume here was calculated with the assumption that the DNA fragments will diffuse to a sample zone length of 5 cm. The corresponding base pair concentration would be around 5×10^{-10} M, which is a comfortable range for fluorescence detection.

Operational Protocol

The principles underlying capillary PCR of individual DNA molecules are outlined in Fig. 1. First, the DNA was diluted into the PCR cocktail containing the dynamic labeling intercalating dye SYBR Green I and filled into the fused-silica capillary that is partially coiled inside the thermal cycler. Unbounded dye fluoresces weakly, introducing a minimal background. Since the reaction mixture was homogeneous, the very few copies of DNA molecules would distribute randomly along the capillary (Fig. 1a). Second, PCR was performed and the target DNA was amplified exponentially. Unlike traditional PCR in 200 μL thin-wall polypropylene tubes, the very small inner diameter of the capillary prevents the amplified DNA from diffusing around substantially (Fig. 1b). Because of the small volume of the narrow sample zones (~15 nL), the localized PCR products yield fairly high local concentrations, which helps to improve the LOD by 2-3 orders of magnitude. The dissolved SYBR Green I would bind to the amplified double-stranded DNAs to increase the local fluorescence intensity. Finally, when driven out of the capillary, the individual sample zones would move at the same velocity (Fig. 1c). At the window, LIF was detected by the PMT and each sample zone would show up as one peak in the electropherogram. Therefore, by counting the number of peaks in the electropherogram, the number of starting molecules could be determined (Fig. 1d).

Peak Picking

For low-copy PCR, the primers that are in large excess tend to form nonspecific products, notably primer-dimers. Since the primer-dimers are also double-stranded oligonucleotides, they would be labeled by the intercalating dyes as well. In the capillary the primer-dimers would produce a background signal throughout the portion of the capillary that is inside the thermal cycler. Fluctuations in this background signal is the major source of interference in peak picking. However, this fluctuation is fairly flat comparing to the sharp (localized) peaks of specific products. By properly setting the edge slope and peak width, specific peaks could be discriminated against the background by using standard chromatographic software (Grams32, Galactic Industries).

There was always a giant peak in the front part of the electropherogram. Its peak height increased as the primer-dimer background increased. We believe this peak might be related to the primer-dimer formed at the interface between the reaction mixture inside the thermal cycler and that outside. Since this giant peak showed up in both control and normal experiments, it can be neglected in our data interpretation. In fact, we used its peak height as an estimation of the primer-dimer background to set the minimum peak height in the peak picking process.

Modifications of PCR Protocol

Some earlier research showed that the fused-silica surface was not as friendly to the PCR as polypropylene. Investigation of microfabricated chips even proved that native silicon completely inhibited PCR reactions.[39, 40] Previous studies in our group[23, 24] revealed that a high concentration of BSA in the PCR mixture could prevent surface inhibition. PVP

dynamic coating was also employed since it could help suppress electroosmotic flow (EOF) during electrophoresis.[41] A low concentration of PVP added into the reaction mixture does not affect the PCR reaction, which was confirmed by gel-electrophoresis. As shown in Fig. 2, the amplification yield of PCR with 0.2% PVP in the cocktail is about the same compared to the one without PVP. Here, to provide a good initial coating, 1% PVP was used to flush the capillary before each run.

Modifications were also made to the thermal-cycling protocol. The hot-air thermal-cycling protocol for 1.02 mm o.d. × 0.56 mm i.d. soft glass capillaries (Idaho Technology) did not work for the 30-μm i.d. fused-silica capillaries. Longer annealing and extension times were needed despite the large surface-to-mass ratio. The reason could be that in such a small i.d. capillary, the rate determination step for the reaction is the diffusion of the small molecules in the mixture. However, the total reaction time was comparable to that of PCR reaction in polypropylene vials.

Intercalating Dyes

The on-line PCR reaction with LIF detection requires the dynamic labeling dye to be present in the reaction mixture. Three different ds-DNA intercalating dyes were tested and compared: YOYO-1, PicoGreen, and SYBR Green I. They have some properties in common: (1) the dye-DNA complex fluoresces strongly at 488-nm excitation, whereas the excess dye does not and (2) they only label double-stranded DNAs, so the excess single-stranded primers and dNTPs would not fluoresce, producing a minimal background. The three dyes were added individually into the reaction mixture before PCR to test for compatibility. Off-line PCR products were loaded onto the commercial slab gel with ethidium bromide stain to

evaluate the reaction yield (Fig. 2). It was found that YOYO-1 completely inhibited the reaction. PicoGreen did not hurt the amplification, since a clear DNA band of the correct size was observed. But, PicoGreen cannot endure extreme temperature cycling, after which the ds-DNA labeling property was totally lost. This was proven by a regular CE run. When independently prepared PCR product was injected into the capillary, no fluorescent DNA peak was found at 488-nm excitation. Fortunately, the third dye, SYBR Green I, was found to be suitable. It could sit in the reaction mixture during thermal cycling and did not hurt the amplification. It could also stand the extreme temperatures and maintain the labeling ability (shown in Fig. 2). Therefore, SYBR Green I was chosen as the DNA stain for on-line PCR reaction.

Elution of Product Zones

Pressure was initially used as the driving force to push the PCR products out of the capillary after reaction. But, PCR products of about 10 copies of DNA molecules showed severe peak overlap in the 50-cm effective length of the capillary due to the band broadening (Fig. 3b). A simple experiment proved that this band broadening was not from the initial band width but was due to the parabolic profile of the hydrodynamic flow. 1-cm of fluorescently labeled DNA sample plug was injected into the capillary repeatedly for 5 times. These sample zones were separated by 10-cm buffer plugs in between. We found that the 1-cm initial sample plug was broadened to about 10 cm when driven out by pressure. Instead, if electrokinetic pumping was used as the driving force, much better peak shapes were observed. In this way, much higher peak capacity could be achieved (less overlap) with higher sensitivity detection (less dilution).

PCR of human β-globin gene

A 110-bp fragment of the β-globin gene was amplified with specific primers from human genomic DNA. On electromigration after PCR, 4 distinct amplified DNA peaks (Fig. 4b) can be seen. Fig. 4a was the control experiment without DNA template in the reaction mixture. In Fig. 4b, not all amplified peaks have the same heights or areas. This is attributed to the known variability of exponential PCR amplification.

In our 8 control experiments (0 copy), the ratios between the primer-dimer background and the giant peak height varied between 0.03-0.06 with a standard deviation of 0.009. Thus, we set 0.08 as the minimum relative peak height for peak picking. The later eluting peaks get broader since the bands migrate over a longer distance. Also, the FWHM of all peaks were less than 1.5 min. These peak widths are consistent with the minimal axial diffusion in small i.d. capillaries, and provide an additional criterion for peak picking.

To show that the peaks in the electropherogram were actually from individual DNA template molecules and not artifacts, we varied the starting number of copies of template molecules. When we increased the number of molecules in the reaction mixture, the number of corresponding peaks in the electropherogram also increased (Fig. 5). However, the number of peaks observed was different from the estimated initial copy number. More than 60 experiments with starting (estimated) copy numbers varying from 0 to 40 were performed with the same PCR conditions to obtain statistical information. A linear relationship between the actual number of peaks and the expected copy number was observed (Fig. 5). The relative standard deviation increased for lower copies of templates, which was expected from counting ($\sqrt{N}$) statistics. However, of the 8 control experiments (0 copy) performed, not a

single one showed any amplified DNA peaks in the electropherogram, which means that no false-positive result was observed. Even if contaminant DNA is present, the primer pair guarantees that only the targeted region is amplified. Furthermore, in no case was the observed peak number larger than the expected peak number. The statistical analysis combined with the results from control experiments confirmed that single copies of targeted DNA molecules were successfully amplified and detected.

The deviation of the slope from 1 was probably due to the inaccuracy in the initial concentration and the improper handling of the low-copy human β-globin solution. The question remains as to whether amplification is 100% effective. One explanation of the slope in Fig. 5 is that only 1 out of 4 copies of template resulted in an amplified zone (fluorescent peak). Wall effects may still be present despite the added BSA. The expansion and contraction of the liquid during thermal cycling can result in dilution (axial spreading) and therefore a lower amplification yield. Whether ineffective amplification or the loss of material in handling these low concentrations of DNA is ultimately responsible for the slope in Fig. 5 will have to be resolved by counting the DNA molecules in independent experiments. For example, our single-molecule imaging scheme[10, 11] can in principle be used to count the true number of template molecules being introduced into the capillary tube before PCR. From a practical point of view, optimizing conditions to assure a high yield so that amplified zones are produced from every molecule will be important for adaptation to disease diagnosis. In the present study, what we can conclude is that the detection limit is no worse than 4 copies of template.

HIV-1 *gag* amplification

For clinical diagnosis, PCR detection of HIV-1 often requires finding low-copy-number blood-borne infectious agents in the presence of high-copy-number host DNAs. For instance, amplification from 20 μL of blood would involve about 1.6×10^5 diploid human genomes in 1 μg of DNA.[42] Based on this fact, HIV-1 negative control DNA at concentration of 10μg/ml (human placenta DNA) was present in our experiment for each run to mimic the abundant host nucleic acid usually present in the test samples for PCR detection from blood.

Individual copies of HIV-1 virus DNA were also detected based on a similar protocol to that for the β-globin gene. The 115 bp HIV-1 *gag* fragment and the 142 bp HIV-1 *gag* fragment were both successfully amplified by capillary PCR. The primer pair SK38/39 (amplifying the 115 bp fragment) was used for the detection of HIV in many research labs and has been shown to work well at relatively high copy numbers. However, in low-copy PCR, the nonspecific primer-dimer formation by this primer pair severely suppressed the formation of the specific PCR product and produced a very high background fluorescence. Instead, the primer pair SK145/431 (amplifying the 142 bp fragment) in the *gag* region showed much higher amplification yield and lower primer-dimer background and thus was chosen here for single-copy capillary PCR. Figure 6 shows the electropherogram of PCR amplification from 5 positive HIV-1 DNA template molecules. Again, no peaks were observed in control experiments (with HIV-1 negative DNA).

CONCLUSIONS

In summary, we demonstrate a novel and sensitive single-molecule screening method

by PCR inside 30-μm i.d. fused-silica capillary. SYBR-Green I is added along with the PCR reaction for dynamic fluorescent labeling. Individual DNA molecules of human β-globin gene and HIV-1 virus DNA are successfully amplified and detected in the capillary. This opens up the possibility of disease diagnosis at its very early stage when only very few cells were infected. The problem reduces to identifying the suitable primer pairs for each disease marker. The feasibility for continuous flow PCR monitoring,[28, 43] along with the well-developed capillary array electrophoresis techniques,[44-46] will provide the high throughput and high sensitivity for large-scale clinical diagnosis. For example, one drop of blood (50 μL) can be distributed to 140 capillary tubes of the dimensions employed here. Simultaneous reaction and subsequent parallel detection[24] should allow screening of every copy of DNA in the sample.

ACKNOWLEDGEMENT

The Ames Laboratory is operated for the U.S. Department of Energy by Iowa State University under contract No. W-7405-Eng-82. This work was supported by the Director of Science, Office of Biological and Environmental Research and Office of Basic Energy Sciences, Division of Chemical Sciences, and by the National Institutes of Health.

REFERENCES

1. Moerner, W. E.; Orrit, M. *Science* **1999,** *283*, 1670-1676.

2. Xu, X.; Yeung, E. S. *Science* **1997,** *276*, 1106-1109.

3. Xu, X.-H.; Yeung, E. S. *Science* **1998,** *281*, 1650-1653.

4. Weiss, S. *Science* **1999,** *283*, 1676-1683.

5. Van Orden, A.; Keller, R. A.; Ambrose, W. P. *Anal. Chem.* **2000,** *72*, 37-41.

6. Yan, X.; Grace, W. K.; Yoshida, T. M.; Habbersett, R. C.; Velappan, N.; Jett, J. H.; Keller, R. A.; Marrone, B. L. *Anal. Chem.* **1999,** *71*, 5470-5480.

7. Agronskaia, A.; Schins, J. M.; de Grooth, B. G.; Greve, J. *Anal. Chem.* **1999,** *71*, 4684-4689.

8. Taylor, J. R.; Fang, M. M.; Nie, S. *Anal. Chem.* **2000,** *72*, 1979-1986.

9. Castro, A.; Shera, E. B. *Anal. Chem.* **1995,** *67*, 3181-3186.

10. Shortreed, M. R.; Li, H.; Huang, W.-H.; Yeung, E. S. *Anal. Chem.* **2000,** *72*, 2879-2885.

11. Ma, Y.; Shortreed, M. R.; Yeung, E. S. *Anal. Chem.* **2000,** *72*, 4640-4645.

12. Saiki, R. K.; Scharf, S.; Faloona, F.; Mullis, K. B.; Horn, G. T.; Erlich, H. A.; Arnheim, N. *Science* **1985,** *230*, 1350-1354.

13. Ou, C. Y.; Kwok, S.; Mitchell, S. W.; Mack, D. H.; Sninsky, J. J.; Krebs, J. W.; Feorino, P.; Warfield, D.; Schochetman, G. *Science* **1988,** *239*, 295-297.

14. Rayfield, M.; DeCock, K.; Hayward, W.; Goldstein, L.; Krebs, J. W.; Kwok, S.; Lee, S.; McCormik, J.; Moreau, J. M.; Odehouri, K.; Schochetman, G.; Sninsky, J. J.; Ou, C. Y. *J. Infect. Dis.* **1988,** *158*, 1170-1176.

15. Fiscus, S. A. *Methods Mol. Med.* **1999,** *20*, 129-139.

16. Larzul, D.; Guigue, F.; Sninsky, J. J.; Mack, D. H.; Brechot, C.; Guesdon, J. L. *J. Virol. Meth.* **1988,** *20*, 227-237.

17. Kaneko, S.; Miller, R. H.; Feinstone, S. M.; Unoura, M.; Kobayashi, K.; Hattori, N.; Purcell, R. H. *Proc. Natl. Acad. Sci. (USA)* **1989,** *86*, 312-316.

18. Young, K. Y.; Resnick, R. M.; Myers, T. W. *J. Clin. Microbiol.* **1993,** *31*, 882-886.

19. Morrison, K. E.; Lake, D.; Crook, J.; Carlone, G. M.; Ades, E.; Facklam, R.; Sampson, J. S. *J. Clin. Microbiol.* **2000,** *38*, 434-437.

20. Buffrini, L.; Grignolo, M. C.; Rovetta, G.; Monteforte, P. *Drugs Exp. Clin. Res.* **2000,** *26*, 67-70.

21. Lachaud, L.; Dereure, J.; Chabbert, E.; Reynes, J.; Mauboussin, J. M.; Oziol, E.; Dedet, J. P.; Bastien, P. *J. Clin. Microbiol.* **2000,** *38*, 236-240.

22. Inoshima, Y.; Morroka, A.; Sentsui, H. *J. Virol. Methods* **2000,** *84*, 201-208.

23. Zhang, N.; Yeung, E. S. *J. Chromatogr. B* **1998,** *714*, 3-11.

24. Zhang, N.; Tan, H.; Yeung, E. S. *Anal. Chem.* **1999,** *71*, 1138-1145.

25. Zhang, Y.; Tan, H.; Yeung, E. S. *Anal. Chem.* **1999,** *71*, 5018-5025.

26. Pang, H.-M.; Yeung, E. S. *Nucl. Acids Res.* **2000,** *28*, e73, i-viii.

27. Woolley, A. T.; Hadley, D.; Landre, P.; deMello, A. J.; Mathies, R. A.; Northrup, M. A. *Anal. Chem.* **1996,** *68*, 4081-4086.

28. Kopp, M. U.; deMello, A. J.; Manz, A. *Science* **1998,** *280*, 1046-1048.

29. Khandurina, J.; McKnight, T. E.; Jacobson, S. C.; Waters, L. C.; Foote, R. S.; Ramsey, J. M. *Anal. Chem.* **2000,** *72*, 2995-3000.

30. Rasmussen, R.; Morrison, T.; Herramnn, M.; Wittwer, C. *Biochemica* **1998,** *2*, 8-11.

31. Morrison, T. B.; Weis, J. J.; Wittwer, C. T. *BioTechniques* **1998,** *24*, 954-962.

32. Espy, M. J.; Ross, T. K.; Teo, R.; Svien, K. A.; Wold, A. D.; Uhl, J. R.; Smith, T. F. *J. Clin. Microbiol.* **2000,** *38*, 3116-3118.

33. Machida, U.; Kami, M. et al. *J. Clin. Microbiol.* **2000,** *38*, 2536-2542.

34. Grace, M. B.; Buzard, G. S.; Hughes, M. R.; Gore-Langton, R. E. *Anal. Biochem.* **1998,** *263*, 85-92.

35. Vogelstein, B.; Kinzler, K. W. *Proc. Natl. Acad. Sci. (USA)* **1999,** *96*, 9236-9241.

36. Xue, Q.; Yeung, E. S. *Nature* **1995,** *373*, 681-683.

37. Craig, D. B.; Arriaga, E. A.; Wong, J. C. Y.; Lu, H.; Dovichi, N. J. *J. Amer. Chem. Soc.* **1996,** *118*, 5245-5253.

38. Tan, W.; Yeung, E. S. *Anal. Chem.* **1997,** *69*, 4242-4248.

39. Cheng, J.; Shoffner, M. A.; Hvichia, G. E.; Kricka, L. J.; Wilding, P. *Nucl. Acids Res.* **1996,** *24*, 380-385.

40. Shoffner, M. A.; Cheng, J.; Hvichia, G. E.; Kricka, L. J.; Wilding, P. *Nucl. Acids Res.* **1996,** *24*, 375-379.

41. Gao, Q.; Yeung, E. S. *Anal. Chem.* **1998,** *70*, 1382-1388.

42. Chou, Q.; Russell, M.; Birch, D. E.; Raymond, J.; Bloch, W. *Nucl. Acids Res.* **1992,** *20*, 1717-1723.

43. Reed, K. C. *Austra. Biotech.* **1996,** *6*, 280-281.

44. Mathies, R. A.; Huang, X. C.; Quesada, M. A. *Anal. Chem.* **1992,** *64*, 2149-2154.

45. Taylor, J. A.; Yeung, E. S. *Anal. Chem.* **1993,** *65*, 956-960.

46. Ueno, K.; Yeung, E. S. *Anal. Chem.* **1994,** *66*, 1424-1431.

FIGURE CAPTIONS

Figure 1. Schematic diagram of on-line capillary PCR. (a) at the beginning of the reaction; (b) during amplification; (c) electromigration after the reaction; and (d) idealized electropherogram.

Figure 2. Gel-electrophoresis of the 142-bp PCR product (stained with ethidium bromide) from HIV-1 DNA under various conditions. Lanes 1, 9 and 11, blank; lane 2, reaction mixture contained no dye; lane 3 and 4, Picogreen was added in the reaction mixture; lanes 5 and 6, YOYO-1 was added in the reaction mixture; lane 7, reaction mixture with SYBR Green I; lane 8, 25-bp DNA ladder; lane 10, reaction mixture with SYBR Green I and 0.2% PVP; and lane 12, 50-bp DNA ladder.

Figure 3. PCR amplification of the 110-bp human β-globin gene and elution by pressure. (a) Control experiment, no human genomic DNA template; and (b) amplification with a total of 10 starting template molecules in the capillary.

Figure 4. PCR amplification of the 110-bp human β-globin gene and elution by electro-migration. (a) Control experiment, no human genomic DNA template; and (b) amplification with a total of 10 starting template molecules in the capillary.

Figure 5. Correlation of expected copy number to detected peak number for 110-bp human β-globin gene.

Figure 6. Capillary PCR of 142-bp fragment from 5 copies of starting HIV-1 DNA and driven out by electromigration.

Capillary PCR Amplification

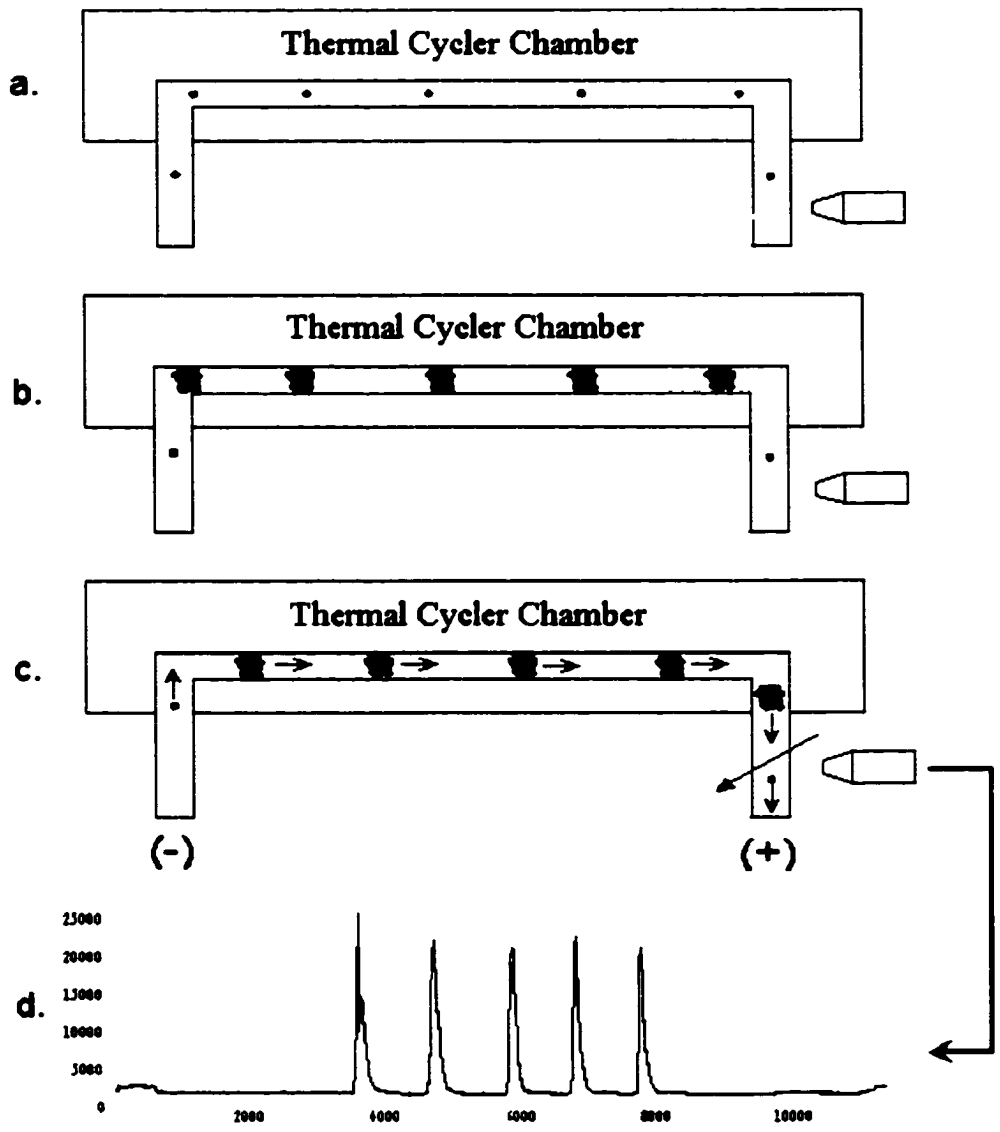

FIGURE 1

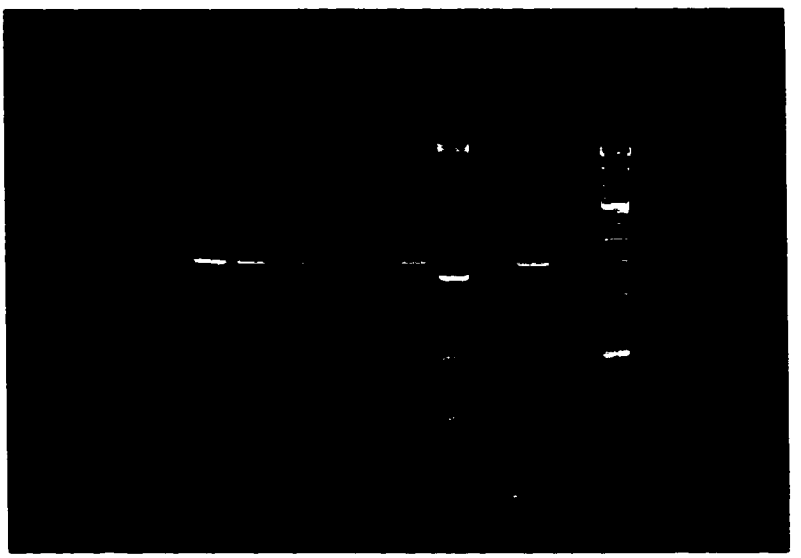

FIGURE 2

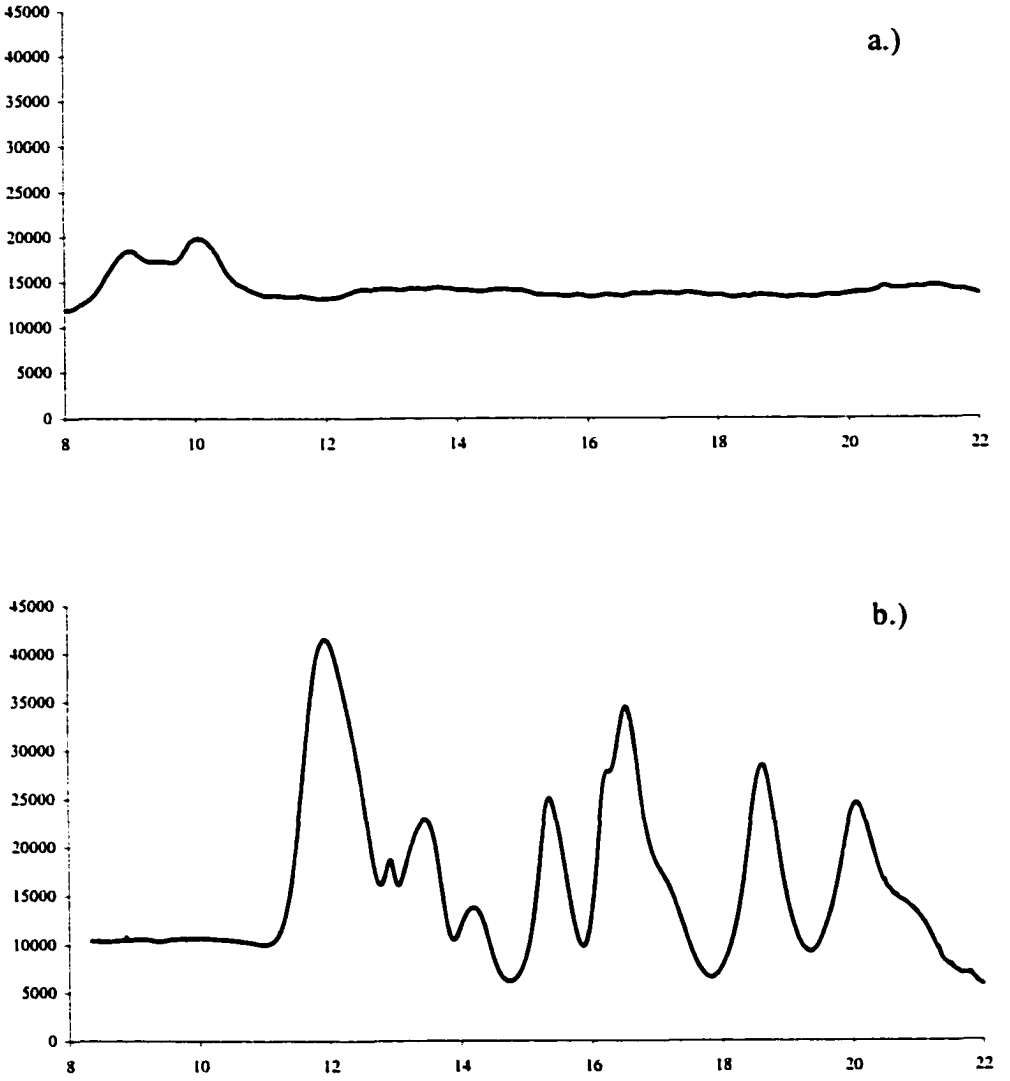
a.)
45000
40000
35000
30000
25000
20000
15000
10000
5000
0
8
10
12
14
16
18
20
22
b.)
45000
40000
35000
30000
25000
20000
15000
10000
5000
0
8
10
12
14
16
18
20
22
Time (min)

FIGURE 3

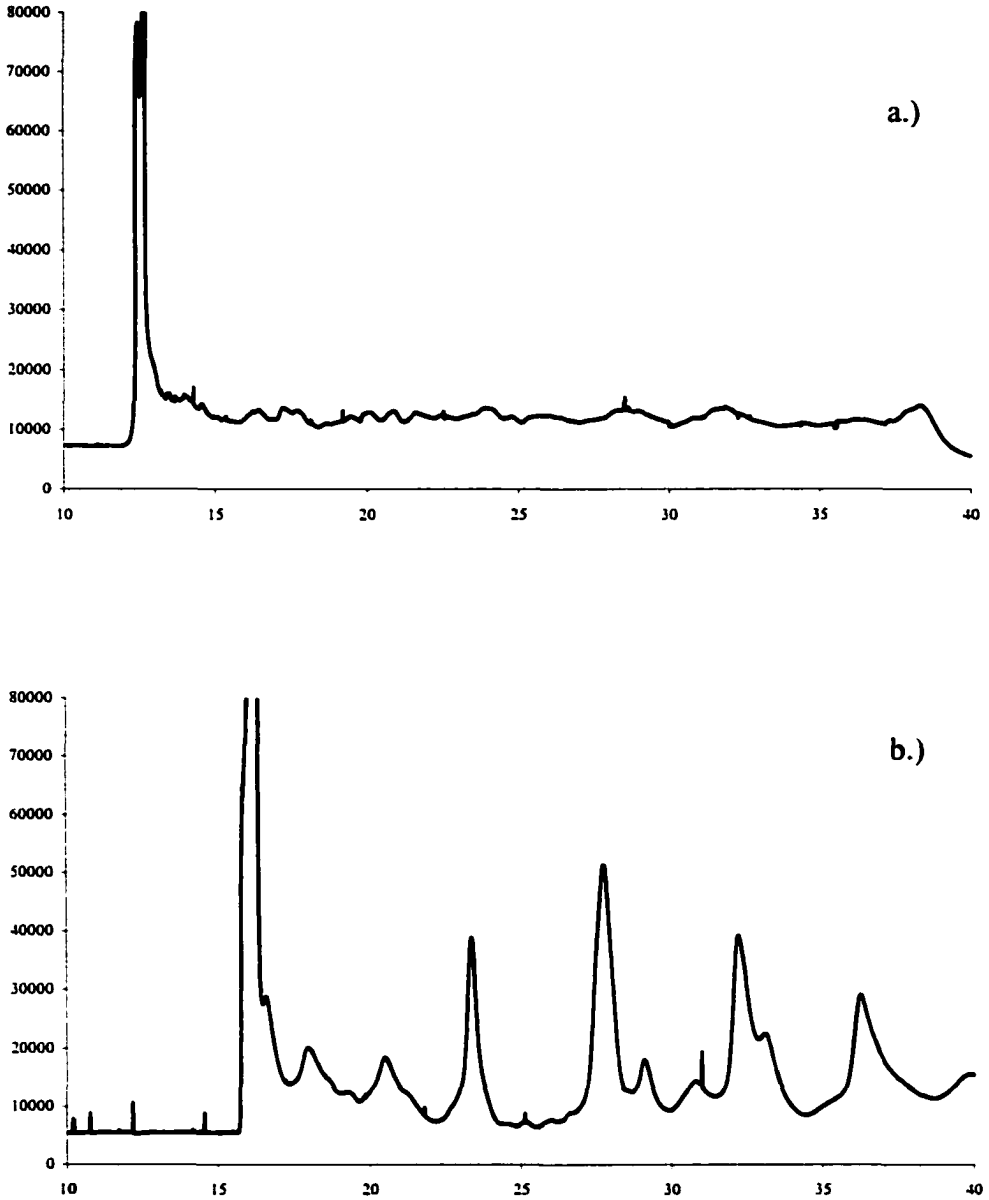
80000
70000
60000
50000
40000
30000
20000
10000
0
10
15
20
25
30
35
40
a.)
b.)
Time (min)

FIGURE 4

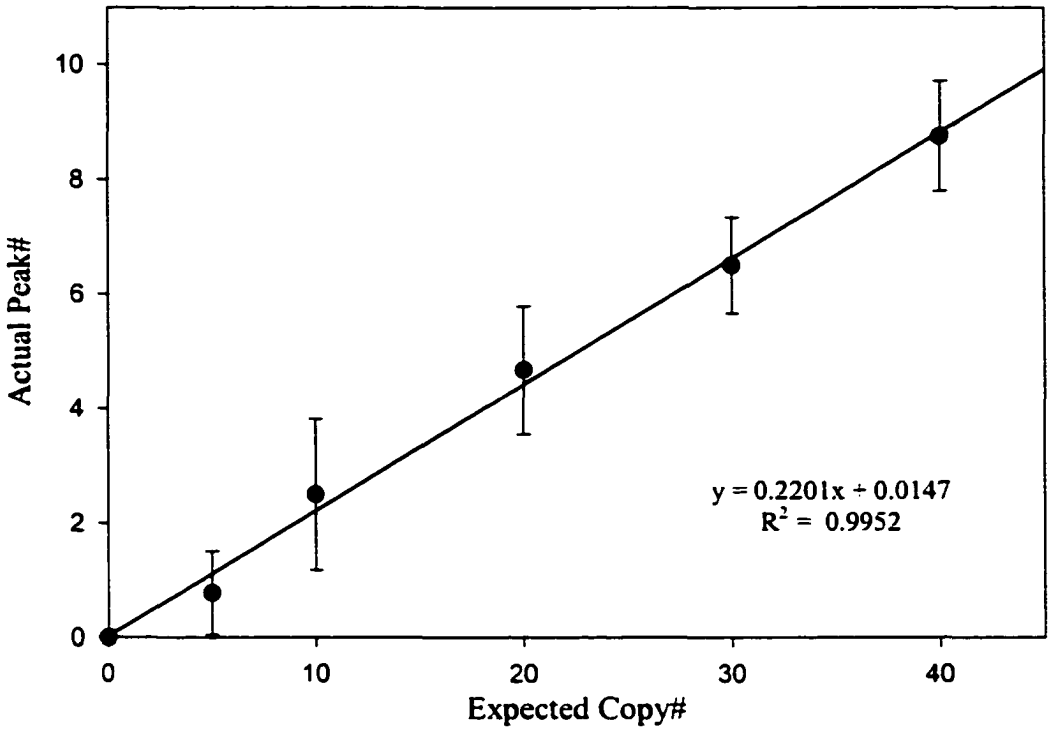
Actual Peak#
Expected Copy#
y = 0.2201x + 0.0147
R² = 0.9952
0
2
4
6
8
10
0
10
20
30
40

FIGURE 5

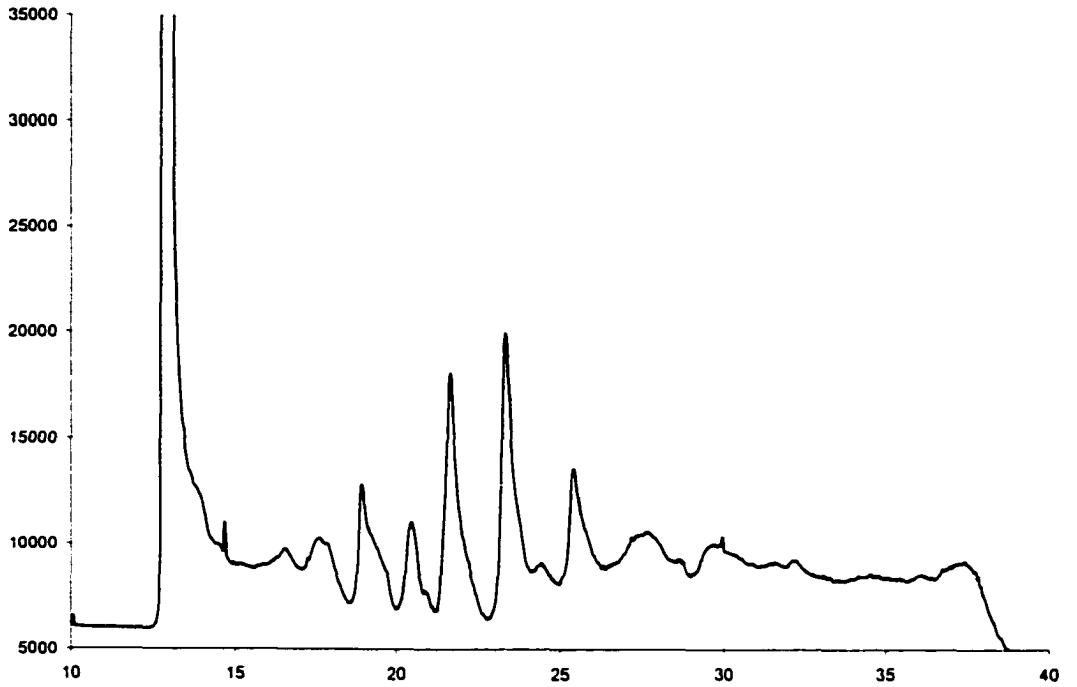
35000
30000
25000
20000
15000
10000
5000
10
15
20
25
30
35
40
Time (min)

FIGURE 6

CHAPTER 4. SELECTIVE DETECTION OF INDIVIDUAL CELLS BY CAPILLARY POLYMERASE CHAIN REACTION

A paper submitted for publication

Hanlin Li and Edward S. Yeung

ABSTRACT

On-line capillary polymerase chain reaction (PCR) coupled with laser-induced fluorescence detection was successfully demonstrated for individual human cells. A single 50-μm i.d. fused-silica capillary served both as the reaction vessel and for isolating single cells. SYBR Green I dye was added into the reaction mixture for dynamic fluorescent labeling. Because of the small i.d. of the capillary, PCR-amplified DNA fragments from single cells were localized in the capillary, providing discrete product zones with concentrations at readily detectable levels. By counting the number of peaks in the capillary via electromigration past a detection window, the number of starting cell templates could be determined. With selective primer design, only the cell containing the DNA of interest was detected. Amplification of the 295-bp fragment from individual human lymphoblast cell β-actin gene was demonstrated. On-column cell counting provided positive correlation between the starting cells templates and the final PCR products. This opens the possibility of highly selective and sensitive disease diagnosis at a very early stage.

INTRODUCTION

There is no doubt that the advent of polymerase chain reaction (PCR) has shed a new light on molecular biology. Outstanding achievements have been made in the applications of PCR methodology in the area of clinical microbiology and diagnosis of human diseases. For instance, in the diagnosis of human infectious diseases, a number of important human viruses, such as HIV,[1, 2] hepatitis viruses[3, 4] have been detected by PCR with high sensitivity and specificity. Genetic disease diagnosis with PCR has been employed in prenatal diagnosis, preimplantation diagnosis[5], forensic analysis[6, 7], disease therapy[8], gene therapy and investigation of oncogenes[9, 10]. PCR is particularly useful when the amount of genetic material is very limited. In recent studies, the sensitivity of PCR has reached an extreme level where a single copy sequence within a single cell or a few cells can be detected[11]. The area of diagnostic science most affected by the advent of this ultra-sensitive single-cell PCR has undoubtedly been pre-implantation genetic analysis[12, 13, 14], which was used to investigate numerous genetic disorders before pregnancy has occurred, including cystic fibrosis, the Huntington's fragile X, Duchenne's muscular dystrophy and others[15, 16, 17]. Interest in examining the genetic nature of single cells has not been limited only to the field of prenatal diagnosis, but also has a great impact in immunology and oncology researches, where it was used to examine changes in the B or T cell lymphocyte receptors[18,19] or to determine the clonal origin of tumors[20].

Other than the applications stated above, we believe that single-cell PCR would also have a huge potential in early stage disease diagnosis. At the early stages of diseases, particularly cancer, only a few cells out of a large population are affected. These will not be

detectable in a homogenized cell sample. Fortunately, the high selectivity of PCR provides a solution to this problem. By designing specific primers to the gene in question, only the DNA region of interest will be amplified. It is relatively straightforward for only the mutant or exogenous DNA to be amplified and detected in a large excess of normal DNAs. The ability to amplify DNA from single cells suggests that, technically at least, it might be feasible to perform diagnosis of certain DNA defects in very few malignant cells while healthy cells are in large excess.

Traditional single cell PCR usually involves micromanipulation of cells[13, 21, 22], where sophisticated setup and special techniques are required, which might hinder the application of this technique to clinical diagnostics. Isolated single cells were then transferred to PCR reaction vessels for amplification. However, to achieve single molecule sensitivity, two or more sequential PCRs usually have to be performed, often using nested sets of primers[13, 23, 24], where carry-over contaminations could be problematic. Another method often used for low copy number amplification is whole genome amplification[25, 26], or more correctly termed primer extension pre-amplification (PEP), in which the entire genome was first amplified, thus providing enough DNA for subsequent PCRs.[15] Unfortunately PEP also has two major disadvantages: it is time consuming, for PEP usually takes 8-12h; the amplification is random, in practice, only ~80% of the genome is effectively amplified. The remaining 20% of the genome, which may contain the gene of interest, may not be amplified at all.[27] We proposed here a simple detection scheme of online coupling of PCR reaction in capillary tubes, where only a one-step PCR is needed for detection and no micromanipulation is involved. The same 50μm i.d. fused silica capillary was used for both PCR reaction and electromigration for post-PCR analysis. Detection of single molecule was made possible by

reducing the reaction volume in the capillary and using laser-induced fluorescence (LIF) detection. Previously, single starting DNA molecules were successfully amplified and detected with this design.[28]

The aim of the present work was to amplify specific gene fragment from isolated single cells using the same device and correlate the number and position of the cells with post-PCR electrophoresis results. Therefore, information of PCR efficiency at single cell level could be obtained. Amplification of β-actin gene in individual human lymphoblast cells was performed. We demonstrate here the apparatus and methods that permit the direct integration of online cell lysis, PCR amplification, on-column hybridization and CE components on a single capillary. No pipetting or manual transfer of liquid was required between amplification and analysis steps, thereby simplifying the procedure and reducing opportunities for contamination. Our integrated system is applicable to all types of single cell PCR amplifications, because a general intercalating dye rather than sequence-specific fluorescent probes was used for PCR product monitoring. Thus, no complicated or expensive target-specific probe chemistry is required for fluorescence detection of the PCR product.

EXPERIMENTAL SECTION

Cell Culture

Lymphoblast cell lines (GM03798, male, Homo sapiens) were obtained from Coriell Cell Repositories (Camden, NJ) and grown in RPMI 1640 culture medium supplemented with 15% heat inactivated fetal bovine serum (Life Technologies, NY), 2mM L-glutamine, 100 U/ml penicillin and 100 μg/ml streptomycin (Sigma, MI). Cells were cultured in T25

tissue culture flasks with 10~20 ml growth medium in an upright position. Culture flasks were incubated at 37°C in an atmosphere of 5% CO_2 in air with loose caps.

Cell Lysis

Fresh cells were taken from culture medium every day, and the cell density was counted with Hemocytometer (Hausser Scientific, Horsham, PA). The cells were then pelleted from culture medium by centrifugation at 60g for 10 minutes, washed once with Hanks' Balanced Salt Solution (HBSS) (Invitrogen, Carlsbad, CA) and then lysed with three different approaches. Unless specified, the reagents used here were all from Sigma-Aldrich (MI).

1. Proteinase K lysis: cell suspension containing 250 μg/ml proteinase K (Roche Boehringer Mannheim, IN) was incubated at 50°C for 2 hours, then at 95°C for 5 minutes to deactivate the enzyme.
2. Lysing with surfactants: three lysis buffer with three different surfactants were tested: 0.05% SDS in phosphate-buffered saline (PBS) solution (1 mM KH_2PO_4, 3 mM $Na_2HPO_4 \cdot 7H_2O$ and 150 mM NaCl, pH 7.4); 0.2% Triton X-100 in 10 mM Tris-HCl, 150 mM NaCl, 1 mM EDTA, pH 7.4; 1% NP40 (Roche Boehringer Mannheim, IN) in 10 mM Tris-HCl, 150 mM NaCl, 1 mM EDTA, pH 7.4.
3. Boiling lysis: cells were re-suspended in hypotonic lysis buffer (50 mM NaCl, 10 mM Tris-HCl, pH 8.0) right before adding to the PCR cocktail and heated at 95°C for 5 minutes before PCR.

Cell Counting

Cell density was counted in bulk culture suspension with a hemocytometer. Typan blue (Life Technologies, NY) was used to stain cells, where dead cells take the dye and appear blue under the microscope and live cells remain transparent. According to the counted cell density, a limiting dilution was made to achieve the density of 1~15 cells in the reaction region of the capillary (~1 μl). The actual number of cells within reaction capillary was then verified by one of the following counting methods:

Flow LIF Method.

SYTO16 (1 μM, Molecular Probes, Eugene, OR) was included in the cell suspension, which could easily penetrate cells and stain nucleic acids. Without binding to the nucleic acids, SYTO16 only shows minimal background, while significant enhanced fluorescent signal at 520 nm emission maxim could be observed after binding. Labeled cell suspension was filled into the capillary and then driven out by gravity. The photo multiplier tube (PMT) (Hamamatsu, Bridgewater, NJ) was placed downstream to monitor the fluorescent signal from cells. The number of cells in the capillary was determined by the number of fluorescent bursts flowing by the detection window.

LIF Imaging Method.

A frame transfer CCD camera (Roper Scientific, Trenton, NJ) was used to record the cell flow instead of PMT in this method. Cell suspension stained with SYTO16 was introduced into 75μm i.d. square and round capillaries, respectively. The fluorescent image of the detection window was vertically collected and magnified by a 10× microscope objective and projected into the CCD camera. The camera was operated in the external synchronous mode. 1000 frames were acquired at frequency of 5 Hz with 10 ms exposure

time for each frame. All images are stored and processed with Winview Software (Roper Scientific). Based on the number of cells appeared in each frame and the actual frame dimension, real cell density in the capillary was resolved.

Partial Dark Field Method.

No SYTO16 or other cell stain was used with this technique. The cells were screened and counted visually by partial dark field microscopy. To obtain a " partial dark field", an occulting disk was placed between the light source and the condenser of the microscope (Olympus CK2, Leeds Precision Instruments, MN). Unlike the normal dark field microscopy, which is most effective for planar surface, the disk only blocks part of the light in the view field. In this way, the capillary wall was not so bright as that of dark field view while it also provided much better contrast than that of mere bright field viewing. The reaction capillary was inserted through two PEEK Tubing Sleeves (381μm ID, Upchurch Scientific, Oak Harbor, WA) mounted on the microscope slide, so that the capillary could be tracked in the field of view while pulling the capillary through the sleeves. The suspension of cells in the PCR cocktail was introduced into the reaction capillary manually by syringe. Both ends of the capillary were sealed with Microtight Unions (Upchurch Scientific, Oak Harbor, WA) to prevent cells from moving in the capillary. The actual number of cells in the reaction region was counted by pulling the capillary under the microscope and the positions of each cell were also recorded. The capillary was then transferred to the reaction set-up for on-line lysing, PCR and electrophoresis.

Polymerase Chain Reaction

PCR of human β-actin gene with lymphoblast cells were first offline optimized in 200 μl thin-wall polypropylene vials and 250 μm i.d. fused-silica capillaries before moving on to online capillary reaction. Resuspended lymphoblast cells were added into 12 FailSafe PCR PreMixes (Epicentre, Madison, WI) with various amounts of $MgCl_2$ and FailSafe PCR Enhancer (with betaine). The 20 μl reaction mixtures had the following compositions: 10 μl FailSafe PCR PreMixes (A-L), 500 μg/ml bovine serum albumin (Idaho Technology, Salt Lake City, UT), 0.4% (w/v) poly(vinylpyrrolidone) (PVP) (MW = 1,000,000 Polysciences, Warrington, PA), 0.5 μM of each primer (forward primer: 5'-TCACCCACACTGTGCCCATCTACGA-3'; reverse primer: 5'-CAGCGGAACCGCTCATTGCCAATGG-3', synthesized by the DNA facility at Iowa State University, Ames, IA), 1:50,000 dilution of DNA staining dye SYBR Green I (Molecular Probes, Eugene, OR), 0.25 unit/μl FailSafe PCR Enzyme Mix and ~10^3 cells.

Conventional PCRs in 200 μl thin-wall polypropylene vials were carried out in GeneAmp 9700 system (Applied Biosystems, Foster City, CA) at the following temperatures: denaturation at 95°C for 5 min; 35 cycles of 94°C 30 s, 54°C 30 s, 72°C 1 min; and 72°C for 7 min. Reaction products were loaded onto 4% high resolution agarose E-Gels (InvitroGen, Carlsbad, CA) to examine the optimal condition.

The PCR protocol was fine tuned for fused silica capillary in 250 μm i.d., 365 μm i.d. capillaries with total length of 25 cm (~12.5 μl reaction volume). Six parallel reactions with different FailSafe PCR recipes were tested in each run. Each PCR cocktail has the final composition of 1×FailSafe PCR PreMix (A, B, C, F, G, I, respectively), 500 μg/ml bovine

serum albumin, 0.4% PVP, 0.5μM of each primer, 1:50,000 dilution of DNA staining dye SYBR Green I, 0.25 unit/μl FailSafe PCR Enzyme Mix and ~500 cells. Capillaries were sealed with MicroTight unions (Upchurch Scientific, Oak Harbor, WA) and PCR was performed in a Rapid Air Cycler (Idaho Technology, Salt Lake City, UT) using 95°C for 5 min, 94°C 30s, 54°C 30s, 72°C 1 min for 35 cycles and 72°C for 7 min. PCR products from capillary PCR were then pushed out and loaded onto slab gel to examine the yield.

Slab Gel Electrophoresis

The sizes of the PCR product was confirmed by slab gel electrophoresis using 4% high-resolution agarose E-Gels (Invitro Gen, Carlsbad, CA). 50 bp ladders (Life Technologies, Grand Island, NY) were loaded on the gel and co-migrated with the DNA sample. The total volume for each sample well was 20 μL. The image was taken under a UV lamp.

Capillary Electromigration

The setup for capillary PCR was described in detail previously. In brief, a 100 cm long capillary was coiled partially inside the air cycler where the amplification was performed (Figure 1). The 488-nm Ar^+ laser beam (Uniphase, San Jose, CA, model 2213-75SLYW) was filtered with a 488nm interference filter (Melles Griot, Irvine, CA) and focused by a convex lens onto the capillary. The fluorescent signal was collected by a 10× microscope objective into the photomultiplier tube (Hamamatsu, Bridgewater, NJ). A 520-nm interference filter (Oriel, Stratford, CT) was placed before PMT to prevent scattered laser

light from entering the detector. A high voltage power supply (Glassman High Voltage Inc, Whitehorse Station, NJ) was used for electrophoresis. The analog signal was sampled at 2Hz with a 22-bit ADC board (IO Tech, Cleveland, OH) controlled by a program written in LabVIEW (National Instruments, Austin, TX) running on a desktop computer.

The same capillary was used for both cell PCR reaction and electromigration in this experiment. PCR reaction mixture containing cells was pushed through the reaction capillary by an airtight Hamilton syringe. The number of cells within the reaction region was visually counted by partial dark field viewing before on-line PCR. After the reaction, a +15 kV DC high voltage was applied to both ends of the capillary. Since 0.4% PVP was employed in the reaction mixture as well as the running buffer, electroosmotic flow was effectively suppressed. Selectively amplified DNA zones would move toward the anode and passed through the detection window. When combined with amplified ds-DNA, the fluorescence of SYBR Green I was greatly enhanced, which made it possible for the LIF detection of PCR product.

The running buffer for the electromigration contains 50mM KCl, 50mM Tris-HCl, 3.0 mM $MgCl_2$ (pH 8.3, Fisher Scientific, Hanover Park, IL) 500μg/ml BSA, 1:10,000 dilution of SYBR Green I in 1×TAE, and 0.4% MW 1,000,000 PVP.

RESULTS AND DISCUSSION

Our previous work successfully demonstrated on-line capillary PCR of individual DNA molecules coupled with laser-induced fluorescence detection[28]. Because of the small i.d. of the fused silica capillary and its associated minimal axial diffusion, highly sensitive and selective single molecule screening was achieved, which opens the possibility of disease

diagnosis at a very early stage. Here, we tried to develop diagnosis methods directly from individual cells. Sophisticated sample preparation was no longer required, which greatly simplified the operating protocol and had the potential of greatly improving the diagnosis throughput.

The principles underlying capillary PCR of individual cells were similar to those of the amplification of individual DNA molecules, which were described in detail previously. In brief, PCR cocktail containing lymphoblast cells and dynamic DNA intercalating dye SYBR Green I was filled into the 50 μm i.d. capillary. The very few copies of cells would distribute randomly along the capillary. During the heating step of PCR, cells were lysed and genomic DNAs were released into PCR reagents. Since both sides of the capillary were submerged in leveled buffer vials, DNAs would stay locally and get amplified. Unlike traditional PCR in 200 μl tubes, the very small inner diameter of the capillary prevented the amplified DNA from diffusing substantially. So the amplified PCR products would be confined in tight sample zones with very small volume, which yielded fairly high local concentrations. These DNA sample zones were then driven out by electromigration with each zone reflected by a peak in the electropherogram, corresponding to one copy of starting cell. In principle, the number of cells in a sample could be measured simply by counting the number of peaks in the electropherogram.

Cell counting

Different from previous efforts in single molecule PCRs[28, 29], the number of starting templates was actually counted instead of an estimation of genome equivalents based on

limiting dilution. We developed three procedures to count the actual number of cells been loaded into the reaction capillary. A detailed example of each method follows.

The *flow LIF* method used a PMT to monitor the laser-induced fluorescence from the cells flowing by the detection window. Because the cells were ~5 μm in diameter each, each stained cell would introduced a spike in the flow-gram as it flowed by the detection window. Figure 2a was a typical flow-gram for lymphoblast cell at concentration of ~200/μl (estimated by hemocytometer). There were some major peaks in the flow-gram with peak intensity as high as over 2000 mV. But the number of major peaks was much less than the number of cells estimated by the hemocytometer. Even when the minimum peak height was lowered to 300, only 38 peaks were picked up while with the 32 cm effective length 50 μm i.d. capillary filled with the cell suspension, there should be approximately 125 cells. However, there are hundreds of minor peaks in the flow-gram, which might due to complex cell culture matrix. It was really difficult to set an appropriate threshold to differentiate the cell peaks from the background spikes. We tried to defocus the laser beam, so the cells in different part of the capillary might be excited more uniformly. The baseline was much cleaner, but again only 33 peaks were counted, which was only ~24% counting efficiency (data not shown),

The *CCD Imaging* method utilized the 2D pixels to take images of the inner capillary zone at fairly high frame rate. It was more straightforward than PMT detection, because the fluorescent signal from cells could be easily differentiated from background signal based on both signal intensity and dimension. Figure 2b showed a couple of fluorescent images of a cell and background signal in a 50 μm i.d. round capillary taken by CCD camera. Figure 2b(1) was the buffer background. The laser scattering from the capillary wall could be seen.

The fluorescent image of each particle showed up as diamond shape in the round capillary as seen in Figure 2b(2-4). But the fluorescence intensity varied a lot from particle to particle. Similar to that of the flow LIF method, there was no obvious cut-off between the actual cell and other miscellaneous junk. If all bright spots were counted, they were too much over-populated compared to the hemocytometer estimation.

However, imaging by square capillary gave very consistent results. Figure 2c showed 4 images of 75 × 75 μm i.d. square capillary taken by the same CCD imaging setup. Almost every cell imaged was really bright and round in shape (Figure 2c(2-4)), while the unknown interference particles were weak and much smaller in actual size. The superiority of the square capillary over the round capillary could be explained by the intrinsic focusing property and larger scattering effect of round capillaries, which made it difficult to distinguish cell signals. By setting the proper threshold, the cell number could be counted precisely with a simple program. For the counting experiments shown in Figure 2c, 23 cells were counted in a total of 1000 frames. Since the hydrodynamic flow rate was 33 pixel/frame and each pixel was 1.06 μm in actual field size, the corresponding cell concentration was ~116 cells/μl, which correlated very well with the ~120 cells/μl concentration measured with hemocytometer.

Although counting by CCD camera is fast and automatic, the cell stain would complicate the PCR reaction with problems like compatibility with reagents, competing with SYBR Green I stains, affecting reaction efficiency etc. So, we also tested a third approach, *Partial Dark Field Microscopy*. By partially blocking the converged light from the condenser, the cells in the PCR cocktail inside the reaction capillaries could be clearly observed with 100× or 200× magnification as shown in Figure 2d. It was simple and

straightforward. No cell stain was needed. The counting results also correlated very well with the hemocytometer results. Once the cells were injected into the capillary, both ends of the capillary were sealed during the counting process and hydrodynamically leveled during thermal cycling. There was no axial flow other than diffusion. The final amplification zones should be consistent with the initial cell locations. For this reason, we recorded the counting process in VHS videotapes and the initial cell locations were marked for later comparison.

Cell lysis.

The first and most important step in single-cell PCR is cell lysis, so that DNA could be released and be accessible to PCR reagents. The most widely used cell-lysing reagent for DNA isolation is proteinase K[30, 31]. The advantage of using proteinase K is that it will not only break down the cell membranes and expose DNAs, but also digest some intracellular proteins that may prohibit PCR reactions. Our preliminary data showed that proteinase K was indeed very efficient in lysing the lymphoblast cells. Unfortunately, proteinase K itself is not compatible with PCR reagents. An extra digestion step must be included before adding in PCR mixture, which would involve manual liquid transfer between steps and is not suitable for our integrated closed system.

We also tested another category of common lysing reagents, surfactants. Our off-line PCR results showed that charged surfactants, such as SDS, prohibit the amplification reaction at concentrations higher than 0.03%, while normally effective lysing concentration is 0.05% ~ 0.1%; neutral surfactants such as Nonidet P 40[32], Triton X-100 etc. were friendly to PCR reactions, but showed poor performance in cell lysis.

The third lysing method, a combination of heat and osmotic pressure, was proved to be most compatible with the integrated on-line capillary PCR. Cell pellet was re-suspended in the hypotonic lysis buffer right before adding into PCR cocktail. A preheating step at 95°C for 5 minutes before the capillary thermal cycling would further complete the cell lysis. In such a way, we could combine the on-column cell lysis with single-cell capillary PCR. A one-step process could integrate the sample preparation, sample amplification and product analysis into a single capillary, with no sample transferring in between.

Modifications of PCR Protocol.

As has been noted by previous studies of PCR in capillaries[28, 33], it was essential to include BSA in the capillary PCR, presumably to block non-specific adsorption of DNA and polymerase to silica surface. We generally used 500μg/ml final concentration of BSA in the reaction. Also, 0.4% PVP was added both into the reaction mixture and the running buffer. The use of PVP in PCR systems is not new. PVP was used as a PCR enhancer[34]and also employed to remove phenol-containing compounds that inhibit PCR.[35, 36] In a different light, several groups utilized PVP in microchip devices for PCR to coat the glass surface, in order to prevent the polymerase from deactivation by adsorption to the surface.[37, 38] PVP is also known as a dynamic coating reagent that helps suppress electroosmotic flow (EOF) during electrophoresis.[28] Apparently, PCR from a single cell is very demanding on the amplification yield, which is primarily determined by the performance of DNA Polymerase. Therefore, selecting the most efficient enzyme and cocktail recipe becomes critical to the success of reaction. *Taq* DNA polymerase from different suppliers were tested and compared. FailSafe PCR Premix from Epicentre (Madison, WI) is superior in both yield and specificity in DNA

amplification from cells. The enhancement of PCR amplification is most possible due to the addition of betaine (trimethyl glycine) in the enzyme mix. The presence of betaine may protect DNA polymerase from thermal denaturation[39] and improve the yield and specificity of ampification.[40, 41, 42]

SGE results of 6 different PCR cocktail recipes were shown in Figure 3. PreMix A was proved to be the optimal condition for this particular amplification, which gave the highest product yield and lowest amount of non-specific amplicons (also known as primer dimmers) in fused silica capillaries. The same condition was then used for all the following online capillary PCR reactions with lymphoblast cells.

PCR of β-Actin Gene From Individual Lymphoblast Cells.

A 295-bp fragment of the β-actin gene was amplified with specific primers from human lymphoblast cells. Since β-actin gene is a single copy gene and each human cell has two alleles of chromosome, PCR of β-actin gene from individual cells starts from 2 copies of templates. On electromigration after PCR, 7 distinct amplified DNA peaks (Fig. 4b) can be seen. Fig. 4a was the control experiment without cell in the reaction mixture. In Figure 4b, not all amplified peaks have the same heights or areas. This is attributed to the known variability of exponential PCR amplification. Because of the SYBR Green I intercalating dye used in the PCR, only double stranded DNA would be labeled. The primers almost didn't contribute any fluorescence in the background signal.

In order to confirm the peaks in electropherogram was actually from single cell PCR but not artifacts, four sets of negative control experiments were done: PCR with no primer pair; no enzyme; no thermal cycling; and no cell templates. In the first three sets of control

experiments, electromigration gave very clean electropherograms with no observable peaks. There was always a peak in the front part of the electropherogram as shown in Figure 4a, which was consistent with our previous on-line capillary PCR results from individual DNA molecules[28]. We believe this peak might be related to the non-specific products, notably primer-dimers, formed at the interface between the reaction mixture inside the thermal cycler and that outside. Because this peak showed up in both control and normal runs, it could be neglected in our data interpretation.

The noticeable fluctuation in the background signal was most likely due to the nonspecific product, primer-dimers, since, for low-copy PCR the primers were in large excess. Because the primer-dimers were also double-stranded oligonucleotides, they would be labeled by the intercalating dyes as well. However, this fluctuation is fairly flat when compared to the sharp (localized) peaks of specific products. By properly setting the edge slope and peak width, specific peaks could be discriminated against the background by using standard chromatographic software (Grams 32, Galactic Industries, Salem, NH).

Peak Correlation.

Because the partial dark field microscope approach provided a reliable method to count each cell been loaded into the reaction capillary, the total number of cells as well as the initial locations of each cell along the capillary could be marked and recorded prior to PCR reaction. During the electromigration, the electric field was kept constant and the electroosmotic flow was suppressed. The amplified DNA fragments would move at almost constant velocity toward the cathode. Thus, in principle, there should be one to one

correlation between the initial cells and electrophoretic peaks if the amplification is 100% effective. The cell locations should correlate with the corresponding migration times as well.

The capillary was filled with PCR cocktail which contained primer, SYBR Green I, enzyme, etc. The running buffer didn't include the primer and enzyme. It showed less background than the reaction mixture. In the electropherogram, we can see a baseline drop when all the whole capillary of PCR cocktail migrates to the detection window. This baseline drop, along with the giant primer dimer peak at the interface between the reaction mixture inside the thermal cycler and that outside, provided a pretty good estimation of the migration velocity of the primer or primer dimer. Since oligonucleotides larger than 10 bp showed similar mobility in free solution, the primer velocity gave a good indication of the migration velocity of the DNA fragments. In such a way, the initial cell positions could be converted to the corresponding migration time. As shown in Fig.5a, each cell was indicated by a bar at its projected migration time. When the bar diagram was stacked with the obtained electropherogram, they provide a direct correlation of the initial cell position and the final amplified peaks.

As shown in Figure 5, each cell was approximately matched with one electrophoretic peak. This gave the most solid proof of the success amplification of the on-line single cell PCR. As discussed earlier, isolated cells got amplified at their initial spots. The axial diffusion was almost negligible. However, as shown by the difference in peak heights, the amplification efficiency varied a lot from cell to cell, which we attributed to the known variability of exponential amplification and insufficient cell lysing. From a practical point of view, optimizing conditions to ensure a high yield so that unambiguous amplified zones are produced from every molecule will be important for adaptation to disease diagnosis. On the

other hand, occasionally, some peaks showed up where no matching cells were observed. Possible explanation was that some cells died during cell culture or sample handling, so DNAs were released into the cell suspension, which were "invisible" during cell counting. But during the thermal cycling, these isolated copies of DNA were also amplified since they shared the same sequence as the live cells.

CONCLUSIONS

In summary, we demonstrated a sensitive single cell screening method by on-line PCR inside a 50-μm-i.d. fused silica capillary. Lymphoblast cells were directly loaded into PCR cocktail and on-line lysed by hypotonic buffer right before thermal cycling. SYBR-Green I was added along with the PCR reaction for dynamic fluorescent labeling. Human β-actin gene within individual lymphoblast cells was successfully amplified and detected in the capillary. This opens up the possibility of disease diagnosis at its very early stage when only very few cells are infected. Online counting of individual starting cell provided direct correlation of the starting templates and final PCR products. The feasibility for continuous-flow PCR monitoring,[43,44] along with the well-developed capillary array electrophoresis techniques, will provide the high throughput and high sensitivity for large scale clinical diagnosis.

ACKNOWLEDGEMENT

The Ames Laboratory is operated for the U.S. Department of Energy by Iowa State University under contract No. W-7405-Eng-82. This work was supported by the Director of

Science, Office of Biological and Environmental Research and Office of Basic Energy Sciences, Division of Chemical Sciences, and by the National Institute of Health.

REFERENCES

1. Ou, C. Y.; Kwok, S.; Mitchell, S. W.; Mack, D. H.; Sninsky, J. J.; Krebs, J. W.; Feorino, P.; Warfield, D.; Schochetman, G. *Science* **1988**, 239, 295-297.

2. Christopherson, C.; Kidane, Y.; Conway, B.; Krowka, J.; Sheppard, H.; Kwok, S. *J. Clin. Microbiol.* **2000**, 38(2), 630-634.

3. Kaneko, S.; Miller, R. H.; Feinstone, S. M.; Unoura, M.; Kobayashi, K.; Hattori, N.; Purcell, R. H. *Proc. Natl. Acad. Sci. U.S.A.* **1989**, 86, 312-316.

4. Allen, M. I.; Gauthier, J.; DesLauriers, M.; Bourne, E. J.; Carrick, K. M.; Baldanti, F.; Ross, L. L.; Lutz, M. W.; Condreay, L. D. *J. Clin. Microbiol.* **1999**, 37(10), 3338-3347.

5. Handyside, A. H.; Pattinson, J. K.; Penketh, R. J.; Delhanty, J. D.; Winston, R. M.; Tuddenham, E. G. *Lancet* **1989**, 1, 347-349.

6. Sullivan, K. M.; Mannuci, C. P.; Kimpton, C. P.; Gill, P. *Biotechniques* **1993**, 15, 636-641.

7. Findlay, I.; Taylor, A.; Quirke, P.; Frazier, R.; Urquhart, A. *Nature* **1997**, 389, 555-556.

8. Nyvold, C.; Madsen, H. O.; Ryder, L. P.; Seyfarth, J.; Engel, C. A.; Svejgaard, A.; Wesenberg, F.; Schmiegelow, K. *J. Immunol. Methods* **2000**, 233(1-2), 107-118.

9. Cantley, L. C.; Auger, K. R.; Carpenter, C.; Duckworth, B.; Graziani, A.; Kapeller, R.; Soltoff, S. *Cell* **1991**, 64, 281-302.

10. Ortiz, B. Hannah; Ailawadi, Monica; Colitti, Cristiano; Muto, Michael G.; Deavers, Michael; Silva, Elvio G.; Berkowitz, Ross S.; Mok, Samuel C.; Gershenson, David M. *Cancer Res.* **2001**, 61(19), 7264-7267.

11. Li, H. H.; Gyllensten, U. B.; Cui, X. F.; Saiki, R. K.; Erlich, H. A.; Arnheim, N. *Nature* **1988**, 335, 414-417.

12. Hahn, S.; Zhong, X. Y.; Troeger, C.; Burgemeister, R.; Gloning, K.; Holzgreve, W. *Cell. Mol. Llife Sci.* **2000**, 57, 96-105.

13. Garvin, A. M.; Holzgreve, W.; Hahn, S. *Nucleic. Acids Res.* **1998**, 26(15), 3468-3472.

14. Rechitsky, S.; Verlinsky, O.; Amet, T.; Rechitsky, M.; Kouliev, T.; Strom, C.; Verlinsky, Y. *Mol. Cell. Endocrinol.* **2001**, 183(Suppl. 1), S65-S68.

15. Wells, D.; Sherlock, J. K.; Handyside, A. H.; Delhanty J. D. A. *Nucleic Acids Res.* **1999**, 27, 1214-1218.

16. Druky, K. C.; Liu, M. C.; Lilleberg, S.; Kipersztok, S.; Williams, R. S. *Mol. Cell. Endocrinol.* **2001**, 183(Suppl. 1), S1-S4.

17. Handyside, A. H.; Lesko, J. G.; Tarin, J. J.; Winston, R. M. L.; Hughes, M. R. *New Engl. J. Med.* **1992**, 327, 905-909.

18. Gellrich, S.; Lukowsky, A.; Schilling, T.; Rutz, S.; Muche, J. M.; Jahn, S.; Audring, H.; Sterry, W. *J. Invest. Dermatol.* **2000**, 115(4), 620-624.

19. Attuil, V.; Bucher, P.; Rossi, M.; Mutin, M.; Maryanski, J. L. *Proc. Natl. Acad. Sci. USA* **2000**, 97(15), 8473-8478.

20. Weinberg, R. A. *Sci. Am.* **1996**, 275, 62-70.

21. Takabayashi, H.; Kuwabara, S.; Ukita, T.; Ikawa, K.; Yamafuji, K.; Igarashi, T. *Prenat. Diagn.* **1995**, 15, 74-77.

22. Von, E. F.; Michel, S.; Günther, M.; Schimmel, B.; Claussen, U. *Hum. Genet.* **1996**, 99, 266-270.

23. Grace, M. B.; Buzard, G. S.; Hughes, M. R.; Gore-Langton, R. E. *Anal. Biochem.* **1998**, 263(1), 85-92.

24. Attuil, V.; Bucher, P.; Rossi, M.; Mutin, M.; Maryanski, J. L. *Proc. Natl. Acad. Sci. USA* **2000**, 97(15), 8473-8478.

25. Zhang, L.; Cui, X. F.; Schmitt, K.; Hubert, R.; Navidi, W.; Arnheim, N. *Proc. Natl. Acad. Sci. USA* **1992**, 89, 5847-5851.

26. Kristjansson, K.; Chong, S. S.; Vandenveyver, I.B.; Subramanian, S.; Snabes, M. C.; Hughes, M. R. *Nat. Genet.* **1994**, 6, 19-23.

27. Findlay, I. *British Med. Bulletin* **2000**, 56(3), 672-690.

28. Li, H.; Xue, G.; Yeung, E. S. *Anal. Chem.* **2001**, 73, 1537-1543.

29. Kalinina, O.; Lebedeva, I.; Brown, J.; Silver, J. *Nucleic Acids Res.* **1997**, 25(10), 1999-2004.

30. Taylor, R. W.; Taylor, G. A.; Durham, S. E.; Turnbull, D. M. *Nucleic Acids Res.* **2001**, 29(15), e74.

31. Roers, A.; Montesinos-Rongen, M.; Hansmann, M. L.; Rajewsky K.; Küppers, R. *Eur. J. Immunol.* **1998**, 28, 2424-2431.

32. Cheng, T.; Shen, H.; Giokas, D.; Gere, J.; Tenen, D. G.; Scadden, D. T. *Proc. Natl. Acad. Sci. USA* **1996**, 93, 13158-13163.

33. Zhang, N.; Tan, H.; Yeung, E. S. *Anal. Chem.* **1999**, 71(6), 1138-1145.

34. Bickley, J.; Hopkins, D.; in: Saunders, G.; Parkes, H., (Eds.), *Analytical Molecular Biology-Quality and Validation* **1999**, 81-102, Thomas Graham House, UK 1999, pp.81-102.

35. Koonjul, P. K.; Brandt, W. F.; Farrant, J. M.; Lindsey, G. G. *Nucleic Acids Res.* **1999**, 27(3), 915-916.

36. Kim, C. S.; Lee, C. H.; Shin, J. S.; Chung, Y. S.; Hyung, N. I. *Nucleic Acids Res.* **1997**, 25(5), 1085-1086.

37. Kopp, M.; de Mellow, A.; Manz, A. *Science* **1998**, 280, 1046-1048.

38. Giordano, B. C.; Copeland, E. R.; Landers, J. P. *Electrophoresis* **2001**, 22, 334-340.

39. Santoro, M. M.; Liu, Y.; Khan, S. M. A.; Hou, L.; Bolen, D. W. *Biochemistry* **1992**, 31(23), 5278-5283.

40. Weissenteiner, T.; Lanchbury, J. S. *BioTechniques* **1996**, 21(6), 1102-1108.

41. Henke, W.; Herdel, K.; Jung, K.; Schnorr, D.; Loening, S. A. *Nucleic Acids Res.* **1997**, 25(19), 3957-3958.

42. Weissensteiner, T. *Nucleic Acids Res.* **1998**, 26(2), 687.

43. Reed, K. C. *Australas. Biotechnol.* **1996**, 6, 280-281.

44. Kopp, M. U.; de Mello, A. J.; Manz, A. *Science* **1998**, 280, 1046-1048.

FIGURE CAPTIONS

Figure 1. Schematic diagram of on-line capillary PCR setup.

Figure 2. (a) Flow-gram of SYTO16 labeled cells with PMT detection; (b) Fluorescent images of cell flow in a 75μm i.d. round capillary, where cells were stained with SYTO16 and frame 1 was the buffer background. The CCD camera exposure time was 10 ms and the frame rate was 5 Hz. The objective was 10×; (c) Fluorescent images of cell flow in a 75μm × 75μm square capillary. Cells were stained with SYTO16 and frame 1 was the buffer background. Exposure time, 10 ms; frame rate, 5 Hz; objective, 10×; (d) Image of cell in a 50μm i.d. round capillary viewed by partial dark field microscopy with 100× magnification. Cells were suspended in PCR reaction mixture without using cell stain.

Figure 3. Gel electrophoresis of the 295-bp PCR product (stained with ethidium bromide) from human lymphoblast cells with different PCR Premixes (FailSafe PCR 2× Premix): Lanes 1, 3, 10 and 12, blank; lanes 2 and 11, 50-

bp DNA ladder; lane 4, PCR with Premix A; lane 5, PCR with Premix D; lane 6, Premix E; lane 7, Premix G; lane 8, Premix H; lane 9, Premix I.

Figure 4. PCR amplification of the 295-bp human β-actin gene and elution by electromigration. (a) Negative control experiment, no human cell template; and (b) with cell template in the capillary.

Figure 5. Correlation of cells starting locations with amplified peaks. The dots were marked positions of cells before reaction, and the bars indicated calculated peak positions based on the migration velocity and the cell locations. The electropherogram showed the actual amplified peaks.

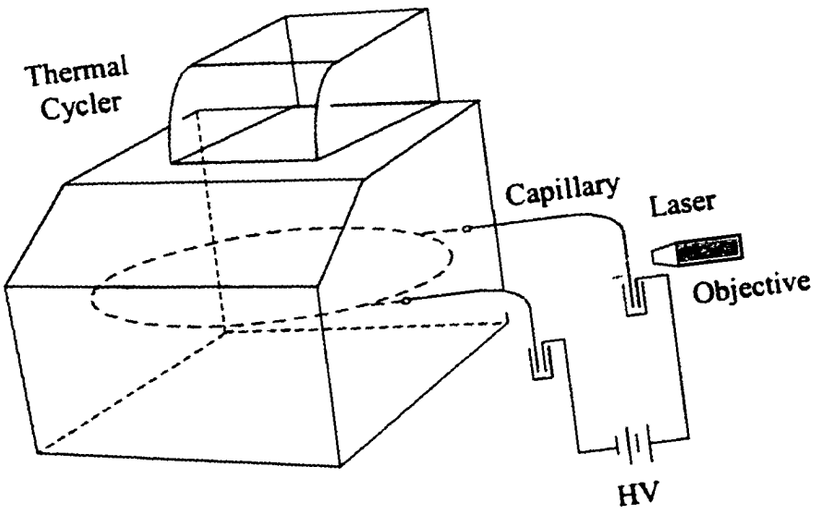

FIGURE 1

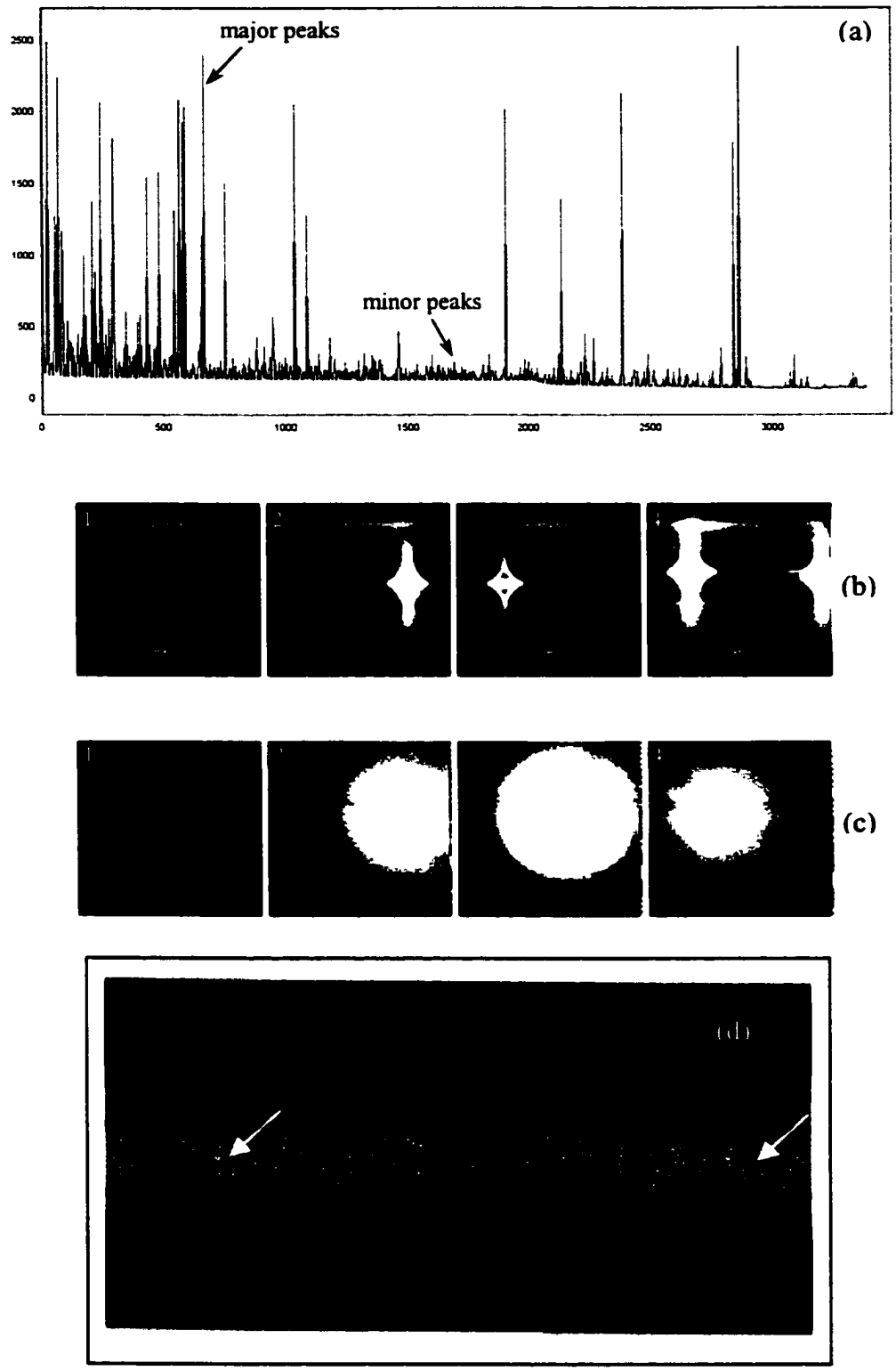
major peaks
(a)
minor peaks
2500
2000
1500
1000
500
0
0
500
1000
1500
2000
2500
3000
(b)
(c)
(d)

FIGURE 2

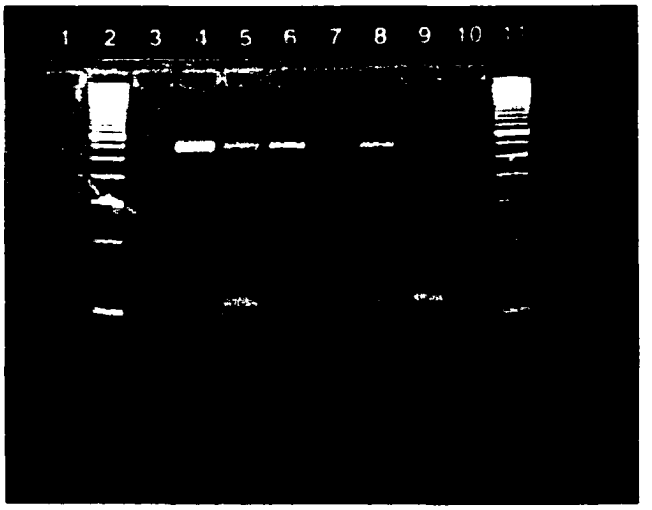

FIGURE 3

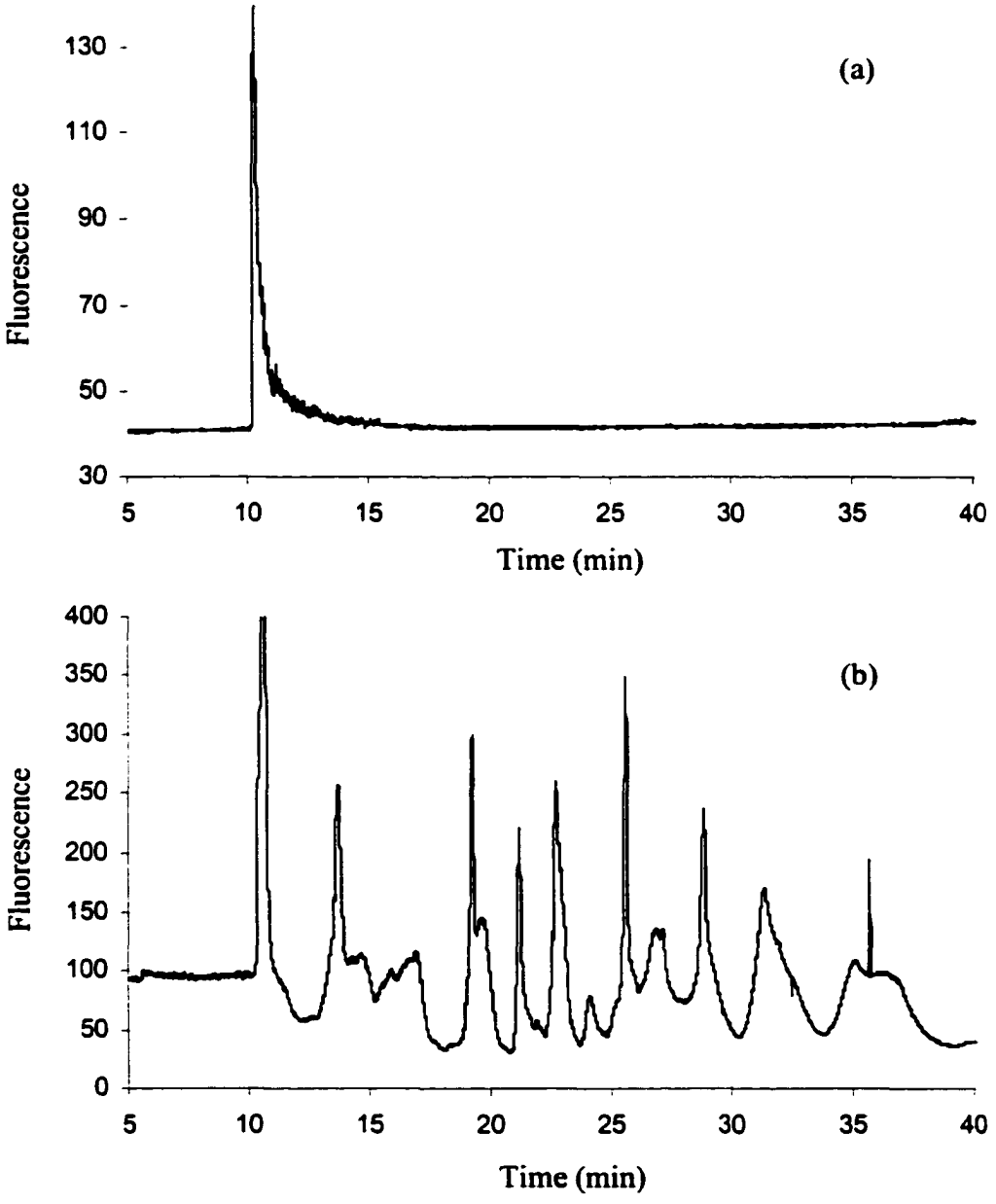
(a)
Fluorescence
130
110
90
70
50
30
5
10
15
20
25
30
35
40
Time (min)
(b)
Fluorescence
400
350
300
250
200
150
100
50
0
5
10
15
20
25
30
35
40
Time (min)

FIGURE 4

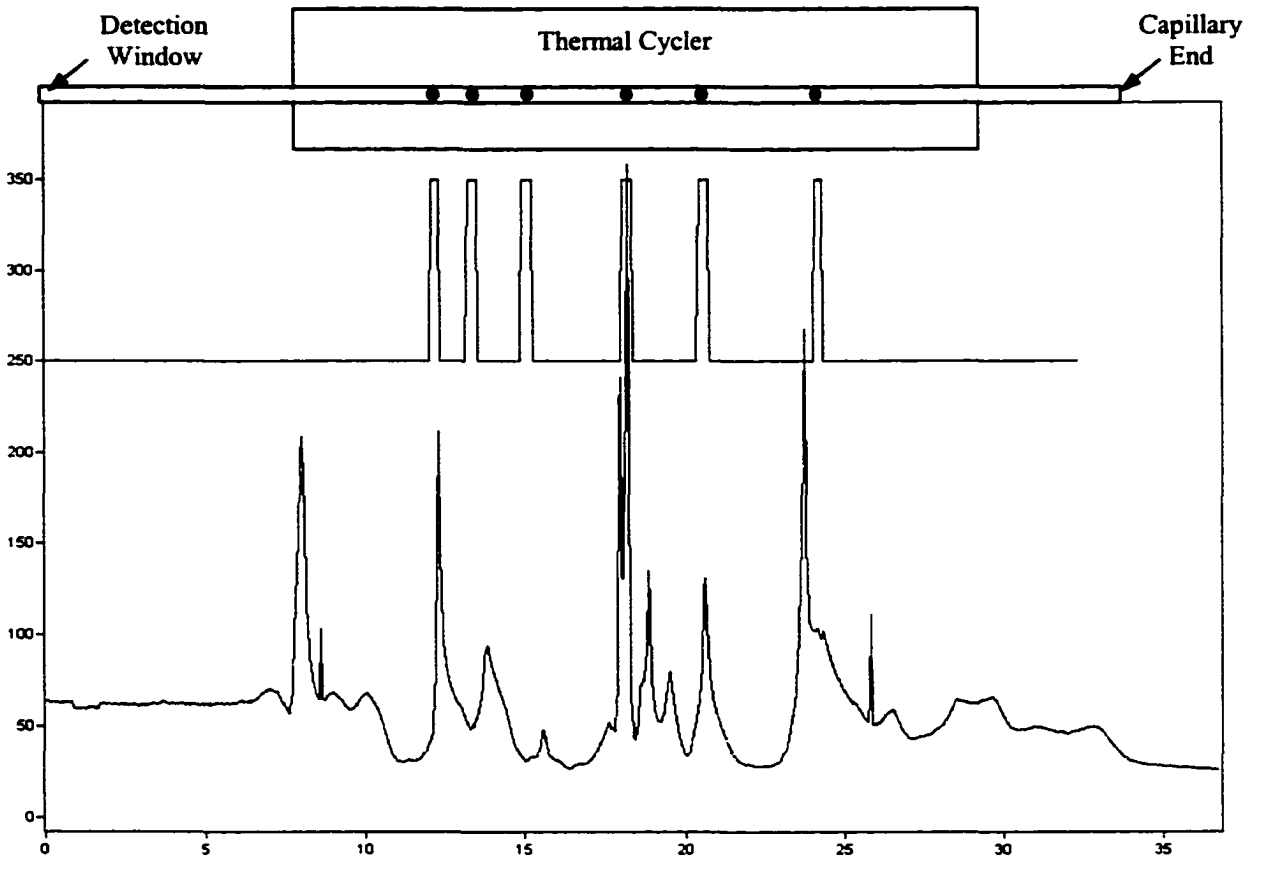
Detection Window
Thermal Cycler
Capillary End
350
300
250
200
150
100
50
0
0
5
10
15
20
25
30
35

FIGURE 5

CHAPTER 5. GENERAL CONCLUSIONS

The emphasis in health care will continue to evolve from management to prophylaxis. There is usually a better chance for therapy if the disease could be recognized at an early stage. Genetic analysis at single cell level is unarguably at the vanguard of several modern scientific arenas including the etiology and diagnosis of disease. However, sensitivity beyond what is presently available is needed to establish molecular profiles for species that are now inaccessible because they are present at low concentrations in tissues or at small quantities in a single cell.

The work in this dissertation has described two novel high sensitive approaches for single molecule genetic analysis. First, we demonstrated a laser induced fluorescence imaging method that allows screening many single molecules at a time based on their electrophoretic mobilities. Each molecule was labeled with fluorescence dye and tracked under a CCD camera by a scientific microscope. Three different procedures were developed to measure the individual molecular mobilities, multi-frame method, streak method, and multi-spot method. Based on their difference in mobility, 2k and 49k bp DNA fragments were unambiguously differentiated. Unlike intensity-based methods, photobleaching and variations in excitation intensity do not interfere with the measurements. Since the measurement only depends on being able to follow a molecule for a few milliseconds in solution, tens of thousands of molecules can be screened every second. Preliminary development of automatic image analysis software was also accomplished, which ensured the ultimate high throughput of this approach for early stage disease diagnosis.

The second single-molecule screening approach we schemed was by online PCR inside a 30-μm-i.d. fused-silica capillary. The capillary was used both as the reaction vessel and for isolating single molecules. SYBR-Green I was added along with the PCR reaction for dynamic fluorescent labeling. Individual DNA molecules of human β-globin gene and HIV-1 virus DNA are successfully amplified and detected in the capillary. This opens up the possibility of disease diagnosis at its very early stage when only very few cells are infected. The problem reduces to identifying the suitable primer pairs for each disease marker.

The online capillary PCR has been further applied to direct amplification of crude biological samples. Individual lymphoblast cells were loaded into the PCR cocktail and on-line lysed by hypotonic buffer in the reaction capillary right before thermal cycling. Human β-actin gene within individual lymphoblast cells was successfully amplified and detected in the capillary without labor-intensive sample preparation. Online cell counting with partial dark field microscopy well correlated the initial cell positions and the final amplified DNA peaks.

For the future efforts, several other interesting applications can be envisioned based on these two single-molecule screening methods. Provided the availability of appropriate labeling dye, very short DNA, e.g. 30 bp, can be monitored by CCD imaging even when it is labeled with only one fluorophor. So specific primers could be labeled as probes for mutant DNA based on single molecule Taqman assay. By labeling the antibodies, the individual antigen molecules could be easily screened as well by single molecule immunoassay, which has the potential as a highly sensitive alternative to ELISA. For the online capillary PCR, its feasibility for continuous-flow PCR monitoring, along with the well-developed capillary array electrophoresis techniques, will also provide the high throughput and high sensitivity

for large-scale clinical diagnosis. And we believe the combination of the lowest possible detection limit and the broadest applicability to biomolecules represents the final frontier in bioanalysis.

APPENDIX. SUPPORTING INFORMATION FOR CHAPTER 2

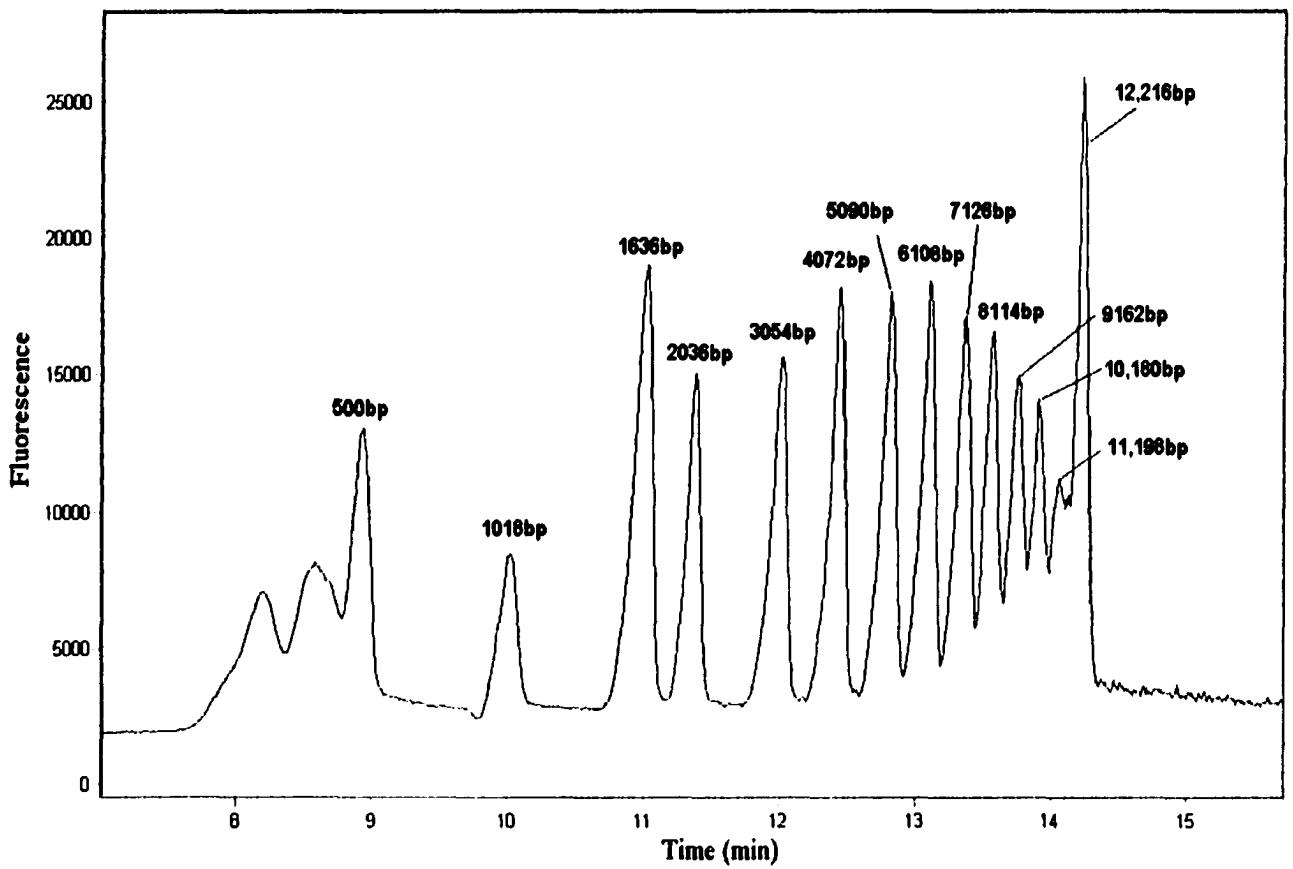

FIGURE 1 Separation of 1 Kb DNA ladder in 10 mM Gly-Gly buffer with 0.05% (w/v) M_r 8 000 000 PEO, pH 8.2.

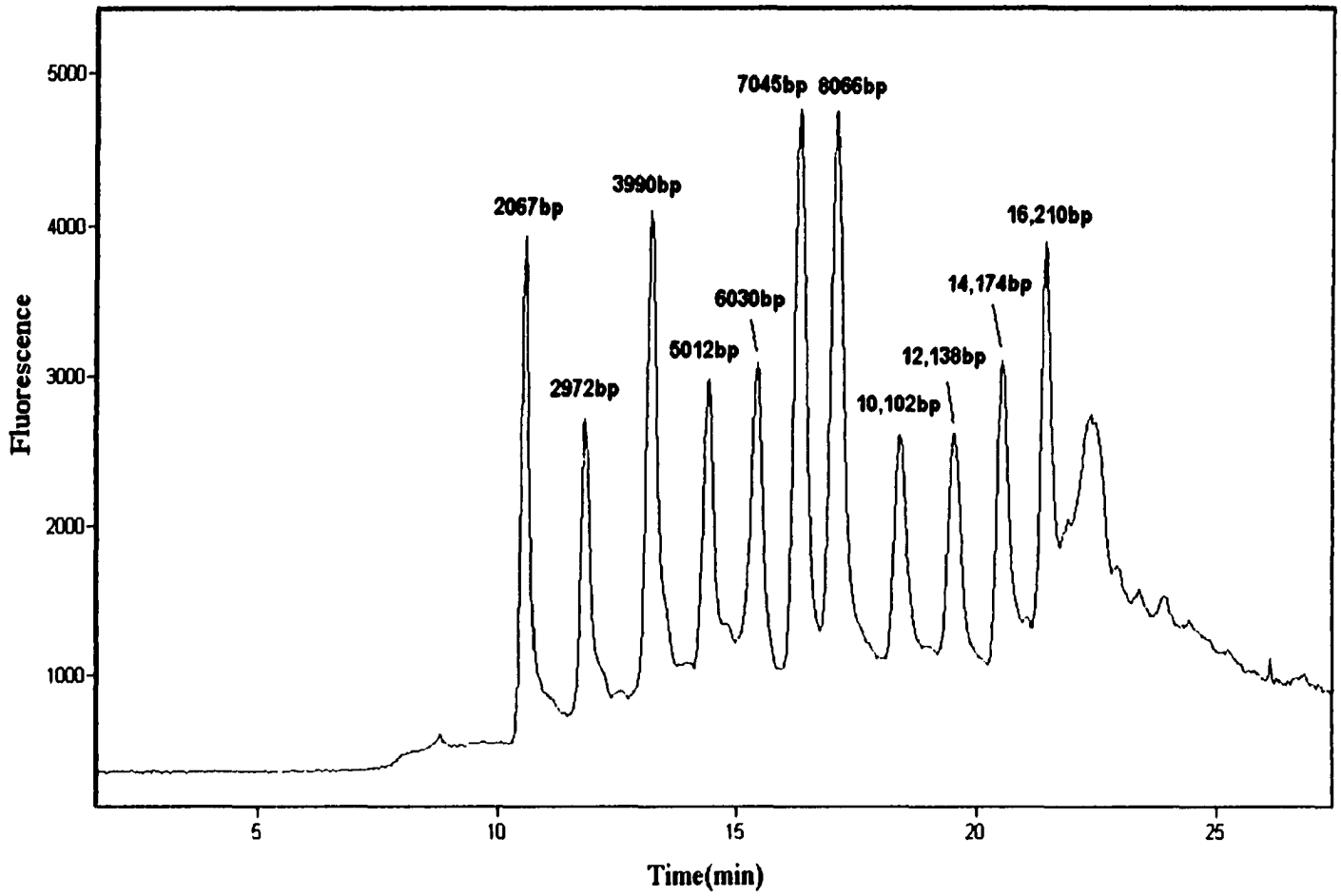

FIGURE 2 Separation of supercoiled 1Kb DNA ladder in 10 mM Gly-Gly buffer with 0.05% (w/v) Mr 8 000 000 PEO, pH 8.2.

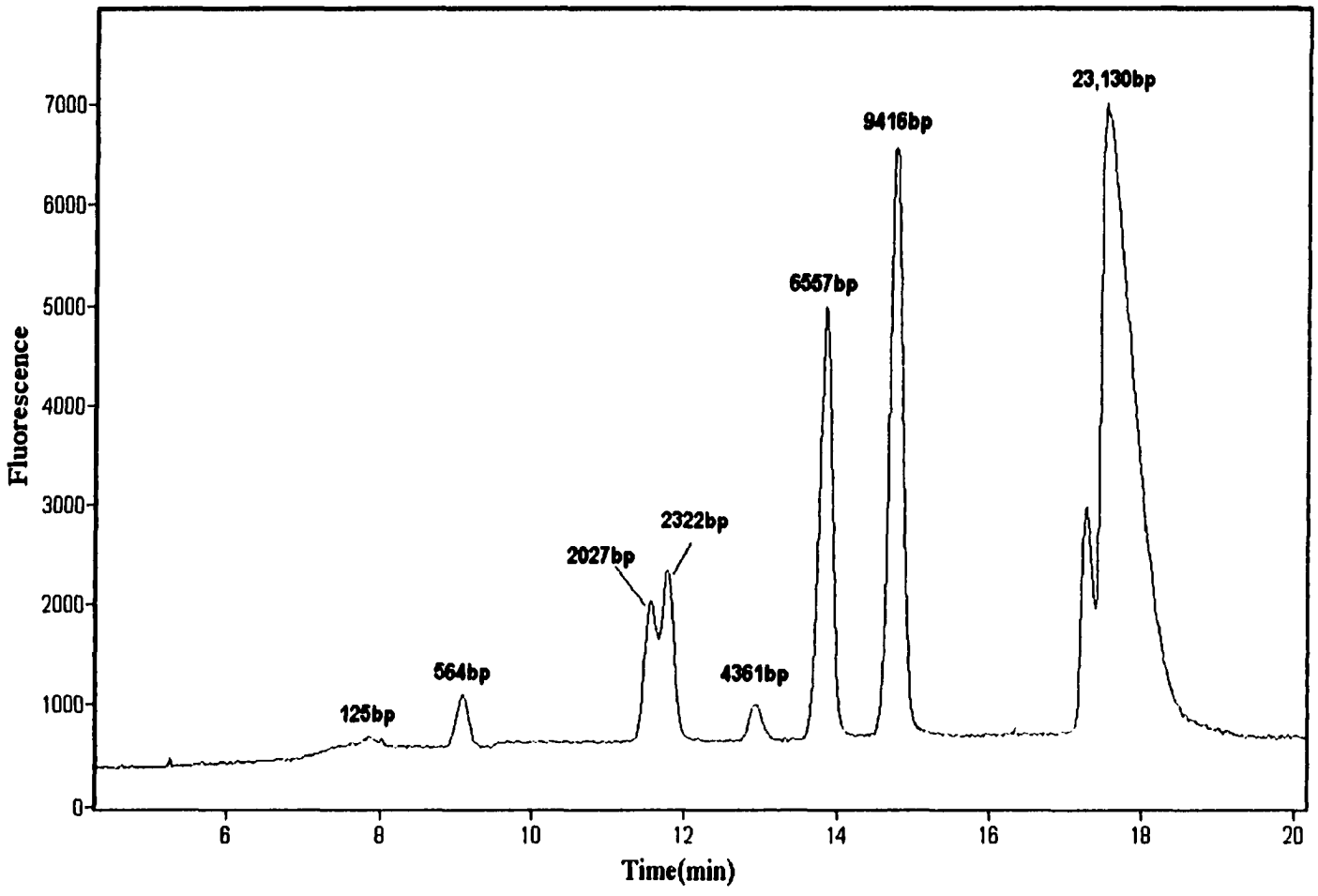

FIGURE 3 Separation of lamda/*Hind* III fragments in 10 mM Gly-Gly buffer with 0.05% (w/v) Mr 8 000 000 PEO, pH 8.2.

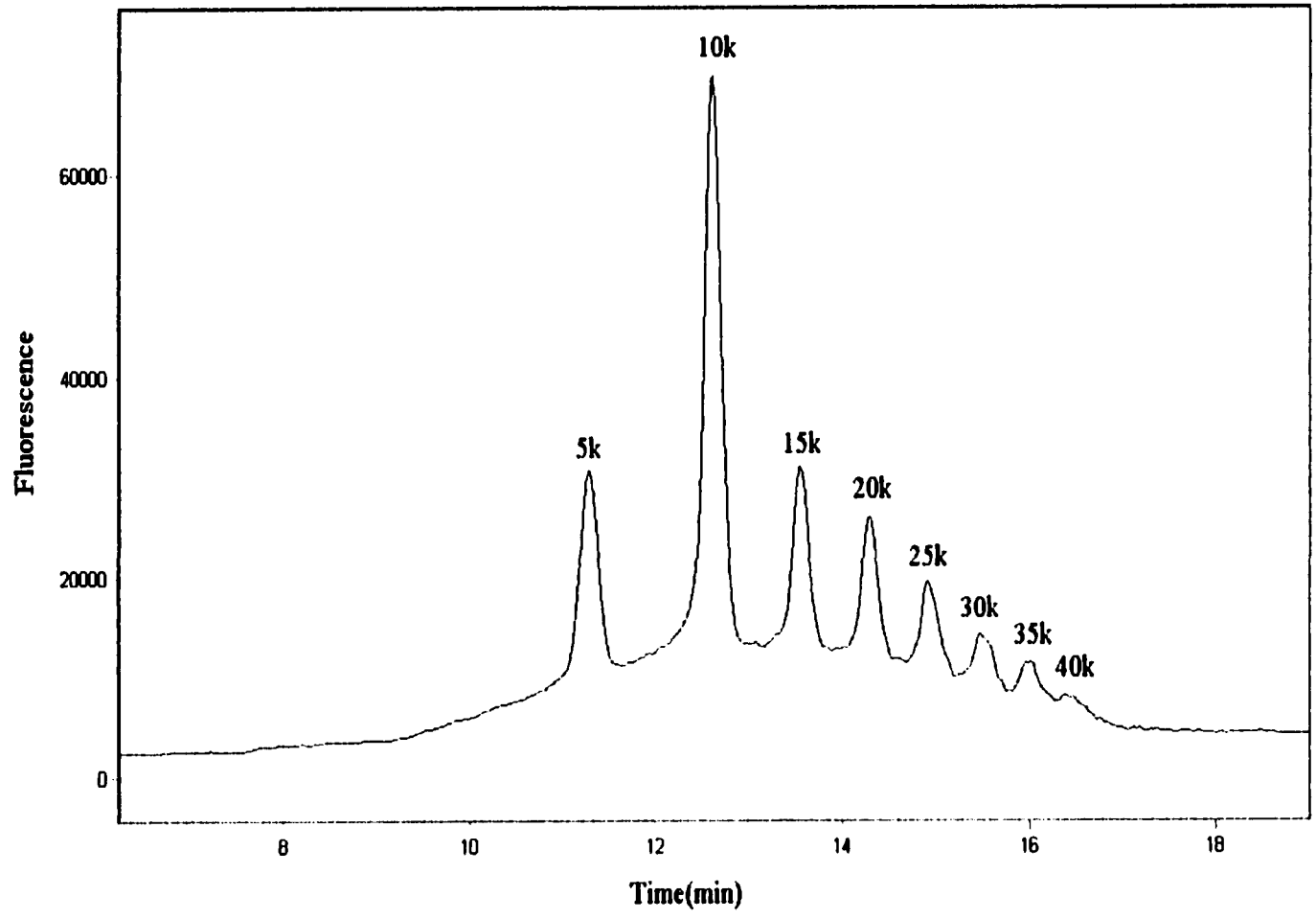

FUGURE 4 Separation of 5 Kb DNA ladder in 10 mM Gly-Gly buffer with 0.05% (w/v) Mr 8 000 000 PEO, pH 8.2.

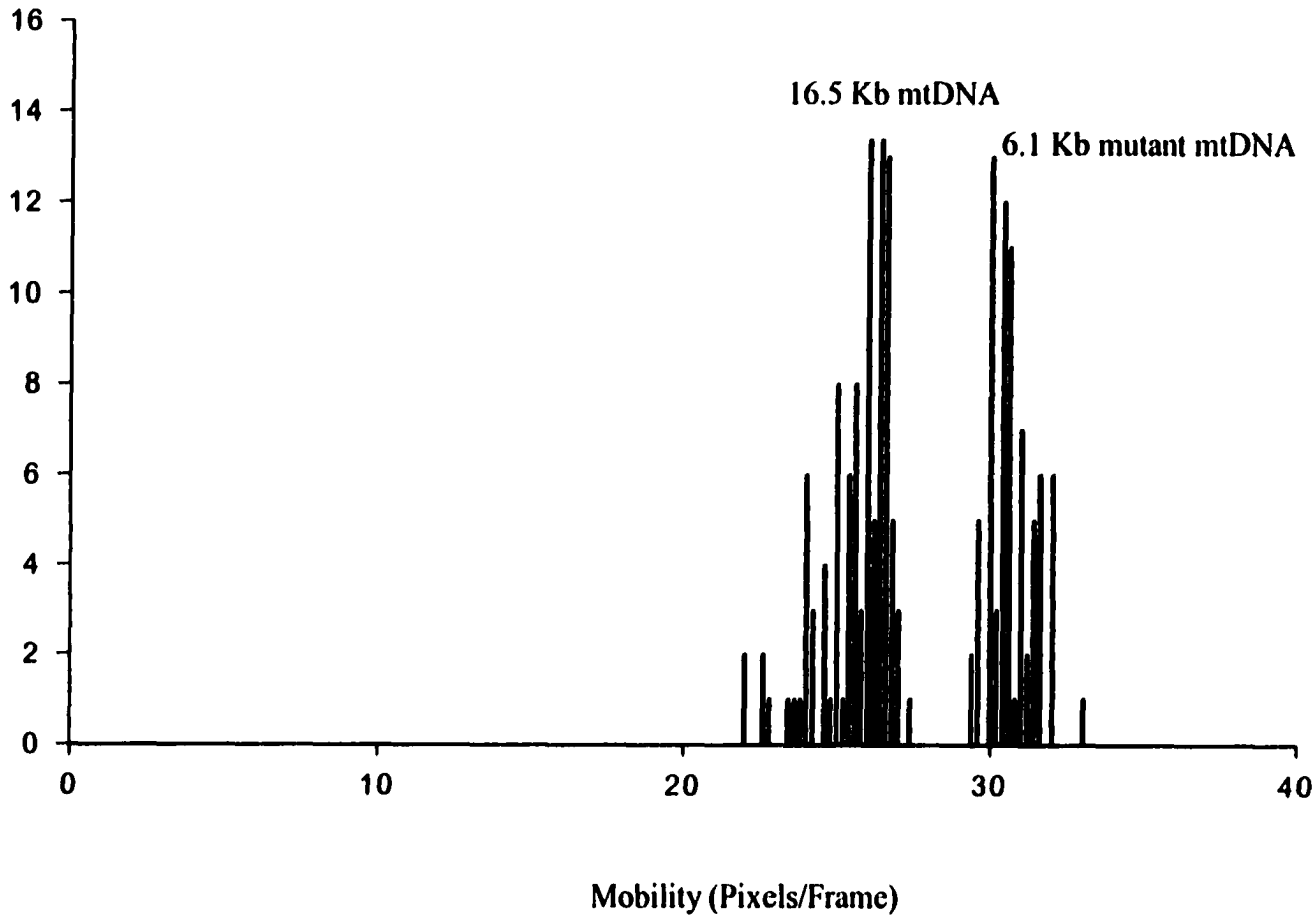

FIGURE 5 Mobility histogram from single-molecule images for a mixture of 16.5 kbp normal human mitochondria DNA and 6.1 kbp mutant mitochondria DNA associated with diabetes. The separation was performed in 50 mM Gly-Gly buffer with 0.3% (w/v) Mr 600 000 PEO, pH 8.2. Confident classification of every fragment is achieved.

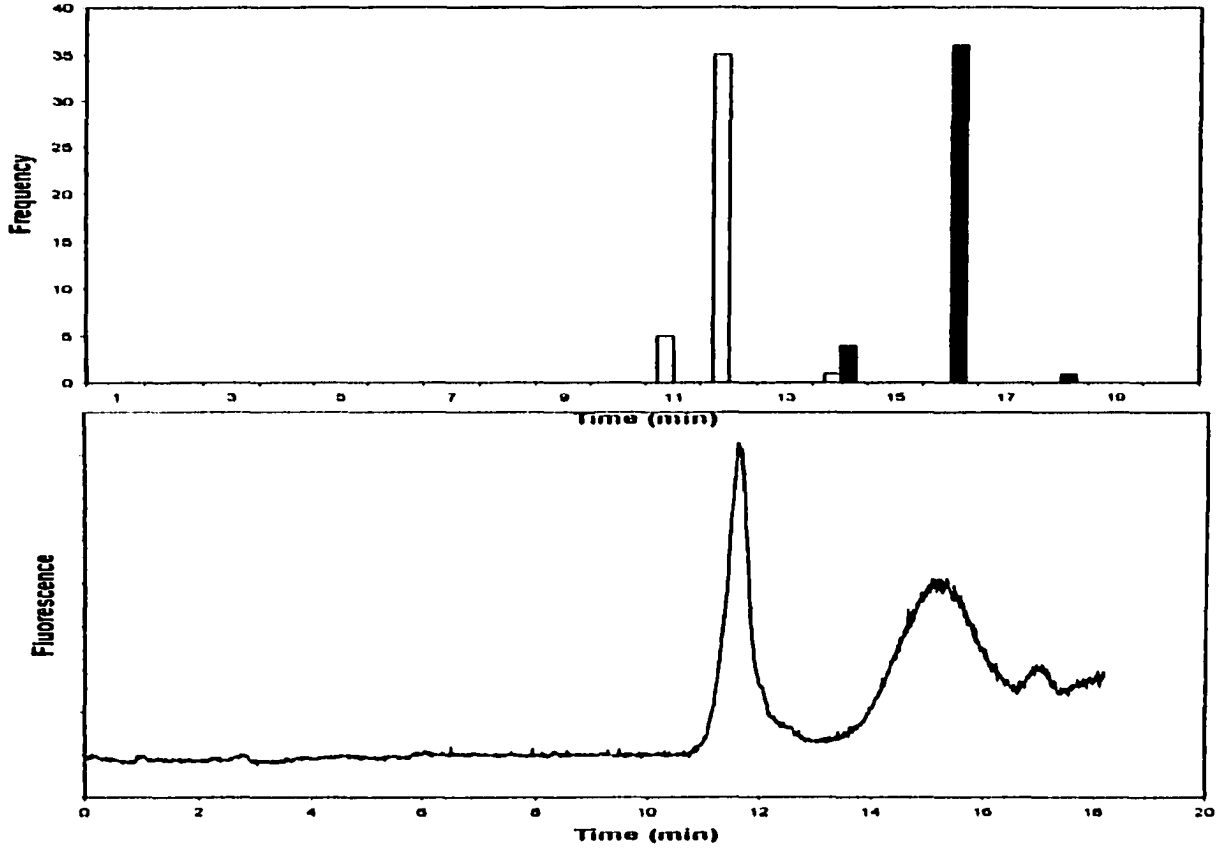

FIGURE 6 Comparison of bulk electropherogram (bottom) with histograms of migration times predicted from single-molecule mobilities (top). Results are depicted for digoxin immunoassay (β-phycoerythrin-labeled digoxigenin, left, *vs.* its immunocomplex, right). Separation was performed in 50 mM Gly-Gly buffer with 0.3% Mr 1 000 000 PVP, pH 8.2.

ACKNOWLEDGEMENT

First of all, I would like to express my heartfelt appreciation to my major professor, Dr. Edward S. Yeung. I would like to thank him for his continuous support and encouragement, for his patience and inspiration throughout the past four and a half years. His knowledge, creativity, persistence and dedication to science had shown me what comprises a great scientist. I sincerely admire him because he is not only a brilliant scientist but also a decent person in all aspects. Things I learned from him will benefit my whole life.

I am also grateful to my committee members, Dr. Beitz, Dr. Espenson, Dr. Houk, and Dr. Johnson, for their precious time and advice.

My sincere thanks go to Dr. Michael Shortreed, Dr. Yinfa Ma, and Dr. Weihua Huang for cooperating with me in different research projects. It was a valuable and pleasant experience to me.

I would also like to thank all Dr. Yeung's group members, both past and present. Wei Wei, Takashi Anazawa, Jinjian Zheng, Craig Aspinwall, Yan He, Homing Pang, Yonghua Zhang, Xiaoyi Gong, Nanyan Zhang, David Gao, Hui Su, Jason Gruenhagen, Michael Christodoulou, Wenwan Zhong, Frank Li and all the others who gave me a lot of help in my research. I also want to thank all the Dr. Yeung's group members for their friendship and the wonderful time I had with them. It is a great family that I will never forget.

Finally, I would like to dedicate this dissertation to my parents and my husband. It is my parents who brought me to this beautiful world, provide me a happy family, and give me their endless love. It is my husband, Gang Xue, who has been giving me his unconditional love, support, encouragement and endurance, and teaching me to keep optimistic and never

give up. I feel so grateful and fortunate to be able to spend the rest of my life with him. Millions of thanks to my parents and my husband, it is them who make my life wonderful.

This work was performed at Ames Laboratory under Contract No. W-7405-Eng-82 with the U.S. Department of Energy. The United States government has assigned the DOE Report number IS-T 2101 to this dissertation.